Dipartimento di fisica e astronomia
Università degli studi di firenze

Scuola di Dottorato in Scienze

Dottorato di Ricerca in Fisica - XXIII ciclo
SSD FIS/02

Dissertation in Physics

to Obtain the Degree of

Dottore di Ricerca
in Fisica

Title:

Partition Functions of Non-Abelian Quantum Hall States

presented by

Giovanni Viola

Supervisor	Andrea Cappelli
Coordinator	Alessandro Cuccoli
Referees	Eddy Ardonne Domenico Seminara

December 2010

To my Parents

Overview

The fractional quantum Hall effect is a collective quantum phenomenon of two-dimensional electrons placed in a strong perpendicular magnetic field ($B \sim 1 - 10$ Tesla) and at very low temperature ($T \sim 50 - 500$ mK). It manifests itself in the measure of the transverse (σ_{xy}) and longitudinal (σ_{xx}) conductances as functions of the magnetic field. The Hall conductance σ_{xy} shows the characteristic step-like behavior: at each step (plateau), it is quantized in rational multiples of the quantum unit of conductance e^2/h: $\sigma_{xy} = \nu\frac{e^2}{h}$; furthermore, at the plateaus centers the longitudinal resistance vanishes. These features are independent on the microscopic details of the samples; in particular, the quantization of σ_{xy} is very accurate, with experimental errors of the order $10^{-8}\Omega$. The rational number ν is the *filling fraction* of occupied one-particle states at the given value of magnetic field.

The fractional Hall effect is characterized by a non-perturbative gap due to the Coulomb interaction among electrons in strong fields. The microscopic theory is impracticable, besides numerical analysis; thus, effective theories, effective field theories in particular, are employed to study these systems. The first step was made by Laughlin, who proposed the trial ground state wave function for fillings $\nu = \frac{1}{2s+1} = \frac{1}{3},\ \frac{1}{5}, \cdots$ describing the main physical properties of the Hall effect. One general feature is that the electrons form a fluid with gapped excitations in the bulk, the so-called incompressible fluid. In a finite sample, the incompressible fluid gives rise to edge excitations, that are gapless and responsible for the conduction properties. Therefore the low-energy effective field theory should describe these edge degrees of freedom.

The Laughlin theory revealed that the excitations are "anyons", *i.e.* quasiparticles with fractional values of charge and exchange statistics. The latter is a possibility in bidimensional quantum systems, where the statistics of particles is described by the braid group instead of the permutation group of higher-dimensional systems. Each filling fraction corresponds to a different state of matter that is characterized by specific fractional values of charge and statistics. The braiding of quasiparticles can also occur for multiplets of degenerate excitations, by means of multi-dimensional unitary transformations; in this case, called *non-Abelian* fractional statistics, two different braidings do not commute. The corresponding non-Abelian quasiparticles are degenerate for fixed positions and given quantum numbers.

Non-Abelian anyons are candidate for implementing topological quantum computations according to the proposal by Kitaev and others. Since Anyons are non-perturbative collective excitations, they are less affected by decoherence due to local disturbances.

Experimental observation of non-Abelian statistics is a present challenge.

The *topological fluids*, such as the quantum Hall fluid can be described by the Chern-Simon effective field theory in the low-energy long-range limit. The Chern-Simon theory is a gauge theory with symmetry algebra $\mathfrak{g}$. Witten's work showed the connection between the Chern-Simon theory and the rational conformal field theory (RCFT). For the applications to quantum Hall physics, this gives two results: i) the wave functions are correlators of the rational conformal field theory with Affine algebras $\widehat{\mathfrak{g}}$, and ii) on spaces with boundaries, *e.g.* a disc or annulus, the Hilbert space of the edge modes is given by the same conformal theory. Therefore, the low-energy effective field theories for Hall fluids are rational CFT, that live on the two-dimensional space or, in the case of edge modes, on the space-time boundary (*e.g.* the cylinder for a droplet of Hall fluid). Once the rational CFT has been proposed for wave functions, it also describes the low energy excitations on the edge.

Conformal field theories describe each anyon by an appropriate field, the fusion between anyons and their braiding properties coincide with the fusion rules of the operator algebra and the monodromy properties of the conformal blocks, respectively. The basic quasiparticles correspond to the sectors in the theory. In the conformal description the Verlinde's formula implies that the braiding matrix, the fusion rules and the quantum dimensions are function of the $\mathcal{S}$ modular transformation of the partition function; the latter is a fundamental quantity in the theory.

While the Laughlin states are described by the Abelian CFT with $\widehat{U(1)}$ symmetry (the chiral Luttinger liquid), more involved theories describe the non-Abelian anyons. Moore and Read proposed the $\widehat{U(1)} \times$ Ising theory for the plateaus at $\nu = 5/2$. In the literature, this approach has been generalized to other states in the second Landau level, that are supposed to be non-Abelian fluids: their wave functions are conformal blocks of rational conformal field theories $\widehat{U(1)} \times \widehat{\mathfrak{g}}$. Here $\widehat{U(1)}$ describes the charge part of the theory and the other factor $\widehat{\mathfrak{g}}$ is the neutral part of the edge modes characterized by an Affine symmetry algebra $\widehat{\mathfrak{g}}$ or a coset $\widehat{\mathfrak{g}}/\widehat{\mathfrak{h}}$. The most relevant proposals are: the Read-Rezayi and anti-Read-Rezayi states, the Bonderson-Slingerland hierarchy, the Wen non-Abelian fluid and the non-Abelian spin-singlet state. These theories describe different filling fractions $\nu = 2 + \frac{p'}{p}$ and have been supported by numerical simulations.

This thesis concerns the study of edge excitations of Hall states, in particular their modular invariant partition functions. This quantity provides a complete definition of the Hilbert space and its decomposition into sectors; moreover, the fusion rules, the selection rules for the fields, are built in. In this thesis, we obtain a straightforward method to derive the modular invariant partition functions for edge excitations in the annulus geometry. Starting from the two choices of: i) the conformal field theory $\widehat{\mathfrak{g}}$ of the neutral part of excitations, and ii) Abelian field representing the electron, the charge and statistics of all excitations can be self-consistently found without further physical input. The annulus geometry is chosen because it enjoys the modular symmetry where the edge modes living on two circles realize the holomorphic and anti-holomorphic parts of the theory. The disk and Hall bar geometries can also be obtained by taking limits of the annulus.

The partition function is derived by considering the role of the electron field in the Hall fluid: this is a spin one-half Abelian field, that must possesses integer exchange statistics with all the other excitations in the fluid. Once these conditions are considered, the derivation of the partition function is unique. We observe that these conditions are also required by invariance under modular transformations of the partition function, that have clear physical meaning for Hall systems.

In the last part of the thesis, we compute experimental signatures of non-Abelian statistics by using the partition function. We describe the Coulomb Blockade current peaks, both at zero and non-zero temperatures (determining the low-lying energy spectrum) and study the thermopower, the ratio of electric and thermoelectric conductances (measuring the so-called quantum dimension). We show that the derivation of the peak patterns from the partition function is very simple, both at zero and finite temperatures. All these experimental predictions are worked out in details for the prominent non-Abelian states in the second Landau level. These experimental quantities are alternative to the interference effects that would directly test the braiding properties of quasiparticles.

The thesis is organized as follows: in chapter 1 we recall some general aspects of planar physics: quantum Hall effect, Chern-Simons theory and quantum statistics in two dimensions. The chapter 2 introduces the reader to the conformal field theory and its connections with Chern-Simons theory, anyons model and the Hall fluids. In chapter 3 we discuss the derivation of the partition function for Hall fluids in the second Landau level, the technical details are reported in appendix B. In the chapter 4, the physical applications of the partition function are analyzed. Appendix A also reports the derivation of the partition function and the Coulomb peak patterns for the Jain states, that are Abelian states in the first Landau level.

The work of this thesis is based on the papers:

A. Cappelli, G. Viola and G. R. Zemba,
Chiral Partition Functions of Quantum Hall Droplets,
Annals Phys, **325** (2010) 465,
`arXiv:0909.3588v1 [cond-mat.mes-hall]`
A. Cappelli and G. Viola
Partition Functions of Non-Abelian Quantum Hall States,
`arXiv:1007.1732v2 [cond-mat.mes-hall]`;
submitted to J. Phys. A.

Other author's publications:

S. Caracciolo, F. Palumbo and G. Viola,
Bogoliubov transformations and fermion condensates in lattice field theories,
Annals Phys. **324**, (2009) 584,
`[arXiv:0808.1110 [hep-lat]]`.

Acknowledgments

I want to express the highest gratitude to my supervisor Andrea Cappelli, for having introduced me to the topics of this thesis, for his charming approach towards research and for his deep knowledge of physics. I hope I will make all his precious teaching mine, bringing it with me for the future.

I also thank Guillermo Zemba for his contribution to the project of this thesis and for all the important hints that he has given to my work.

I acknowledge many fruitful discussions with Ivan D. Rodriguez, Dario Ferraro, Lachezar S. Georgiev, Giancarlo Ferrera, Jacopo Bechi, Sergio Caracciolo and Masudul Haque. They all have contributed in different ways to the improvement of my knowledge and my critical approach towards physics, stimulating my passion for research.

This work has been realized at the Physics and Astronomy Department of the University of Florence. Finally, I want to thank all the special people that I have met during these years and that have been sharing this experience with me. My staying in Florence would not surely have been such a fun without all the friends I have met here.

Contents

Chapter 1

Introduction

In this chapter we recall some aspects of planar physics that are relevant for this thesis. We introduce the quantum Hall effect (QHE) and its wave function description, then we discuss the Chern-Simons theory (CS) that provides the effective field theory for low-energy excitations of *topological fluids*, such as bidimensional electron gases (2DEG) in perpendicular magnetic fields. Afterwards, the aspects of exchange statistics in planar systems are presented. In the last part, we discuss experiments that have been devised for observing fractional charge and fractional statistics in QHE.

1.1 Integer Quantum Hall effect

The quantum Hall effect takes place in two dimensional electrons (typically in GaAs heterostructures) subjected to strong perpendicular magnetic fields (1 T $\lesssim B \lesssim$ 10 T) and very low temperatures (10 mK $\lesssim T \lesssim$ 500 mK); for a review on QHE see [1, 2, 3, 4]. The experimental set up is shown in figure 1.1.

The experimental data show the characteristic step-like behavior: as a function of the magnetic field, the Hall resistance $R_H = R_{xy}$ displays plateaus in correspondence with deep minima of the longitudinal resistance R_{xx}, as shown in figure 1.2. These plateaus occur at quantized values of the resistance, that are rational multiples of the quantum unit of resistance h/e^2:

$$R_{xy} = \frac{h}{e^2}\frac{\hat{p}}{p'} = \frac{h}{e^2}\frac{1}{\nu}\,, \qquad\qquad R_{xx} = 0\,. \tag{1.1}$$

The quantum Hall effect was observed for the first time in 1980 by K. Von Klitzing, G. Dorda and M. Pepper [6]. In that experiment, only the integer plateaus were observed, *i.e.* $\nu = 1,\ 2,\ \cdots$. The fractional plateaus were observed in experiments by Tsui, Stormer and Gossard, *e.g.* $\nu = \frac{1}{3},\ \frac{1}{5},\ \cdots$ in the 1982 [7]. The two phenomena are called Integer Quantum Hall Effect (IQHE) and Fractional Quantum Hall Effect (FQHE) respectively: they are examples of quantum mechanical behavior for a macroscopic quantity such as the resistance.

From scaling arguments [5], the conductance g and the conductivity σ in a box of size L in d space dimension are related by $g = \sigma L^{d-2}$. It follows that the case $d = 2$ is

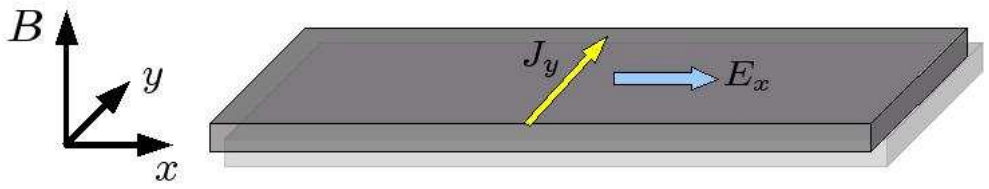

Figure 1.1: The experimental setup of the quantum Hall system. The Hall resistance is measured between the two horizontal edges of the bar.

special since σ can be obtained form the resistance R without the knowledge of the size of the sample. Therefore, we can have extremely precise measures of conductivity [3].

At the plateaus, the inverse of the Hall resistance yields the conductivity σ_{xy},

$$\sigma_{xy} = \nu \frac{e^2}{h} , \tag{1.2}$$

that is proportional to the *filling fraction* $\nu \equiv N_{\rm e}/N_{\Phi_0}$, with $N_{\rm e}$ the number of electrons and N_{Φ_0} the flux through the area of the 2DEG in units of the flux quantum $\Phi_0 = hc/e$. Since the conductance tensor σ_{ij} is off-diagonal, a dissipationless transverse current flows in response to the applied electric field. The Hall resistance does not follow the classical behavior, which would be linear in the applied magnetic field. The values of the Hall resistance in the middle of the plateaus are independent on the microscopic details of the samples, the experimental errors on its measure are very small, of order 10^{-8} Ω.

The values in (1.1) are valid in the zero-temperature limit. The deviations at finite temperature, at least for a small range of T, are proportional to $e^{-\widetilde{T}/T}$, where $\widetilde{T}$ is proportional to the gap in the excitations spectrum. An indication of a finite gap is given by the absence of Ohmic conductance.

As it will be clear in the following, the fractional quantum Hall effect is a non-perturbative quantum phenomenon that requires effective descriptions. The universality of the rational conductivity values suggests that the approaches based on low-energy effective field theories are relevant, as in the cases of critical phenomena of statistical mechanics. The experimental observations [8] makes it clear that the low-energy effective degrees of freedom are defined on the edge.

1.1.1 Landau levels

In strong magnetic fields, the electrons are spin polarized for most of the materials used in experiments: the large Zeeman splitting freezes the spin degrees of freedom. The Hamiltonian of a single electron, with effective mass m and charge e, is

$$\hat{H} = \frac{1}{2m} \left(\hat{\mathbf{p}} - \frac{e}{c} \mathbf{A} \right)^2 , \tag{1.3}$$

where $\mathbf{A}$ is the external field, $\nabla \times \mathbf{A} = B$. It is convenient to first discuss the geometry of the infinite plane and of the finite disc. From the analysis of the of cyclotron motion

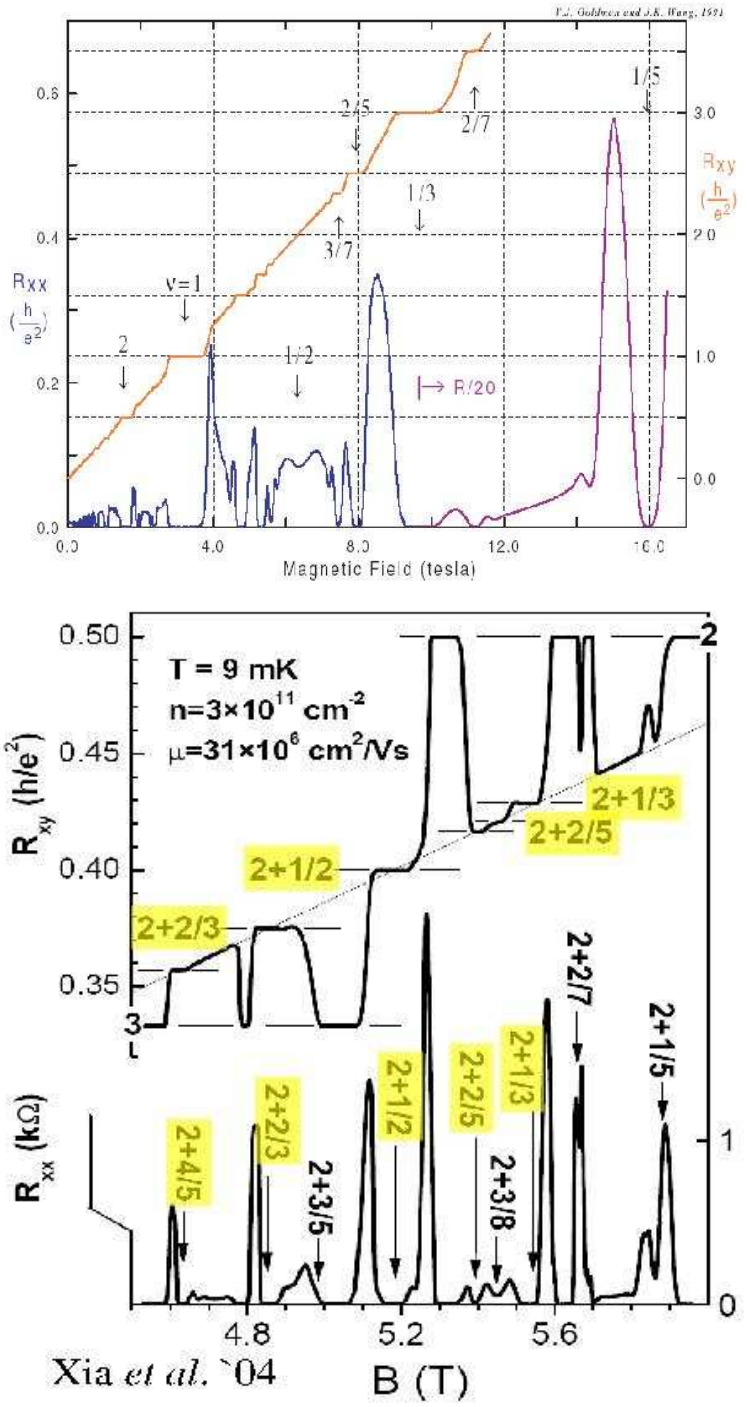

Figure 1.2: Top: overview of Hall and longitudinal resistance R_H and R_{xx}, respectively, [9]. Bottom: enlarged view of the R_H and R_{xx} for filling fractions $2 < \nu < 3$ [10]. Major FQHE states are marked by arrows.

of the electron [1], the energy and magnetic length are obtained: these are, respectively, $\hbar\omega_c = \hbar\frac{eB}{mc}$ and $\ell_B = \sqrt{\frac{2\hbar c}{eB}}$. The flux through a disc with radius ℓ_B, is equal to the quantum of flux Φ_0 that plays a fundamental role the theory of QHE [4, 11]. The flux through the whole area of the sample are quantized in units of Φ_0.

The Hamiltonian in (1.4) and the corresponding Schödinger equation are gauge invariant, but the momenta $\hat{\mathbf{p}}$ is not; it is convenient to fix the symmetric gauge $\mathbf{A} = (-\frac{By}{2}, \frac{B}{2}, 0)$ and introduce the complex coordinates $z = x + iy$ and $\bar{z} = x - iy$. The Hamiltonian can be expressed in terms of a pair of creator and annihilation operators $\hat{a}$ and $\hat{a}^\dagger$ (see *e.g.* [1]). A second independent couple $\hat{b}$ and $\hat{b}^\dagger$ is introduced, since the initial phase space is $4-$dimensional. The Hamiltonian and the angular momenta $\hat{J}$ can be written in terms of them as follows:

$$\hat{H} = \hbar\omega_c(\hat{a}^\dagger\hat{a} + 1/2) \qquad \text{and} \qquad \hat{J} = \hbar(\hat{a}^\dagger\hat{a} - \hat{b}^\dagger\hat{b})\,. \tag{1.4}$$

The eigenvalues of $\hat{H}$ and $\hat{J}$ are $E_n = \hbar\omega_c(n + 1/2)$ and $J_{n,l} = \hbar(n - l)$, respectively (with $n,\ l \in \mathbb{N}$); their eigenvectors denoted by $\eta_{n,l}(z, \bar{z})$ are reported in [1]. The Landau levels (LLs) are degenerate with respect to angular momentum excitations; the energy gap between two levels ($\hbar\omega_c$) is proportional to B. Thus, for large magnetic fields we can consider only the lowest Landau level (LLL). In a single LL, the phase space is reduced from 4 to 2 dimension. The wave functions $\eta_{0,l}$ are localized on circles of radius $\sqrt{l}\ell_B$. Therefore in the disk geometry, the LLs have finite degeneracy $\propto (R/\ell_B)^2$.

The single particle problem can be solved analytically in different geometries (usually the plane, the sphere and the torus) and the general expression of the single-particle states is $\eta_{n,l}(z, \bar{z}) = \psi(z, \bar{z})_{n,l}F_n(z, \bar{z})$. The first term depends on the genus of the surface and on the quantum numbers; the second factor $F_n(z, \bar{z})$ is geometrical and dependents on the energy level.

Hereafter, we consider the plane and mostly the lowest Landau Level for which $\psi(z, \bar{z})_{0,l} = \frac{z^l}{l!\sqrt{\pi}}$ and $F_n(z, \bar{z}) = e^{-\frac{|z|^2}{2}}$, in the notation $\ell_B = 1$. The system is characterized by the filling fraction ν. Since the number of one-particle states per unit of area is $\frac{B}{\Phi_0}$, the density of occupied states is given by $\nu = \frac{\rho}{B/\Phi_0}$ (in term is the of electrons density ρ). For integer values of ν, all the states in the lowest ν levels are occupied (assuming spin-polarized electrons) and the multi-particle wave function can be obtained by standard Slater's determinants. For $\nu = 1$ it is given by the Vandermonde determinant,

$$\Psi_1(\{z_i\}, \{\bar{z}_i\}) = \prod_{0\le i<j\le N_e} (z_i - z_j)\ e^{-\frac{1}{2}\sum_i |z_i|^2}\,. \tag{1.5}$$

Since all the states in the LLL are full, the excitations are gapped and correspond to jumps of electrons to the next LL. Moreover the density is constant. Thus, the electrons form a fluid which has a gap for density fluctuations, *i.e.* it is incompressible [12]. This is a key point for the observation of the plateau.

A simple computation shows that the conductivity tensor σ_{ij} for the states with integer filling $\nu = n$ is given by $\sigma_{xx} = 0$ and $\sigma_{xy} = -\sigma_{yx} = \frac{e^2}{h}n$ [1, 2], in accordance with experiments. Therefore, the simple quantum mechanical description of free electrons

is able to capture some basic features of the IQHE. Note that the Hall conductance is correct only for discrete values of B such that ν are exactly integers. The existence of the plateaus in $\sigma_{x,y}$ requires to consider also the effect of impurities inside the sample [1]. In the following, we suppose that the values of the magnetic field is in the middle of the plateaus and we describe physical properties that do not depend on impurities.

1.2 Fractional Quantum Hall effect

The fractional quantum Hall Effect is a very interesting nonperturbative quantum phenomenon, that has been analyzed by new methods and techniques: theoretical, numerical and experimental. The best observed filling fractions in LLL are the Laughlin series ($\nu = 1/(2k+1)$) and the Jain hierarchy ($\nu = m/(2ms \pm 1)$). The plateaus in second LL (SLL) ($\nu = 2 + \frac{p'}{\hat{p}}$) will be particularly relevant for this thesis. Each plateau corresponds to a different collective state of matter, that can be characterized by a new type of order, the so-called topological order [2] and its excitations have specific fractional quantum numbers.

At fractional ν, the ground state of the non-interacting Hamiltonian is highly degenerate, but the observations of plateaus requires an unique ground state and a gap (*i.e.* an incompressible fluid) [1]: therefore, the interaction between electron must be taken in account. Fractional plateaus are less stable respect to the integer ones, they are observed in cleaner and colder samples [6, 7], and their energy gap is smaller than in IQHE. At the observed fractions, the interactions between electrons are able to lift the degeneracy and to create a nonperturbative gap and so an incompressible ground state [1, 3].

1.2.1 Laughlin wave function

A paradigmatic method for analyzing the FQHE was found by Laughlin [3], and then further developed, among others, by Haldane and Halperin [13], Jain [1], Wen et. al., Moore and Read [14] and Ardonne and Schoutens [15, 16]. Since a microscopic theory of nonperturbative interacting electrons is very difficult, Laughlin proposed a trial wave function that reproduces the main properties of the state at a given filling fraction. He considered an expression involving powers of the Vandermonde, as follows:

$$\Psi_p(\{z_i\},\{\bar{z}_i\}) = \prod_{0\le i<j\le N_e} (z_i - z_j)^p \; e^{-\frac{1}{2}\sum_i |z_i|^2}\,, \tag{1.6}$$

for odd integer p values (even if boson are considered). The filling fraction is obtained by the ratio $\nu = \frac{N_e^2}{2J_{tot}}$ where N_e is the number of electron and J_{tot} is the total angular momenta of the state. Therefore Ψ_p describes the experimentally observed plateau at $\nu = 1/p = 1/(2s+1)$ [7] and is called the Laughlin wave function.

Numerical analyses confirm that this wave function has large overlap with the exact numerical ground state of the few-body problem: moreover, it minimizes the Coulomb energy for the given ν value [17]. The analogy with a two-dimensional plasma [17] proves

that the states Ψ_p have constant density; since they are gapped, they describe incompressible fluids. Laughlin's wave functions are also the exact ground states of model short-range two-body potentials, the Haldane pseudo-potential [3]. These potentials encode the electron repulsion at short distance due to the Coulomb potential.

According to the Laughlin theory, the quasiholes are vortices in the incompressible fluid [3, 4], they are local deformation of the density. The wave functions with one and two quasiholes are, respectively:

$$\Psi_{p;qp}(\eta; z_1, \cdots, z_N) = \prod_{i=1}^{N} (z_i - \eta) \Psi_p(z_1, \cdots, z_N)\,, \tag{1.7}$$

$$\Psi_{p;2qp}(\eta_1, \eta_2; z_1, \cdots, z_N) = (\eta_1 - \eta_2)^{\frac{1}{m}} \prod_{i=1}^{N} \left((z_i - \eta_1)(z_i - \eta_2)\right) \Psi_p(z_1, \cdots, z_N)\,. \tag{1.8}$$

Laughlin noticed that the quasiholes have fractional charges $Q = e/p$; furthermore, and under the exchange of two of them, the wave function acquires a fractional phases $\vartheta = \pi/p$ [17]. These were the first examples of *fractionalization* of quantum numbers. The fractional charge was experimentally confirmed in shot noise experiments [18]; indications of fractional statistics have been found in interferometry experiments [19]. We will discuss these results in section 1.5.

1.2.2 Jain Series

Besides Laughlin's ones, the most stable plateaus in LLL are at filling fractions $\nu = m/(2sm \pm 1)$, with m and s two positive integers. These states were first explained by the Haldane-Halperin hierarchical construction [13, 20], that can also be understood by using effective field theory (see section 1.3 and [20]). The idea is that starting from a given filling fraction $\nu = 1/p$ quasiparticles (quasiholes) are created by changing the magnetic field. When the latter particles reach a finite density, they can condensete in a new Laughlin states of quasiparticles at $\nu_1 = 1/p_1$ for an even integer p_1. Then, the superposition of the two states creates a new incompressible Hall fluids with $\nu = 1/(p \pm \frac{1}{p_1})$; where $\pm$ stands for condensation of quasiholes and quasiparticles, respectively. This process can be iterated m times (the level of the hierarchy), therefore there can be m successive condensations of the excitations.

The Haldane-Halperin hierarchical construction produces states for too many filling fractions that are not observed. A classification of the most stable is provided by in the Jain theory [1] or by the approach proposed in [12].

According to Jain, the fractional fluids are described by IQH states, $\nu^* = m$, of *composite fermions*: these particles are composed by an electron with $2s$ elementary fluxes Φ_0 attached (an even number of fluxes is required to maintain the fermionic statistic of the composite objects). For integer filling $\nu^* = m$, the composite particles form an incompressible fluids, and are assumed to be weakly interacting. The total flux paired with the electrons is $2s\Phi_o\rho$ and is subtracted from the flux of the external field; therefore, the composite fermions are subjected to the remaining field $B^* = B - 2s\Phi_o\rho$. As a consequence, the filling fraction for composite fermions ν^* is related to that of

the original electrons by $\nu = m/(2sm+1)$; this physical picture reproduces the series of observed plateaus (similarly for negative series $\nu = m/(2sm-1)$). The presence of weakly interacting excitations subjected to a reduced magnetic field B^* has been indeed observed experimentally [3].

The Jain theory provides the expressions of the wave functions of composite electron states with and without the excitations. The ground states wave functions for $\nu = m/(2sm+1)$ are given by the products $\Psi_J = \mathcal{P}_{LLL}\Delta^{2s}\chi_m$, where χ_m are the wave functions for m completely filled LLs and $\Delta := \prod_{i<j}(z_i - z_j)$ is the Vandermonde factor describing the flux attached to each electrons. $\mathcal{P}_{LLL}$ is the projection on the LLL. The excitations can be realized by removing a composite electron in one of the filled LL described by χ_m. These excitations have minimal fractional charge $1/(2sm+1)$. More details on Jain's theory can be found in [1].

1.2.3 The Halperin states

In the Haldane-Halperin hierarchy, there are some states that are relevant for this thesis. Until now the spin was consider polarized: but, there exists same cases in which the Zeeman splitting is not large and the electron spin must be taken in account [21]; indeed non-polarized spins states have been observed [22, 23]. Spinful electrons imply double occupation of single-particles states. This is implemented by the following Halperin wave function [21], where the electrons are labelled by $\uparrow$, $\downarrow$ for the spin direction (the Gaussian factor is omitted):

$$\Psi_{m,m',n}(\{z_i^{\uparrow}\},\{\bar{z}_i{}^{\uparrow}\};\{z_i^{\downarrow}\},\{\bar{z}_i^{\downarrow}\}) = \Psi_m(\{z_i^{\uparrow}\},\{\bar{z}_i{}^{\uparrow}\})\Psi_{m'}(\{z_i^{\downarrow}\},\{\bar{z}_i{}^{\downarrow}\})\prod_{i,j}(z_i^{\uparrow}-z_j^{\downarrow})^n\,. \quad (1.9)$$

Note that the electrons with opposite spins are coupled by the third factor. The filling fraction for this states is $\nu = \frac{m+m'-2n}{mm'-n^2}$. The spin-singlet cases are recovered for $m = m' = n+1$; m must be an even integer to satisfy the Pauli principle. In these cases the numbers $N^{\uparrow}$, $N^{\downarrow}$ of electrons with opposite spin are the same. The excitations in these fluids are considered in section 2.5.1.

1.2.4 Second Landau level

Moore-Read State

For all the observed plateaus in the LLL, the values of ν have odd integer denominators. In the second LL (SLL) the observation of one plateau at $\nu = 5/2$ [24] suggests the possibility of new phenomena associated to even-denominator fillings. Other even denominator Hall states are also found [25]. Although the nature of $\nu = 5/2$ state is not completely established [26], we shall discuss the best-known proposal by Moore and Read of a spin-polarized state [4]: for $\nu = 2 + 1/2$ the LLL is completely full with electrons with opposite spin, while the second LL is supposed to be half filled and spin polarized.

This plateau cannot be explained by the previous theories, since the odd denominator is a consequences of the fermionic statistics of the fundamental degrees of freedom.

The even denominator suggests that the Hall state is realized by a fluid of bosons, that could be Cooper pairs [27]. Following Jain's proposal, the strongly interacting gas of electrons in the half-filled level can be mapped into a gas of composite fermions (one electron plus 2 quantum fluxes) at $B^* = 0$. At low temperature and within a parameter range, the lowest ground state of weakly-interacting composite fermions can be a condensate of Cooper pairs, where the attractive interactions could be generated by the mediations of electrons in the LLL. Since the electrons are spin polarized, the condensate must be a $p-$wave superconductor [28]. This is the physical picture that supports the $p-$wave superconductor as the microscopic theory for $\nu = 5/2$.

The $p-$wave superconductor in 2D space dimension reveals interesting features. The Hamiltonian can be diagonalized by Bogoliubov transformation of the fermionic creation and annihilation operators [27, 28], as follows:

$$\hat{H}_{BCS} = \sum_{\mathbf{k}} \left[\xi_{\mathbf{k}} c^\dagger_{\mathbf{k}} c_{\mathbf{k}} + \frac{1}{2} \left(\Delta^*_{\mathbf{k}} c_{-\mathbf{k}} c_{\mathbf{k}} + \Delta_{\mathbf{k}} c^\dagger_{\mathbf{k}} c^\dagger_{-\mathbf{k}} \right) \right] , \quad \begin{array}{l} \alpha_{\mathbf{k}} = u_{\mathbf{k}} c_{\mathbf{k}} - v_{\mathbf{k}} c^\dagger_{-\mathbf{k}}, \\ \alpha^\dagger_{\mathbf{k}} = u^*_{\mathbf{k}} c^\dagger_{\mathbf{k}} - v^*_{\mathbf{k}} c_{-\mathbf{k}}, \end{array} \tag{1.10}$$

where $\xi_{\mathbf{k}} = \varepsilon_{\mathbf{k}} - \mu$ and $\varepsilon_{\mathbf{k}} \simeq \mathbf{k}/(2m)$ is the single-particle kinetic energy and $\Delta_{\mathbf{k}}$ is the gap function (its dynamics is governed by a Landau-Ginsburg action, $\Delta_{\mathbf{k}} \simeq (k_x - ik_y)\Delta$ for small k); μ is a parameter of the theory not necessarily related to the chemical potential of the initial electrons. This theory have two phases: for $\mu < 0$ there is a strong-pairing phase, for $\mu > 0$ a weak-pairing phase (strong/weak-pairing indicates that the wave functions fall exponentially/polynomially when the distance between two quasiparticles grows). The wave function for even N particles is found to be:

$$\Psi(z_1, \cdots, \zeta_n) = \mathrm{Pf}\ [g(z_i - z_j)] \mapsto \mathrm{Pf}\ \left[\frac{1}{z_i - z_j} \right] , \quad \text{for } \mu > 0 \text{ and } |z_i - z_j| \gg 1 \tag{1.11}$$

where Pf is the Pfaffian [29]. The wave function depends on the values of $v_{\mathbf{k}}$ and $u_{\mathbf{k}}$, that are solutions of the Bogoliubov-de Gennes equations for this system. These parameters are two complex numbers with the condition $|v_{\mathbf{k}}|^2 + |u_{\mathbf{k}}|^2 = 1$ and are defined up to a $\mathbf{k}$-dependent common phases $e^{i\phi_{\mathbf{k}}}$. The two phases of the theory are not characterized by different symmetry; indeed the difference between them has *topological* nature: the map between the space of momenta and the space of $(u_{\mathbf{k}}, v_{\mathbf{k}})$ has different topological properties in the two phases as explained in [28] and reference therein.

Now, we will discuss the interesting features that emerge form this system when vortex and boundaries are take in account. Localized vortices, alias quasiholes, in a superconductors look like empty cylinders in the sample with n half integer quantum fluxes (say $\Phi_0/2$) at point R_i. On the edge of the cylinder, new phenomena appear [28]. In the case with N well separated non interacting vortices the gap function near R_i is $\Delta(r) \simeq \Delta(|r - R_i|)e^{i(\theta_i + \Omega_i)}$, here $\theta_i = arg(r - R_i)$ and $\Omega_j = \sum_{i \neq j} arg(r - R_j)$, Δ goes to zero for $r - R_i \mapsto 0$. For this configurations the Bogoliubov-de Gennes equations has N zero energy solutions $(u_{i,\mathbf{k}}, v^*_{i,\mathbf{k}})$, each one localized near one vortex. The corresponding operators $(\alpha_{i\mathbf{k}}, \alpha^\dagger_{i\mathbf{k}})$, obtained from these solution (1.10) are Majorana fermions $\alpha_{i\mathbf{k}} = \alpha^\dagger_{i\mathbf{k}}$. For N even these fermions can be mapped into $N/2$ Dirac fermions $A_l \equiv \alpha_l - i\alpha_{l+N/2}$. The dimension of their Hilbert space (the zero energy space of $\hat{H}_{BCS}$) grows

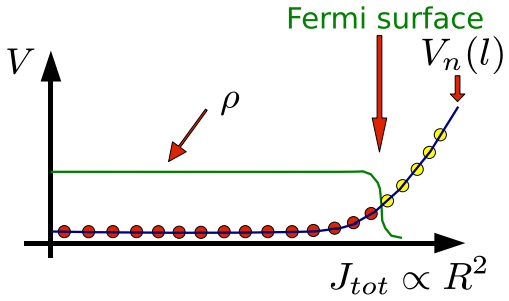

Figure 1.3: The LLL in the disc geometry: energy levels include the confining potential $V(R)$. The Fermi surface in position space is realized along the edge of the sample.

as $(\sqrt{2})^N$ and the elements of the basis can be obtained by standard construction of the Fock space of $N/2$ Dirac fermions. The vacuum $|0\rangle$ is defined as $A_l|0\rangle$ *i.e.* $\alpha_l|0\rangle = i\alpha_{l+N/2}|0\rangle \ \forall \ l$. Each operators α_i depends on all $e^{i\Omega_j}$ and they are not single values as function of R_i: if R_i moves around only the vortex in R_j $\alpha_i \mapsto -\alpha_i$ and $\alpha_j \mapsto -\alpha_j$; this transformation does not depend on the shape of the closed path of R_i and exchanges the basis elements of ground states space. The unitary representations of this monodromy is $U_{ij} = e^{\pi\alpha_i\alpha_j/2}$ and its "square root" $e^{\pm\pi\alpha_i\alpha_j/4}$ is the operations that correspond to the exchange the two vortices. It follows that, for two couples of quasiholes (i, j) and (i, l), their exchange operators do not commute. The Majorana fermions appear also in presence of edges as shown in [27].

In conclusion, the physics of the $p-$wave superconductor shows that the usual vortex excitation have an internal degree of freedom of a Majorana fermion. As a consequence, the many-vortex wave function has additional degeneracies and the exchange statistics takes places in this multidimensional space. It is described by non-commutating unitary transformations, that give rise to non-Abelian statistics in the quantum Hall effect.

It can be shown that non-Abelian statistics is not affected by local perturbations, owing to the special properties of the zero-energy subspace. Therefore, it is a topological feature as ordinary fractional statistics.

Other States second Landau Level

Behind $\nu = 5/2$, other plateaus are observed in the SLL. The state with $\nu = 2 + \frac{2}{5}$ is particular interesting for the applications to the quantum computation to be described in the following. In the next chapter, these state are discussed in the approach based on the effective field theories and conformal field theories (CFTs).

1.2.5 Edge excitations of the incompressible fluids

In the previous sections we observed that the ground states are incompressible fluids with constant density $\rho(z)$. Let us consider the integer-filling case for simplicity. The presence of the confining potential bends the Landau level energy adding a l dependent

term $V_n(l)$: $E_n \mapsto E_{n,l} = (n+1/2)\hbar\omega_c + V_n(l)$ (see Fig. 1.3). Owing to incompressibility, the potential creates a Fermi surface along the edge; the low-energy excitations are particle-holes excitations which are located at the edge of the sample and are massless and one-dimensional. Therefore the low-energy theory of the corresponding Hall fluids is the relativistic field theory of the edge excitations: these modes are the responsible for transport phenomena.

For fractional fillings, the ground states are not easy to describe. Nevertheless, the presence of a confining potential and an incompressible fluid gives rise to edge excitations whose structure can be understood by using conformal field theory, as explained in the following chapters.

The excitations in the bulk are localized deformations of the density, they are charged (with charge $qe/\hat{p}$, $q \in \mathbb{Z}$) and gapped (the gap Δ is of the order of the Coulomb self energy $\Delta \simeq \frac{(qe)^2}{\hat{p}^2}\frac{1}{\ell_B^2}$). The deformation of the density due to a bulk quasiholes is compensate by a change at the edge, due to the constant-density condition, leading to a charge excitations at the edge. Therefore, from the edges all the excitation can be analyzed, both the gapless on the edge and the gapped in the bulk.

1.3 Chern-Simons theory

In section 1.2 we observed that the excitations in quantum Hall fluids have fractional statistics. Moreover we remarked the importance of effective field theory descriptions. This section introduces the effective field theory for these states and show how such excitations can be realized in this framework. The main mechanism to produce statistics transmutation is by magnetic field attachment [11, 30, 31, 32].

Let's consider an impenetrable ultra-thin solenoid perpendicular to the plain placed at the point x_0, that contains a flux Φ . It induces a vector potential $\mathbf{a}$ on the plane, with magnetic field vanishing outside the solenoid. If particles with charges q move on the path γ that encircles the flux l times, its wave function acquires the phases $\frac{q}{c\hbar}\oint \mathbf{a}\cdot d\ell = l\frac{q\Phi}{c\hbar} =: l\vartheta$. This is the Aharonov-Bohm effect. This phases is called a *topological phase*, and is *topological protected* from local perturbation, since it depends only on the topological properties of the path, *i.e.* the winding number l, but not on its shape. The presence of the flux does not change the energy of the particles.

Let's now consider composite objects built by charge q and flux Φ; the Aharonov-Bohm effect produces an additional phase factor ϑ when two of them are exchanged. This phase shift is equivalent to a transmutation of the statistics. At the same time the flux-charge attachment gives rise to a change in angular momenta in such a way that the spin-statistics relation holds [32, 33]. In particular, composite particles with fractional charge $e^*$and flux Φ_0 have fractional statistics.

In 2D systems, quasiparticles with fractional charge are clearly non-perturbative states, that involve $N \mapsto \infty$ microscopic (fermionic) degrees of freedom. It is very difficult to built a microscopic theory for this phenomena, but it is possible to describe them by using effective field theories, that are valid in the low-energy, long-range limit.

The realization of flux-charge attachment in effective field theory is obtained by

using the Chern-Simons (CS) action as follows [2, 20, 31]. A system of charged particles can be described by its conserved matter current j_μ. In two space dimension this current is dual to a gauge fields $\mathbf{a}_\mu$ (different from the external electromagnetic field) such that $j_\mu = \frac{1}{2\pi}\epsilon_{\mu\nu\rho}\partial^\nu \mathbf{a}^\rho$. In the hydrodynamical approach to Hall fluids, j_μ is the density current that describes the low-energy effective degrees of freedom [2, 20]. On the plane, a possible action for gauge field $\mathbf{a}_\mu$ is the Chern-Simons term, that is more relevant (in renormalization-group sense) of the Maxwell term, and naturally occurs in systems without parity and time reversal symmetries such as QHE. For m fluids $\mathbf{a}_{I\mu}$, $I = 1, \cdots, m$, coupled to each other by an integer matrix K_{IJ} and in presence of non-dynamical and external currents $J^s_{I\ \mu}$, the multi-component Abelian Chern-Simons effective theory reads:

$$S = \int_{\mathcal{M}} \left(\frac{1}{4\pi} K_{IJ} \mathbf{a}_{I\mu} \partial_\nu \mathbf{a}_{J\mu} \epsilon^{\mu\nu\rho} + \frac{e}{2\pi} A_\mu t_I \partial_\nu \mathbf{a}_{I\mu} \epsilon^{\mu\nu\rho} + \mathbf{a}_{I\mu} J^s_{I\ \mu} \right) , \tag{1.12}$$

where A_μ is the external electromagnetic field and t_I are the electric charges of $\mathbf{a}_{I\mu}$. The Chern-Simons theory is a topological theory and its Hamiltonian vanishes. It does not introduce propagating degrees of freedom in $2+1$ dimension, as *e.g.* the Maxwell theory, but describes topological effects as follows.

Solving the equations of motion for the field $\mathbf{a}_\mu$ in presence of a point-like static charge $J^s_0 = l\delta(x - x_0)$ gives the charge-field attachment $j_0 = \frac{et}{2\pi k} B + \frac{q}{k} J^s_0$ (this is the expression for only one field $\mathbf{a}_\mu$). In the general case, the filling fractions, the charge and the statistics of the quasiparticles take the following values:

$$\nu = \sum_{I,J} t_I K^{-1}_{I,J} t_J \,, \qquad q = \sum_{I,J} t_I K^{-1}_{I,J} l_J \qquad \text{and} \qquad \vartheta = \pi \sum_{I,J} l_I K^{-1}_{I,J} l_J \,. \tag{1.13}$$

The currents J^s_I are the sources of the fields $\mathbf{a}_I$ and describe static quasiparticles.

The parameters in the action (m, t_I, l_I and K_{IJ}) depend on the topological fluid that is considered. In the Haldane-Halperin hierarchical fluids, m is the level of the hierarchy. For the Laughlin series, $m = t = 1$ and $K = p$, and the quasiparticle with smallest charge has $l = 1$. The Jain series is described by m equal gauge fields (dual to m conserved matter currents j^μ_I which represent the edge degrees of freedom of the m LLs of composite fermions): the parameters is (1.13) are $K_{I,J} = \pm\delta_{I,J} + 2sC_{I,J}$ and $t_I = 1$, with $C_{I,J} = 1\ \forall\ I,\ J$ in a specific basis [12]. Finally, for the spin singlet states (1.9) the matrix K and t read:

$$K = \begin{pmatrix} m & n \\ n & m' \end{pmatrix} , \qquad\qquad t = (1,1) \,. \tag{1.14}$$

For all these cases the values of ν, q and ϑ in (1.13) reproduce the values obtained from the approach through the wave functions outline in the previous section.

This analysis suggests a non-Abelian generalization of (1.12), that would describes the so-called non-Abelian anyons as those occurring in the Moore-Read theory. The non-Abelian Chern-Simons action is [34, 35]:

$$S = \int_{\mathcal{M}} \mathrm{Tr} \left[\frac{k}{4\pi} \left(\mathbf{a} \wedge \mathrm{d}\mathbf{a} + \frac{2}{3} \mathbf{a} \wedge \mathbf{a} \wedge \mathbf{a} \right) + J^s \cdot \mathbf{a} \right] . \tag{1.15}$$

The field $\mathbf{a}$ is a gauge field in a lie algebra $\mathfrak{g}$ and k is the level of the theory. This gauge field theory induces a Aharonov-Bohm phases with matrix values [30] acting on a multiplet of degenerate excitations. The actions (1.12) and (1.15) have interesting common features [20, 34, 35]. They only depend on the topology of the space time (for this reasons they are called topological fields theories). Gauge invariance of the partition function on closed manifolds $\mathcal{M}$, imposes the quantization of the coupling $k \in \mathbb{Z}$; such condition also extended to $K_{I,J}$ in the Abelian case [2, 20]. Even though the Hamiltonian is zero, the dynamics is non trivial for the Manifolds $\mathcal{M}$ with boundaries and with higher genus [36].

1.4 Braiding and Anyons

The last two sections presented examples of excitations with fractional statistics: here a more general argument based on the path integral is presented.

Let's consider a system with N identical particles, living on a manifold $\mathcal{M}$. Their configurations is a point in the manifold * $(\mathcal{M}^N - \Delta)/S_N$. The path-integral amplitude between the configuration X at time t and X' at time t' involves the sum on all the possible paths $(X(t))$ connecting the two configurations. The sum can be splitted as follows ($\mathbf{A}$ is the set of all the paths between initial and final configurations):

$$K(X', t', X, t) = \int_{X(t)\in\mathbf{A}} e^{iS[X(t)]}\mathcal{D}X(t) = \sum_{\gamma} \lambda(\gamma) \int_{X(t)\in\mathbf{A}_\gamma} e^{iS[X(t)]}\mathcal{D}X(t)\,, \qquad (1.16)$$

the path integral is decomposed in contributions from the different homotopy classes of paths $\mathbf{A}_\gamma$. The sets of all equivalence class of closed path and the composition of path give rise to the fundamental homotopy group of $(\mathcal{M}^N - \Delta)/S_N$, $\pi_1\left((\mathcal{M}^N - \Delta)/S_N\right)$ [32, 30] . The factors $\lambda(\gamma)$ are pure quantum effects, that weight differently paths in different homotopy class and cannot emerge from the classical limit. In order to define the quantum evolution, it is necessary to define the action of the fundamental group: this is equivalent to assign the values of $\lambda(\gamma)$ for each class of paths. The quantization procedure forces the wave functions to be a representations π_1 [32, 30].

In the path integral formulation of the problem presented at the beginning of section 1.3, the subsets of paths are labelled by the winding number l ($\mathbf{A}_\gamma = \mathbf{A}_l$) and the corresponding Aharonov-Bohm phases fix the factors $\lambda(\gamma)$.

The homotopy group π_1 of configuration space in three or higher dimensional varieties $\mathcal{M}$ is isomorphic to the permutation group of N objects (S_N) [30, 37]. Since the paths can avoid the point particles by going in the extra dimensions, paths of double exchange of two particles (σ^2) are homotopically equivalent to the trivial path; the possible eigenvalues of the exchange operators (σ) are ± 1. In such cases there are only two possible representations, symmetric (bosons) and anti-symmetric (fermions) under the exchange of two particles [32].

*The configuration space is $\mathcal{M}^N$ minus Δ (the sub-set of $\mathcal{M}^N$ where at least two particles are at the same position), modulus the permutation group S_N (the particles are indistinguishable). The points in Δ must be subtracted from configurations space [32].

The fundamental group of the configuration space in two dimensions is isomorphic to the braid group of N object $\mathcal{B}_N$ [37]; the generators of $\mathcal{B}_N$ are σ_i, which exchange the particle i-th with the $(i+1)$-th counterclockwise they satisfy the Yang Baxter relations ($[\sigma_i, \sigma_j] = 0$ iff $|i-j| > 1$ and $\sigma_i\sigma_{i+1}\sigma_i = \sigma_{1+i}\sigma_i\sigma_{i+1}$). The double exchange σ_i^2 is different from the identity path, thus $\mathcal{B}_N$ are infinite groups and they admit representations of two types [30, 33]: one dimensional and higher dimensional representations. For the former type, σ_i acts on the wave function Ψ of the system as follows:

$$B[\sigma_i]\Psi(r_1, \cdots, r_i, r_{i+1}, \cdots) = e^{i\vartheta_i}\Psi(r_1, \cdots, r_{i+1}, r_i, \cdots)\,. \tag{1.17}$$

These representations are Abelian, i.e. the result of two exchanges of particles does not depend on the order of the exchange, they are labeled by a real number ϑ. Bose-Einstein/Fermi-Dirac statistics are recovered for $\vartheta = 0,\ \pi$, respectively. Particles carrying representations with $\vartheta \neq 0, \pi$ are called anyons [32, 33]. Usually, in these cases, the ground state of the system is non degenerate (if the genus of $\mathcal{M}$ is zero).

Higher-dimensional representations require degenerate states for fixed positions, total spin and the other quantum numbers of the particles. The wave functions are vector multiplets whose label is a new index, a non-Abelian quantum number. Suppose that $\Psi_\alpha(r_1, \cdots, r_N)$, with $\alpha = 0 \cdots \mathtt{D}$ are the elements of the basis of the vector space. The braiding acts on this space as follows:

$$B[\sigma_i]\left(\Psi_\alpha(r_1, \cdots, r_i, r_{i+1}, \cdots)\right) = \sum_{\beta=1}^{\mathtt{D}} [B_i]_{\alpha\beta}\Psi_\beta(r_1, \cdots, r_{i+1}, r_i, \cdots)\,, \tag{1.18}$$

where $\mathtt{D}$ is the degeneracy of the states and depends on N and on the type of anyons considered. The $[B_i]_{\alpha\beta}$ are unitary $\mathtt{D}\times\mathtt{D}$ matrices and the product of two of them can be non-commutative; the particles are called non-Abelian anyons and satisfy non-Abelian statistics [30, 33]. Transformations under exchange of particles are properties of the whole wave functions and not of the single particles.

Bulk excitations on the ground states (far from the boundary) are supposed to have a gap Δ: a gapful spectrum protects the ground state from the spontaneous creations of excitations and thermal activations of excitations is suppressed by a factor $e^{-\Delta/(k_B T)}$. Therefore the only low-energy perturbations of the systems are the braidings [30]. Systems with low energy excitations that are Anyons are said to be in a *topological phase of matter* [30]. Effective field theories for these systems are topological field theories, as discussed in section 1.3. In reals systems of size L, the topological invariance can be broken by terms proportional to $\mathcal{O}\left(e^{-\Delta/T}\right)$ and $\mathcal{O}\left(e^{-L/\xi}\right)$.

1.4.1 Quantum Computations with non-Abelian anyons

Quantum Computation [38] is one of the main challenges for contemporary physics: its aim is to store and elaborate informations by using quantum systems and quantum mechanical processing. At first advocated by Feynman [39], it is potentially much more powerful than classical computation [38]. The basic idea is to store information in q-bits (a Hilbert space of dimension two) and elaborate them by quantum circuits; these

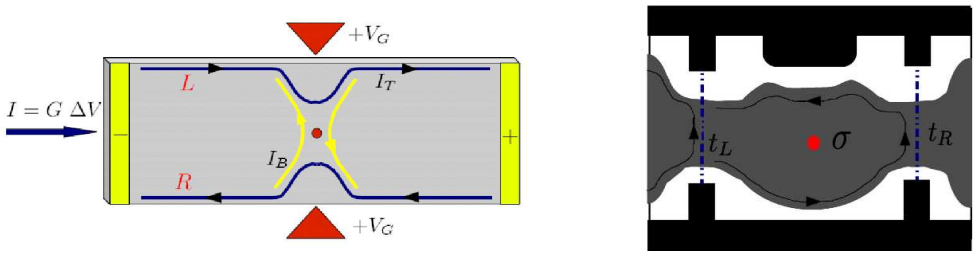

Figure 1.4: Left: shot noise experimental set up. The fluid is squeezed at in one point by a static potential V_G. The point contact introduces an finite inter-edge tunneling amplitude function of V_G. Right: the quantum Hall Fabry-Perot interferometer realized by two constrictions. The electron fluid is represented in the weak backscattering limit.

are sequences of unitary operators acting on the Hilbert space of n q-bits given by the evolution of the quantum state. At the end, the measurement of the state should be specified. These three points are the DiVincenzo criteria.

In order to develop the possible circuits, it is necessary to realize generic transformations of $U(2^n)$, the unitary group of n q-bits. When this is possible, we have an *universal quantum computer*. Every unitary operator in the space of n q-bits can be decomposed into single q-bit gates (elements of $U(2)$) and one two q-bit gate called Controlled-NOT (CNOT) gate that creates entanglement between them [38].

Local errors, thermal noise and decoherence are the main problems in realizing a Quantum Computer. The problem of decoherence could be solved by the so-called Topological Quantum Computations (TQC); in this scheme q-bits are realized by non-Abelian anyons systems and unitary operators are obtained by braiding of Anyons [30, 33]. The advantage in the use of TQC is that informations are stored in the whole wave function of the systems and unitary operators are topologically protected. Both of them are insensitive to local perturbations. Notice that non-Abelianity is required for quantum computations, since one needs unitary transformations complicated enough to allow universal quantum computations. Abelian anyons are insufficient to achieve quantum computations since the wave functions are scalar. The simplest anyons that support Universal quantum computations are the so called Fibonacci anyons [40, 41]; they will be introduced latter in the thesis.

1.5 Experiments of fractional charge and statistics

1.5.1 Measure of the fractional charge by shot noise

In fractional Hall states, the edge excitations flow chirally along the edge and have fractional charges (see [4] and sections 1.2.5). Let us discuss the experiment of tunneling between two edges of a Hall bar as shown in Fig. 1.4. Without the point contact the tunneling is zero and the Hall current is quantized; the presence of the point contact introduces an finite intra-edge tunneling. In the weak-constriction regime, the tunneling

of quasiparticles with smaller fractional charge is dominant. The current I_B between the two edge (L and R) at different chemical potential in this regime is governed by a Poisson process. Indeed the tunneling of charge carriers are rare. At very low temperature, thermal noise is suppressed and there is the shot noise S_I, *i.e.* the quadratic fluctuations of the current due to the discrete nature of the process. By Poisson statistics, the variance of the number of tunneling particles is proportional to the mean value and one finds $S_I \equiv \langle|\delta I(\omega')|^2\rangle|_{w=0} = e^* I$; this determined the charge e^* of the carriers (for more details see [42]). The experimental results support the fractionalization of the charge in Hall states in the Laughlin series [43], $e^* = \frac{e}{p}$ for $\nu = \frac{1}{p}$, and other states, including those in the second LL to be described latter.

1.5.2 Fabry-Perot interferometer

As observed before, fractional-charge excitations also have fractional statistics, within the CS effective field theory approach; therefore the observation of fractional charge is an indication of fractional statistics [30, 33]. A direct observation of fractional statistics should consist in the measure of the phases that the wave function accumulates when one particle encircles another.

Experimental tests of braiding properties are given by interferometric experiments. In the following, we briefly discuss the Fabry-Perot geometry [4, 30, 44]. Another possibility is the Mach-Zehnder interferometer discussed in [4] and the references therein.

In the QH version of the Fabry-Perot Interferometer (see Fig. 1.4, right side) the quasiparticles moving along the upper and lower edges can tunnel between the two edges at the two constrictions R and L with tunneling amplitudes $t_{L/R}$. The tunneling current leads to a fluctuation of the longitudinal conductance σ_{xx}. The probability that the edges modes move from the down-left to the top-left corners is a measure of the braiding between the N_{qp} particles in the bulk (σ in the picture) and the particles that moves on the edge. This probability is given, at lowest order in the amplitudes, by the sum of the contributions of the two possible paths [44, 45],

$$\sigma_{xx} \propto |(t_L U_L + t_R U_R)|\Psi\rangle|^2 = |t_L|^2 + |t_R|^2 + 2\mathrm{Re}\left(e^{i\alpha} t_L^* t_R \langle\Psi|M_{\text{edge bulk}}|\Psi\rangle\right) , \quad (1.19)$$

where $|\Psi\rangle$ is the states of the current at the initial point, $e^{i\alpha}$ is the Abelian Aharonov-Bohm phases due to the external magnetic field and $M_{\text{edge bulk}} = U_L^{-1} U_R$ is the unitary operation that represents the braiding between the particle travelling along the edge and that in the bulk. For weak tunneling, the dominant (most relevant) tunneling is done by the quasiparticle with smallest fractional charge in the theory; moreover, multiple windings are suppressed.

For Abelian states, the braiding effect, *i.e.* the last term in (1.19), is proportional to:

$$2|t_L^* t_R| \cos 2\pi\nu \left(\frac{\Phi}{\Phi_0} - N_{qp}\right) . \quad (1.20)$$

The first contribution is the the Aharonov-Bohm phases due to the field, the second is the monodromy of the quasiparticle on the edge with N_{qp} bulk quasiparticles (with charge νe). The charge of particles on the edge can be measured from the modulation

of σ_{xx} as function Φ; the fractional statistics is also obtained by varying $N_{qp} \mapsto N_{qp} + 1$ *i*.e. by creating quasiparticle in the bulk.

For non-Abelian anyons, the braiding acts in non trivial way on the degenerate wave functions $|\Psi_a\rangle$: $\langle\Psi_a|M_{\text{edge bulk}}|\Psi_b\rangle = M_{ab}$ describes how these states change with braiding. This matrix elements can be calculated by using RCFT techniques [44], and the results is:

$$M_{\sigma,b} = \frac{\mathcal{S}_{\sigma,b}\mathcal{S}_{I,I}}{\mathcal{S}_{b,I}\mathcal{S}_{\sigma,I}}\,, \tag{1.21}$$

where σ indicates the total quasiparticle in the bulk, b the particle moving on the edge and $\mathcal{S}$ is the modular transformation matrix. These quantities will be introduced in the next chapter. For the Moore-Read state at $\nu = 5/2$, $M_{\sigma,b}$ is zero for odd number of quasiparticles in the bulk; this effect could have been observed in experiments [46]. The study of quantities that indirectly measure fractional statistics and non-Abelian fractional statistics will be the main point of this thesis.

Chapter 2

Conformal field theory descriptions of quantum Hall states

In this chapter, conformal field theories (CFT) are presented together with the rational ones (RCFT), that posses a finite number of basic excitations. Then, partition functions on the torus will be discussed and their invariance under modular transformation will be analyzed. Extensive introductions on CFT can be found in [47, 48]. Here, we recall some basic definitions, and the key elements for this work: the modular invariant partition functions and the properties that can be derived from them.

Conformal Field Theories in two space-time dimensions have been intensively developed since the mid eighties, and their important physical applications includes critical behavior in statistical mechanics [48], solid state physics in low dimension [11] and the world-sheet description of string theory [49]. Furthermore, their deep algebraic structures and their connections with many domains of mathematics make them outstanding laboratories of new techniques and ideas [50]. For this thesis, the most interesting topic is the relation between RCFTs and Chern-Simons theories and its application to the description of anyons systems; these relations are introduced in sections 2.4 and 2.3 respectively.

The connection between Quantum Hall fluids and the holomorphic part of RCFTs permits to apply the algebraic methods of these theories. The relation is twofold: since the effective field theory for bulk excitations is a Chern-Simons theory [2, 20], the wave functions of the systems are described by the conformal blocks of the corresponding RCFT; furthermore, the low-energy excitations at the edge are described by the same RCFT. These two connections, based on Witten's fundamental works [34, 35], describes both the braidings properties of the bulk excitations and the edge modes that are responsible for the transport properties in QHE samples. The CFT analysis will be compared with experimental data in chapter 4.

2.1 Operators Algebra

One basic element of CFT is the existence of a numerable basis of local fields $\{\Phi_\Delta(x)\}$, that are eigenvectors of the dilatation operator $\Phi_\Delta(x) = \lambda^\Delta \Phi_\Delta(\lambda x)$, where Δ is the scaling dimensions of the $\Phi_\Delta(x)$. In CFT, the natural coordinates in the plane are complex: $z = x + iy$ and $\overline{z} = x - iy$; they are considered independent until the reality conditions are imposed at the end of the calculations [47]. The conformal transformations are the analytic coordinate transformations $z \mapsto f(z)$. At critical points, all fields $\Phi(z, \bar{z})$ are factorized in holomorphic and anti-holomorphic (called chiral and anti-chiral respectively) parts: $\Phi(z, \overline{z}) = \phi(z)\overline{\phi}(\bar{z})$. The fields obeying the following transformation law under conformal transformations,

$$\Phi_\Delta(z, \bar{z}) = (\partial_z(f(z))^h \left(\partial_{\bar{z}} \bar{f}(\bar{z})\right)^{\bar{h}} \Phi_\Delta(f(z), \bar{f}(\bar{z}))\,, \tag{2.1}$$

are called primary fields. Here h and $\bar{h}$ are the conformal dimensions, that are related to the scaling dimension by $\Delta = h + \bar{h}$. Primary fields acquire the phase $e^{2i\pi(h-\bar{h})}$ under the rotations of 2π of the plane; therefore the conformal spin of Φ_Δ is $s = h - \bar{h}$.

The stress energy tensor is the generator of the conformal transformation: it has two components $T(z)$ and $\overline{T}(\bar{z})$, that are analytic and anti-analytic respectively; their Laurent's expansions are,

$$T(z) = \sum_{n\in\mathbb{Z}} z^{-n-2} L_n\,, \qquad\qquad \overline{T}(\bar{z}) = \sum_{n\in\mathbb{Z}} \bar{z}^{-n-2} \bar{L}_n\,. \tag{2.2}$$

The operators product expansion (OPE) between two stress tensors, is determined by dimension of T and the conformal invariance symmetry; its form is,

$$T(z)T(w) = \frac{c/2}{(z-w)^4} + \frac{2T(w)}{(z-w)^2} + \frac{\partial T(w)}{(z-w)} + \text{regular terms}\,. \tag{2.3}$$

Here, c is the central charge (also called conformal anomaly); it is a positive real number, since $\langle T(z)T(w)\rangle = \frac{c/2}{(z-w)^4}$. The TT OPE is equivalent to the commutation relation of the modes L_n:

$$[L_n, L_m] = (n-m)L_{n+m} + \frac{c}{12}(n^3 - n)\delta_{n+m,0}\,. \tag{2.4}$$

These commutation relations define the Virasoro algebra, that is characterized by the values of central charge c. CFTs possess the symmetry algebra Vir $\times$ $\overline{\text{Vir}}$ where Vir ($\overline{\text{Vir}}$) is the holomorphic (anti-holomorphic) Virasoro algebra with generators L_n ($\overline{\mathrm{L}}_n$) [47, 48, 51]. The theory is characterized by a set of representations of the Virasoro algebra that are one to one relations with the primary fields.

For $c \geq 1$, RCFTs have an extended symmetry algebra that includes Virasoro. One class of extended algebras are the Affine algebras $\widehat{\mathfrak{g}} \times \overline{\widehat{\mathfrak{g}}}$, generalization of the simple Lie algebra $\mathfrak{g}$. The generators of an Affine algebra are the conserved currents $J^a(z)$ and $\overline{J}^a(\overline{z})$; their OPEs is:

$$J^a(z)J^b(w) = \frac{\delta^{ab}k}{(z-w)^2} + \sum_c i f_c^{ab} \frac{J^c(w)}{z-w}\,. \tag{2.5}$$

The structure constants of $\mathfrak{g}$ are f_c^{ab} and k is the level of the algebra. Upon inserting the Laurent expansion of the current $J^a(z) = \sum_n J_n^a(z) z^{-n-1}$ into the OPE, the commutation relations of the Affine algebra $\widehat{\mathfrak{g}}$ as follows:

$$[J_n^a, J_m^b] = \sum_c i f_c^{ab} J_{n+m}^c + kn\delta_{n+m,0} \qquad \text{and} \qquad [J_n^a, \overline{J}_m^b] = 0\,. \tag{2.6}$$

From the Sugawara construction, one obtains the Virasoro algebra embedded in $\widehat{\mathfrak{g}}_k$. The central charge is function of the $\widehat{\mathfrak{g}}_k$ data and reads $c = k\dim(\mathfrak{g})/(k+g)$, where $\dim(\mathfrak{g})$ and g are the dimension of the Lie algebra and the dual Coxter number, respectively (for $\mathfrak{g} = SU(2)$ and $SU(3)$ $dim(\mathfrak{g}) = 2,\ 8$ and $g = 2,\ 3$ respectively). The prototype of field theory with Affine symmetry algebra $\widehat{\mathfrak{g}} \times \overline{\widehat{\mathfrak{g}}}$ is the Wess-Zumino-Witten model [47]: its action is,

$$S^{WZW} = \frac{k}{16\pi} \int d^2 z \mathrm{Tr}(\partial^\mu \mathfrak{g}^{-1} \partial^\mu \mathfrak{g}) + k\Gamma; \tag{2.7}$$

here $\mathfrak{g} = \mathfrak{g}(z, \bar{z})$ is a matrix field with values in $\mathfrak{g}$ and Γ is the Wess-Zumino term. In these models $J(z) = -k(\partial \mathfrak{g})\mathfrak{g}^{-1}$ and $\overline{J}(\overline{z}) = -k\mathfrak{g}^{-1}\overline{\partial}\mathfrak{g}$. For more details see [47].

In this thesis, the relevant CFT have Affine algebras $\widehat{\mathfrak{g}} = \widehat{U(1)},\ \widehat{SU(m)}_k$; furthermore, the parafermionic CFTs are obtained by coset construction of Affine algebras; in particular, $\widehat{\mathfrak{g}}/\widehat{\mathfrak{h}} = \widehat{SU(2)}_k/\widehat{U(1)}^2$, $\widehat{SU(3)}_k/\widehat{U(1)}^2$ [47, 51, 52].

Primary fields are eigenvectors of the Casimirs of the algebra (L_0 for Vir and L_0 and α_0 for $\widehat{U(1)}$); in the case of the Virasoro algebra, we have: $L_0\Phi = h\Phi$ and $\overline{L}_0\Phi = \bar{h}\Phi$. The descendant fields are obtained by successive actions of the generators of the algebra on the primary fields Φ_Δ, for Virasoro algebra:

$$\Phi_{(\{n_i\},\{\bar{n}\}_{j=1\cdots\bar{K}}),\Delta} = L_{n_1} \cdots L_{n_K} \overline{L}_{\bar{n}_1} \cdots \overline{L}_{\bar{n}_{\bar{K}}} \Phi_\Delta\,, \quad n_1 \le n_2 \le n_3 \cdots, \bar{n}_1 \le \bar{n}_2 \cdots\,. \tag{2.8}$$

Similarly descendant fields for Affine algebras are obtained by applying both J_n^a and L_m on Φ_λ, the primary fields labeled by the weights λ of $\mathfrak{g}$. Each primary field and its descendants form a representation of the algebra, denoted by $[\Phi_\lambda]$; the primary field is the highest-weight state. Since all quantities split into holomorphic - anti-holomorphic parts, we will discuss only the holomorphic part.

The OPE of two primary fields ϕ_ν and ϕ_μ can be written:

$$\phi_\nu(z_\nu)\phi_\mu(0) = \sum_\lambda \frac{C_{\nu\mu\lambda}}{z_\nu^{h_\nu + h_\mu - h_\lambda}} \phi_\lambda(0) + \text{descendants contributions}\,, \tag{2.9}$$

where h_λ are the conformal dimensions of ϕ_λ. The coefficients $C_{\nu\mu\lambda}$ are called structure constants. Eq. (2.9) has a clear physical meaning: the composite operator $\phi_\nu\phi_\mu$ is equal to the linear combination of fields on the right side. The set of primary fields in a theory is supposed to form a closed algebra under OPE, thus ensuring the completeness of the excitations of the theory. The identity field I is labeled by $\lambda = 1$; it has vanishing conformal dimension and $C_{1\mu\lambda} = \delta_{\lambda\mu}$. By definition, in a RCFT the number of primary fields, *i.e.* of the irreducible representations of the Affine algebra, is finite, as further discussed in section 2.2.2.

2.2 Partition Functions of CFT

The thermodynamic properties of physical systems at equilibrium are encoded in the (grand canonical) partition function [53]. For one-dimensional quantum systems defined on a circle of radius R with periodic boundary conditions [48, 53], the partition function is:

$$Z = \mathrm{Tr}_{\mathcal{H}} \left[e^{i\Delta X \hat{P}} e^{-\beta(\hat{H}-\mu\hat{N})} \right] , \tag{2.10}$$

where $\hat{P}$, $\hat{H}$ and $\hat{N}$ are the momentum, energy and number operators, respectively, and the trace in (2.10) is on the Hilbert space. In the definition of the grand canonical partition function, it is useful to add a non vanishing spatial translation ΔX; the usual expressions of Z is recovered for $\Delta X = 0$.

If the system is conformal invariant at low energies, the algebraic properties of CFT can be applied for computing of Z. The Hilbert space (holomorphic and antiholomorphic parts) is organized in highest-weight representations $[\phi_\lambda]$ of the (maximal extended) symmetry algebra $\widehat{\mathfrak{g}} \times \bar{\widehat{\mathfrak{g}}}$ (Virasoro algebra, $\widehat{U(1)}$ Affine algebra, W-algebra etc.) [47, 48, 54]. The physical properties of the systems determine the symmetry algebra, for example that of free massless bosons is $\widehat{\mathfrak{g}} = \widehat{U(1)}$ and the highest-weights correspond to the fractional charge [47, 48]. The Hilbert space decomposition is:

$$\mathcal{H} = \bigoplus_{\lambda,\bar{\lambda}} \mathcal{N}_{(\lambda,\bar{\lambda})\in P^k \times P^k} [\phi_\lambda] \otimes [\bar{\phi}_{\bar{\lambda}}] , \tag{2.11}$$

where P^k is the set of label of primary fields. The multiplicities $\mathcal{N}_{\lambda,\bar{\lambda}}$ count the number of times that a pairs of $\widehat{\mathfrak{g}}\times\bar{\widehat{\mathfrak{g}}}$ representations, *i.e.* a sector, appears in the theory and they will be determined by consistency conditions in the following; the $\mathcal{N}$ are non-negative integer and symmetric matrices. For rational CFTs the number of highest weights is finite and these matrices have finite size.

Eq. (2.10) can be rewritten as follows [47, 48]:

$$Z(\tau,\zeta) = \mathrm{Tr} \left[q^{L_0 - c/24} \bar{q}^{\bar{L}_0 - c/24} w^{Q_L} \bar{w}^{Q_R} \right] , \tag{2.12}$$

where $q = e^{2\pi i \tau}$, $w = e^{2\pi i \zeta}$; τ and ζ will be defined latter. $\hat{H}$ and $\hat{P}$ are expressed through L_0 and $\bar{L}_0$: $\hat{H} = L_0 + \bar{L}_0 - c/12$ and $\hat{P} = L_0 - \bar{L}_0$. $\hat{H}$ also includes the Casimir energy proportional to the Virasoro central charge c [47]. The operators Q_L and Q_R are other Casimir operators of the algebras; their choice depends on the system that is considered. For massless free bosons, the so-called chiral Luttinger liquid, $\widehat{\mathfrak{g}} = \widehat{U(1)}$ and the Casimirs are L_0 and α_0; thus, $Q_L = \alpha_0$ and $Q_R = \bar{\alpha}_0$ whose eigenvalues are the values of the charge, the primary field being labelled by the fractional charge $\lambda = a$. In the relativistic domain, where pairs of excitations can be created form the ground state, the number operator $\hat{N}$ is not well defined and the charge Q is used in the grand canonical partition function.

Moving from operator to path-integral formalisms, equations (2.10) and (2.12) become path-integrals on the doubly periodic geometry of the torus [29]: the torus is composed of a spatial circle of length R and a imaginary-time circle of length β for the

temperature. Scale invariance implies that the expression (2.12) only depends on the ratio of periods, the so-called modular parameter τ. The complete identification of the complex parameters τ and ζ is:

$$\tau = \frac{\Delta x}{2\pi R} + i\frac{\beta}{2\pi R}\,, \qquad \zeta = \frac{\beta V_0}{2\pi R} + i\frac{\beta\mu}{2\pi R}\,. \tag{2.13}$$

The real part ΔX in τ introduces a twist in the time periodic boundary condition; V_0 is the electric potential coupled with the charge.

Since the Hilbert space is decomposed in representations (2.11), the trace in (2.12) can be reduced to the sum of characters $\theta_\lambda(\tau,\zeta)$ [47] of these representations, as follows:

$$\theta_\lambda(\tau,\zeta) = \mathrm{Tr}_{[\phi_\lambda]} e^{2\pi\tau(L_0 - c/24)} w^{Q_L}\,, \tag{2.14}$$

$$Z(\tau,\zeta) = \sum_{\lambda,\lambda' \in P^k \times P^k} \mathcal{N}_{\lambda,\lambda'} \theta_\lambda(\tau,\zeta)\bar{\theta}_{\lambda'}(\bar{\tau},\bar{\zeta})\,. \tag{2.15}$$

The partition functions has been rewritten as the sum over different sectors, that are in finite number for RCFT. In each sector in (2.14), all the descendants of the corresponding primary fields contribute. The characters θ_λ are known functions and they encoded all the informations of the representations. The sum in the definition of the characters (2.14) converges for $\mathrm{Im}\tau = \frac{\beta}{2\pi R} > 0$, that is naturally satisfied.

2.2.1 Modular invariant partition function

The torus $\mathbb{T}^2$ can be described as the complex plane $z \in \mathbb{C}$ modulus the lattice of the translations Λ generated by two complex numbers ω_1 and ω_2, which are the periods, $(z \approx z + n_1\omega_1 + n_2\omega_2)$: $\mathbb{T}^2 = \mathbb{C}/\Lambda$. Scale invariance permits the rescaling of lenghts, thus we characterize the torus by the modular parameter $\tau = \omega_2/\omega_1$, with $\mathrm{Im}\tau > 0$. The geometry of the torus is left invariant by the discrete coordinate transformations which replace the periods $\omega_1,\ \omega_2$ with the equivalent ones $\omega_1' = a\omega_1 + b\omega_2,\ \omega_2' = c\omega_1 + d\omega_2$, with $a,\ b,\ c,\ d \in \mathbb{Z}$ and $ad - cb = 1$. These transformations form the modular group $\Gamma \equiv PSL(2,\mathbb{Z}) = SL(2,\mathbb{Z})/\mathbb{Z}_2$; its generators are T and S, which act on τ as follows:

$$T:\ \tau \mapsto \tau + 1 \qquad \text{and} \qquad S:\ \tau \mapsto -\frac{1}{\tau}\,. \tag{2.16}$$

Modular transformations have the following geometrical meaning. The transformation T is equivalent to cutting the torus at a given time along the space direction obtaining a cylinder, then twisting the cylinder of one period and then re-attach the twisted boundaries. The other generator S corresponds to exchanging the time and space directions. The complex variable ζ is interpreted as the coordinate of one point on the torus and transforms covariantly:

$$T:\ \zeta \mapsto \zeta \qquad \text{and} \qquad S:\ \tau \mapsto -\frac{\zeta}{\tau}\,. \tag{2.17}$$

The two generators satisfies the relations $(ST)^3 = S^2 = C$, where C is the charge conjugation matrix, that maps ζ in $-\zeta$.

Modular invariance is the requirement of the RCFT to depend on the geometry of the torus but not on the specific set of coordinates used to describe it. It is natural in reparametrization invariant theories like in the world-sheet description of the string theory. It is implemented in any RCFT applications: we shall latter interprete the modular invariance condition in physical terms in the context of QHE. In the more familiar application of CFT to statistical systems in two space dimensions, we consider the spins on the square, for example. In order to rewrite the partition function as the trace of the transfer matrix [48], we must choose the time direction; there are two possible choices, so two expressions of the partition function that are equal by S invariance, that exchanges time and space. Moreover, translation invariance produces the second invariance (T) of the partition function.

The modular reparametrizations of the torus imply the following invariances of the partition function:

$$Z\left(\frac{-1}{\tau},\frac{-\zeta}{\tau}\right) \stackrel{S}{=} Z\left(\tau,\zeta\right) \stackrel{T}{=} Z\left(\tau+1,\zeta\right) \ . \tag{2.18}$$

These conditions are naturally satisfied in any path-integral calculation. In the algebraic approach of RCFT outlined in the previous section, they can be used as consistence conditions to determine the unknown multiplicities $\mathcal{N}_{\lambda,\bar{\lambda}}$. In order proceed, we must know the transformation law of the characters θ_λ in (2.14); it turns out that the characters of RCFT form a linear unitary representations of the modular group [47, 51], as follows,

$$T: \qquad \theta_\lambda(\tau+1,\zeta) = \sum_{\mu=1}^{\mathrm{N}} \mathcal{T}_{\lambda\mu}\theta_\mu(\tau,\zeta) = e^{2\pi(h_\lambda - c/24)}\theta_\lambda(\tau,\zeta)\,, \tag{2.19}$$

$$S: \qquad \theta_\lambda(\frac{-1}{\tau},\frac{-\zeta}{\tau}) = e^{i\alpha}\sum_{\mu=1}^{\mathrm{N}} \mathcal{S}_{\lambda,\mu}\theta_\mu(\tau,\zeta)\,, \tag{2.20}$$

that is projective due to the $\lambda-$independent phase $\alpha \neq 0$; $\mathrm{N} = |P^k|$ is the number of primary fields (the matrix $\mathcal{S}$, $\mathcal{T}$, $\mathcal{N}$ are $\mathrm{N}\times\mathrm{N}$ matrices). The matrices $\mathcal{S}$ and $\mathcal{T}$ do not depend on the modular parameters (τ,ζ) and satisfy the relations $(\mathcal{S}\mathcal{T})^3 = \mathcal{S}^2 = \mathcal{C}$.

From the invariance of Z and unitary of the modular representation, it follows that the matrices $\mathcal{N}$ must commute with the $\mathcal{T}$ and $\mathcal{S}$. The invariance under T; imposes the condition $\mathcal{N}_{\lambda,\lambda'} \neq 0$ iff $h_\lambda - h_{\lambda'} \in \mathbb{Z}$; namely, that physical excitations should have integer conformal spin. The invariance under S transformation gives a stronger condition on the multiplicities. It amounts to a completeness condition for the spectrum of the RCFT: upon exchanging time and space, it roughly imposes that the set of states at a given time is the same as that ensuring time propagation [47].

Since the $\mathcal{N}_{\lambda,\lambda'}$ are the multiplicities of sectors, that of the identity including the ground state must be present and be non degenerate: $\mathcal{N}_{I,I} = 1$. A solution of modular conditions is always present and corresponds to the diagonal matrix $\mathcal{N}_{\lambda,\lambda'} = \delta_{\lambda,\lambda'}$. The search of all solutions to (2.18) gives a classification of all possible critical theories, i.e. the universal classes, in two dimensions. For more details see [47, 55].

2.2.2 Verlinde formula

Some interesting algebraic properties of the OPE of conformal fields are encodeed in the fusion coefficients $N_{\nu\mu}^{\lambda}$ of pairs of representations of the chiral algebra, that are defined by:

$$[\phi_\nu] \times [\phi_\mu] = \sum_{\lambda \in P^k} N_{\nu\mu}^{\lambda} [\phi_\lambda] \, . \tag{2.21}$$

This is a rewriting of the OPE (2.9), in which the integers $N_{\nu\mu}^{\lambda}$ count the number of times that the representations $[\phi_\lambda]$ appears in the OPE between ϕ_ν and ϕ_μ. More precisely, they count the number of independent couplings between $[\phi_\nu]$, $[\phi_\mu]$ and $[\phi_\lambda^*]$. It there is only one field $[\phi_\lambda]$ in the fusion of the pairs $[\phi_\nu]$, $[\phi_\mu]$, the OPE is said Abelian, because this is the case of $\widehat{U(1)}$ theory due to the charge conservation. If there are more terms in the r.h.s of (2.21), *i.e.* $\sum_\lambda N_{\nu\mu}^{\lambda} > 1$ for given ν and μ, then the OPE is said non-Abelian. In the latter case, the correlations with the insertion of ϕ_ν and ϕ_μ have several intermediate channels leading to independent terms called conformal blocks [47].

The matrices $(N_\nu)_\mu^\lambda = N_{\nu\mu}^{\lambda}$ commutate among themselves, since the operator algebra is associative. The coefficients $N_{\nu\mu}^{\lambda}$ depends on the algebraic properties of the CFT algebra. They can be determined studying the corresponding three points functions. The fields $[\phi_\nu]$ and $[\phi_\mu]$ are said local between them if on the left side of (2.21) there is only one term, say $[\phi_\lambda]$, and $h_\lambda - h_\nu - h_\mu \in \mathbb{Z}$.

A fundamental relation of RCFT connects the fusion coefficients with the modular $\mathcal{S}$ matrix: it is the so-called Verlinde formula [47, 56]:

$$N_{ij}^{k} = \sum_{n=1}^{p} \frac{\mathcal{S}_{in}\mathcal{S}_{jn}\overline{\mathcal{S}}_{kn}}{\mathcal{S}_{0n}} \, , \tag{2.22}$$

where $\overline{\mathcal{S}}_{kn}$ is the complex conjugate of $\mathcal{S}_{kn}$. This relation implies that the eigenvalues of the matrices N_i are $\mathcal{S}_{in}/\mathcal{S}_{0n}$. It permits to express all the fusion properties in terms of $\mathcal{S}$: it also implies that a consistent set of fields that have closed fusion algebra is given by the representation of modular transformations. The matrix $\mathcal{S}$ can be easily determined by studying the modular invariance of the partition functions.

Quantum Dimension

An important concept in RCFT is the *quantum dimension* d_λ of a representation $[\phi_\lambda]$ of the algebra, that is defined by:

$$d_\lambda \equiv \frac{\mathrm{Tr}_\lambda 1}{\mathrm{Tr}_1 1} = \lim_{q \mapsto 1^-} \frac{\theta_\lambda(q)}{\theta_1(q)} = \frac{\mathcal{S}_{\lambda 1}}{\mathcal{S}_{11}} \, . \tag{2.23}$$

The last expression is found by using of the modular transformation (2.19) for relating the $q \mapsto 1$ limit ($\tau \mapsto 0$) involving an infinite number of terms in θ_λ with the leading term for $\widetilde{q} = e^{-\frac{2\pi}{\tau}} \mapsto 0$.

The physical meaning of d_λ is found in the asymptotic growth of the number of terms that occurs in the fusion of many fields ϕ_λ, *i.e.* $[\phi_\lambda]^{\otimes n} \simeq d_\lambda^n$. This result is proven

by multiplying n times N_λ matrices and estimating the growth by the contribution of the largest eigenvalues $\frac{\mathcal{S}_{\lambda 1}}{\mathcal{S}_{11}}$ of N_λ, as given by the Verlinde formula (we shall return on this point letter on). Therefore, $d_\lambda = 1$ for Abelian fields and $d_\lambda > 1$ for non-Abelian ones.

Simple Currents

The *simple currents* Φ_e of a Affine algebra $\widehat{\mathfrak{g}}_k$ are primary fields that have Abelian fusion rule with all the other fields. The fusion with simple currents acts as a permutation (A) on the sets of fields in the algebra $N_{e\mu}^{\lambda} = \delta_{A(\mu),\lambda}$; the permutation depends on the Affine algebra that is considered and the choice of Φ_e. The simple currents generates an algebra isomorphic to $\mathbb{Z}_p = \mathbb{Z}/(p\mathbb{Z})$ or products of them.

For example, in the RCFT with Affine algebra $\widehat{SU(m)}_k$ the primary field ϕ_λ are labeled by the weight of $\mathfrak{su}(m)$ $\lambda = (\lambda^1, \cdots, \lambda^{m-1})$, with $\sum_i^{m-1} \lambda_1 \leq k$. The number of primary field for this RCFT is $|P_+^k| = ((m-1)!)^{-1} \prod_{i=1}^{m-1}(i+k)$ and there are $m-1$ simple current labeled by λ_b where $\lambda_b^i = k\delta_{b,i},\ i = 0, \cdots,\ m-1$. Their conformal weight are $h_b = \frac{kb(m-b)}{2m}$ and the fusion rules [47] between a simple currents, ϕ_{λ_b} and a general primary fields ϕ_λ are:

$$\phi_{\lambda_b} \times \phi_\lambda = \phi_{A^b(\lambda)}\,, \tag{2.24}$$

$$\mathcal{A}(\lambda_1, \lambda_2 \cdots, \lambda_{m-1}) := (k - \sum_{i=0}^{m-1} \lambda_i,\ \lambda_1, \cdots,\ \lambda_{m-2})\,. \tag{2.25}$$

2.3 Algebraic properties of anyonic systems

This section briefly summarizes some common aspects of the algebraic formulation of anyons models and of chiral RCFTs, and the relations between them. The simplest cases of consistent anyon models, Ising and Fibonacci anyons, are discussed [40]. A full discussion of the RCFT side can be found in [56], more details on anyons can be found in [33, 30].

In a general quantum systems, there are different classes of particles $\{[a_i]\}_{i=1,\cdots \mathrm{N}}$ (Superselection Sectors); each set is label by the quantum numbers i. The index i is given by the values of conserved quantities (charge, spin ecc...). We suppose that the number of classes is finite (rational anyons models). In the simplest examples, there is only one quasiparticle type per each class. Since quasiparticles can be combined toghether, it is necessary to know what are the results: this information is encoded in the "fusions rules" between two of them, $a_i \times a_j = \sum_k N_{i,j}^k a_k$, each addendum has a diagrammatically representations as in Fig. 2.1. The fusion rules can be interpreted as maps from the couple (i,j) that give the labels k for which $N_{i,j}^k \neq 0$. If $\sum_k N_{i,j}^k > 1$ for at least one j, *i.e.* if there is at least one non-Abelian anyon, the model is called a non-Abelian anyon model. In all systems, there is the identity particle I that has trivial fusion rules with all the other fields, and for each quasiparticles a_i exists its conjugate particles a_i^* such that $I \in a_i \times a_i^*$. All these properties are valid for the operator algebra of the RCFT (2.21).

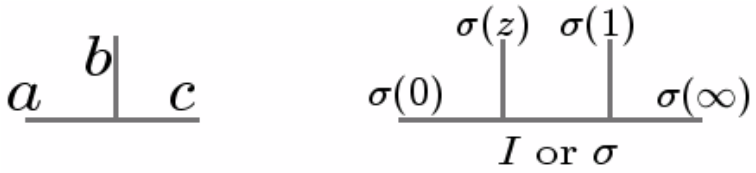

Figure 2.1: On the left: graphical representation of the fusion between the a and b anyons with c as the resulting anyon. On the right: four point function of Ising anyons.

The connection between anyons model and RCFTs [56] can be first explained in the Abelian case [14, 33]. Abelian anyons are labeled by fractional statistics quantum number and fractional charge [33]. The more interesting theories are rational, so the charges are multiplies of a basic fraction, say $\frac{1}{p}$ and the value of p depends on the theory considered. The Abelian fusion rule is the addition of charges $a_q \times a_{q'} = a_{q+q'}$ with $q + q'$ mod p [33]. The algebra is closed iff all the multiplies of $1/p$ are present and this defines an one dimensional lattice [57]. For each anyons a_q at the point z in the plane it is associated a chiral vertex operator $e^{i\frac{q}{\sqrt{p}}\varphi(z)}$ where φ is a chiral free boson with compatified radius p [47]. If q is the fractional charge of the excitation, the fractional statistics is the conformal dimension of the vertex operator $h = \frac{q^2}{2p}$. The representation of the wave function of n Abelian anyons at points $\{z_i\}_{i=1,\cdots,n}$ is realized by the conformal blocks [47, 14] of the n corresponding vertex operators, that can be computed with the standard CFT technique of the Coulomb-gas formalism [47]. The generalizations for m Abelian charges is described by the corresponding RCFT: $\widehat{U(1)}^m_K$ [47].

The simpler examples of non-Abelian anyons are Ising and Fibonacci anyons; the particles contents are $\{I, \psi, \sigma\}$ and $\{I, \tau\}$, respectively, and the non-trivial fusion rules are:

Ising	Fibonacci
$\psi \times \psi = I\,, \quad \psi \times \sigma = \sigma\,, \quad \sigma = I + \sigma$	$\tau = I + \tau\,.$

For these two cases the related RCFTs are the Ising CFT (the $\mathbb{Z}_2$ parafermionic theory $\mathrm{PF}_2 \equiv \widehat{\mathrm{SU}(2)}_2/\widehat{\mathrm{U}(1)}_4$) and a "coarse graining" of the $\widehat{SU(2)}_3/\widehat{U(1)}_6$ extended parafermionic CFT [58], in the sense that in PF_3 there are six fields: three Abelian, that can be put in the same class I, and the others are non-Abelian and are put in the class τ [58]. The super-selection sectors can be considered as classes of chiral primary fields and the fusion rules of the RCFT and the Anyons models match. These two cases constitute examples of a mapping of the RCFTs in anyons models.

The CFT realization of non-Abelian statistics can be exemplified as follows. Suppose to have 4 non-Abelian excitations of Ising model in the bulk (the same analysis applies to Fibonacci anyons). In the CFT formulation, wave functions of the systems are the conformal blocks of 4 spin fields of Ising theory:

$$\langle \sigma(0)\sigma(z)\sigma(1)\sigma(\infty)\rangle = a_1 F_1(z) + a_2 F_2(z)\,. \tag{2.26}$$

The graphical representations of 4-spin fusion is given in Fig. 2.1. The intermediate states given by the fusion of two field on the left side must mach that of the two fields in the right side of the picture [30, 47]. The fusion paths (labeled by intermediate states) are independents since the two corresponding conformal blocks F_1 and F_2 (that are Hypergeometric functions) are independent functions [47, 56]. This is an important results given by the CFT approach, because it permits to verify that the states with non-Abelian particles are degenerate, for fixed positions of the particles. On the contrary, the 4-point wave functions with Abelian fields has only one contribution.

The process can be repeated for n excitations of the same type. By repeated applications of the fusions, one can verify that the number of possible fusion paths (alias the number of different intermediate states) for n quasiparticles of the same type i is given by:

$$\mathcal{D}_i(n) = \sum_{b=1}^{N} \left[(N_i)^{n-1} \right]_a^b \sim d_i^{n-1} , \qquad n \to \infty. \tag{2.27}$$

The positive real number d_i is the quantum dimension of the particle i, and describes how the degeneracy of n-particles state grows with the number of particles. From the Verlinde formula (2.23) the largest eigenvalue of the fusion matrix N_i determines: $d_i = \frac{S_{iI}}{S_{II}}$, One finds for Ising anyons $d_\sigma = \sqrt{2}$ and for Fibonacci τ particles $d_\tau = \frac{1+\sqrt{5}}{2}$ (the golden ratio).

A quantity that characterizes the Anyon model is the *total quantum dimension*:

$$\mathcal{D} = \sqrt{\sum_{i}^{\mathrm{N}} d_i^2} , \tag{2.28}$$

where the sum extendes over all the particles in the model. By use of (2.23), one finds $\mathcal{D} = 1/S_{II}$. For Abelian anyons $\mathcal{D} = \sqrt{p}$, where p is the number of particles; for non-Abelian models $\mathcal{D}$ is bigger than the square root of the number of particles. In the case of Ising and Fibonacci these are 2 and $\sqrt{1 + (1+\sqrt{5})/2}$, respectively.

The algebraic approach to anyon systems gives the representations of the braidings matrices $[B_i]_{\alpha\beta}$ (defined in Eq. (1.18)). In the RCFT description of the Abelian excitations, the phases exchange ϑ (introduced in Eq. (1.17)) are easily determined. Indeed the fusion between two rational Abelian anyons with charge q and q' (in unit of charge $1/p$) is:

$$e^{i\frac{q}{\sqrt{p}}\varphi(z)} e^{i\frac{q'}{\sqrt{p}}\varphi(0)} \simeq z^{(q+q')/p} e^{i\frac{q+q'}{\sqrt{p}}\varphi(0)} , \tag{2.29}$$

so the exchange phase is $\vartheta = \frac{q+q'}{p}$.

For the cases of Ising anyons, the exchange is a bidimensional matrix that can be obtained by studying the analytic continuations of the Hypergeometric functions in Eq. (2.26) [47]. Due to crossing symmetry in CFT, there are only two independent braidings: the spin field in z winds the spin in 0 or in 1. They acts on the basis of the conformal blocks as follows:

$$\begin{pmatrix} F_1 \\ F_2 \end{pmatrix} (ze^{i2\pi}) = \begin{pmatrix} 1 & 0 \\ 0 & -1 \end{pmatrix} \begin{pmatrix} F_1 \\ F_2 \end{pmatrix} (z) , \qquad \begin{pmatrix} F_1 \\ F_2 \end{pmatrix} ((z-1)e^{i2\pi}) = \begin{pmatrix} 0 & 1 \\ 1 & 0 \end{pmatrix} \begin{pmatrix} F_1 \\ F_2 \end{pmatrix} (z) . \tag{2.30}$$

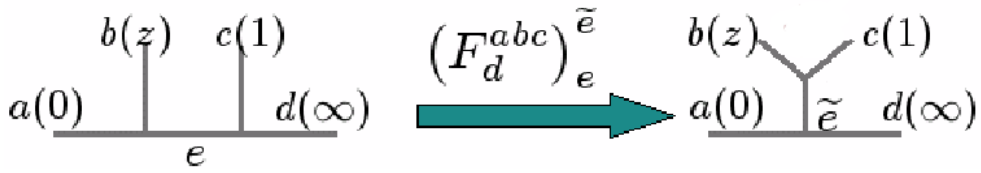

Figure 2.2: Graphical representations of the $F-$move.

This examples shows that the description of non-Abelian statistics in the RCFT approach.

Another aspect of the RCFT approach description is the fusion algebra. This is commutative, since the final state depends only on the initial quantum numbers and does not depend on the order of fusions. The Hilbert space with 4 initial quasiparticles V_{abcd} can be decomposed in two different ways depending on the order of the fusions. Since the space is the same the bases must be related by a unitary matrix F (called $F-$matrix); this is equivalent to the crossing symmetry in CFT [47]. The diagrammatic representations is reported in picture 2.2. For each anyons systems there is a $F-$matrix for all the initial states $F_d^{a,b,c}$. In the case of Ising and Fibonacci Anyons they are 2×2 matrices. The same argument can be reproduced for any number of particles, by repeated action of the elementary change of base of 4 points function [33]. All the different ways must be equivalent, meaning that the $F-$matrix must satisfy some conditions: one of them is the pentagon equations obtained from the study of 5-point functions,

$$(F_5^{12c})_d^a (F_5^{a34})_c^b = (F_d^{234})_c^e (F_5^{1e4})_d^b (F_b^{123})_e^a \,. \tag{2.31}$$

This is a polynomial identity for the $F-$matrices; its solutions are known in simple cases [56], and depend on the fusion coefficients $N_{i,j}^k$ and therefore on $\mathcal{S}$. For Ising and Fibonacci anyons, the expressions for F can be found in [56] and [41].

The non-Abelian braiding matrices (in (1.18)) can be determined by using their compatibility equations with $F-$matrices called hexagon equations. The mathematical details of this procedure can be found in [56, 41, 30]. The general solutions of the pentagon and hexagon equations are unknown for Fibonacci anyons are reported in [56, 41]. In the topological Quantum Computations scheme, all the operations are obtained by the braiding of anyons,therefore the corresponding modular matrix $\mathcal{S}$ becomes of crucial importance.

2.4 Chern Simons-RCFT connection

The Chern-Simons theory encodes the topological properties of fractional statistics and flux attachment of anyons introduced before. In this section we discuss more precisely its connection with RCFT [30, 34, 35]. The connection depends on the manifold $\mathcal{M}$; for physical applications we are interested in two kinds of geometries, $\mathcal{M} = \Sigma \times \mathbb{R}$ and $\mathcal{M} = Y \times S^1$. The two dimensional manifolds Σ and Y, without and with boundary,

respectively, are interpreted as spatial. The other factors $\mathbb{R}$ and S^1 are interpreted as temporal and can be compact for reproducing thermal sums.

Let us first discuss the case of $\mathcal{M} = \Sigma \times \mathbb{R}$. The action is $S = \int \mathrm{dt} \int_\Sigma \mathcal{L}$, the path integral expression of the ground state wave function at time t is:

$$\psi_{gs}(\bar{a}(x)) = \int_{a(x,t)=\bar{a}(x)} \mathcal{D}a(x) e^{iS[a]} \,. \tag{2.32}$$

Witten showed [34] that the expression (2.32) for a CS theory with gauge algebra $\mathfrak{g}$ at level k (whose action is reported in Eq. (1.15)) can related to the partition function of a Wess-Zumino-Witten (WZW) theory with Affine algebra $\widehat{\mathfrak{g}}_k$ (2.7).

For QH physics, it is particular interesting consider the case $\Sigma = \mathbb{T}^2$ (but the argument can be generalized for higher genus surfaces); in this geometry, Witten's relation permits to write the partition function as a quantum mechanical problem with a finite number of states. The set of states is isomorphic to the set P^k of integrable representations of the chiral $\widehat{\mathfrak{g}}_k$ WZW theory [47]. The ground state on the torus is degenerate: this degeneracy is called *topological order* [2] and it is equal to N, the number of primary fields in the corresponding RCFT [59]. For example: for $\widehat{\mathfrak{g}}_k = \widehat{U(1)}_k$ the topological order is k *i.e.* the number of possible values of fractional charges.

In the quantum Hall Effect, we are interested in the wave function with insertions of quasiparticles, that are equivalent to the insertions of time-like Wilson loops in the CS theory [34, 35]. In this case, the wave functions of the $(2+1)$-dimensional theory are conformal blocks of the corresponding WZW theory [47], where each Wilson loops corresponds to a primary fields. The monodromy properties of the conformal blocks determine the statistical properties of the anyons describe by the CS theory [30, 60].

This relation between topological theories and RCFT are well understood since the papers [34] and [35, 61]. In general there are electrons plus some anyons. In the RCFT expression of the wave function, the field for the electron must have ordinary statistics properties and for this reason it must be a simple current [14]. We will come back to this point in the next chapter.

Let us consider now the geometry $\mathcal{M} = Y \times S^1$ with non-empty boundary $\partial\mathcal{M} \neq 0$. For example, we are interested in Y being the disc or the annulus, with one and two boundary circles, respectively. In this case the CS action is not gauge invariant: under the infinitesimal gauge transformation of the field $\mathbf{a} \mapsto \mathbf{a}' = g\mathbf{a}g^{-1} + g\partial_\mu g^{-1}$, the action acquires the boundary terms [20]:

$$\frac{k}{4\pi} \int_{\partial\mathcal{M}} \mathrm{Tr} g^{-1} dg \wedge \mathbf{a} \,. \tag{2.33}$$

In order to have a full gauge invariant theory, the set of gauge symmetries must be reduced to the sub set of transformation such that $\partial_0 g|_{\partial\mathcal{M}} = 0$, for which (2.33) vanishes. With this restricted set of symmetries, the configurations of $\mathbf{a}$ cannot be completely gauged away: the path integral on this reduced set of configurations can be rewritten as that of the corresponding WZW theory [35]. The Hilbert space is isomorphic to that of the chiral WZW, for Y being disk, and of the full WZW for Y the annulus. Thus,

the CS partition function can be rewritten as the partition function of the chiral and full WZW for the disk and the annulus respectively. In the case of the annulus, the two parts, chiral and antichiral, live on opposite edges. In all cases the CS theory that we have described is related to the same RCFT.

Chern-Simons theories are usually assumed as the low-energy effective theories of systems in topological states of matter (that are gapful). The previous results tell us that such systems have both chiral gapless edge modes and gapped bulk excitations. At the same time, "effective" wave function can be determined without attempting the solution of the corresponding Schrödinger equation for the electrons. These relations are very useful since they permit to apply the algebraic methods of CFT to the study of the topological theories.

2.5 QHE wave function and RCFT

The relations sketched in the previous section indicate that RCFTs can be used as effective field theory for the QH states: the RCFT theory describes both wave functions and edge modes. A straightforward proof that a chiral RCFT describes the low-energy edge mode can be given for the IQHE [62] (see below).

2.5.1 Wave function as conformal blocks

In the section 1.2 we summarized some relevant examples of wave functions in LLL, that can be written as conformal blocks of RCFT. This relation [14] was generalized by Moore and Read to trial wave functions for other QH states in the second LL (SLL).

IQHE and Laughlin states

For filling fraction $1/\nu = p$, with p odd, the wave functions were given in Eqs. (1.5) and (1.6). The holomorphic functions in (1.6) can be identified with the conformal blocks of the compatified chiral boson with compactification radius $\sqrt{p}$. This RCFT has $c = 1$ and $\widehat{U(1)}_p$ Affine algebra and is usually called the Luttinger liquid; for details and conventions see [47, 62]. The same relation is valid for the wave functions in presence of quasiholes. Indeed by the Wick theorem one can prove:

$$\Psi_p(\{z\},\{\bar{z}\}) = \langle e^{-i\int d^2z\sqrt{p}\varphi}\prod_i \Phi_e(z_i)\rangle\,, \tag{2.34}$$

$$\Psi_{p;2qp}(\eta_1,\eta_2;\{z\},\{\bar{z}\}) = \langle e^{-i\int d^2z\sqrt{p}\rho_0\varphi}\prod_i \Phi_e(z_i)e^{i1/\sqrt{p}\varphi(\eta_1)}e^{i1/\sqrt{p}\varphi(\eta_2)}\rangle\,, \tag{2.35}$$

where $\Phi_e(z_i) = e^{i\sqrt{p}\varphi(z_i)\rho_0}$. The non-local field ($e^{-i\int d^2z\sqrt{p}\rho_0\varphi}$) is necessary in order to reproduce the Gaussian factor and a nonvanishing result [14, 47] (it corresponds to the background charge in CFT). The computations of the conformal blocks is described for example in [14]. In the following the background charge field will be omitted.

The fractional charge and statistics of the quasiholes can be obtained from the properties of the conformal fields in Eq. (2.35) and match the values obtained in Laughlin's

theory. Noticed that the insertion of one electron field Φ_e does not change the analytic properties of the correlators, because the primary fields $\Phi_{qh} = e^{i1/\sqrt{p}\varphi(\eta_1)}$, that are related to the quasiholes, have integer mutual phase with Φ_e (ϑ defined in (2.29)). The charge operator is $\hat{Q} = \frac{1}{2\pi}\oint J(z)dz$, in RCFT language, where $J(z) = \frac{1}{\sqrt{p}}\partial\varphi(z)$ is the current in the chiral boson theory; the normalization factor is fixed in a such way that the electron field has charge 1.

Halperin states

The relations between conformal blocks and wave functions in the case of the ground state of Halperin fluids Ψ^H, (1.9) with $m = m' = n-1$, is given by the CFT correlators of an equal number $N^\downarrow = N^\uparrow = N$ of two species of electrons field $\Phi_e^\uparrow$ and $\Phi_e^\downarrow$ as follows:

$$\Psi^H(\{z_i^\uparrow\},\{\bar{z}_i{}^\uparrow\};\{z_i^\downarrow\},\{\bar{z}_i^\downarrow\})) = \langle\prod_i^N \Phi_e^\uparrow(z_i)\prod_i^N \Phi_e^\downarrow(z_i)\rangle\,, \tag{2.36}$$

where,

$$\Phi_e^\uparrow = e^{\frac{i}{\sqrt{2}}\left(\sqrt{2m+1}\varphi_c+\varphi_s\right)}\,, \qquad \Phi_e^\downarrow = e^{\frac{i}{\sqrt{2}}\left(\sqrt{2m+1}\varphi_c-\varphi_s\right)}\,, \tag{2.37}$$

the background charge is omitted and $\varphi_{c/s}$ are two chiral boson fields corresponding to the $\widehat{U(1)}^2$ CFT. They are interpreted as the charge and spin fields respectively [14]. The expression of the wave functions for the ground state fixes the compatification radius of both the Affine algebras: they are $p_c = 2(2m+1)$ and $p_s = 2$. The possible primary fields local with respect to both $\Phi_e^\uparrow$ and $\Phi^\downarrow$ are:

$$\Phi_{qh}^\uparrow = e^{\frac{i}{\sqrt{2}}\left(\frac{1}{\sqrt{2m+1}}\varphi_c+\varphi_s\right)}\,, \qquad \Phi_{qh}^\downarrow = e^{\frac{i}{\sqrt{2}}\left(\frac{1}{\sqrt{2m+1}}\varphi_c-\varphi_s\right)}\,, \tag{2.38}$$

and fusion between these two fields only, they are related to the quasiholes of the fluids [14, 30]. The minimal fractional charge is $\frac{1}{2m+1}$, and the locality between quasiholes and electron fixes the values of the spin of the former to be $\sigma_z = \pm 1/2$. The states in presence of quasiparticles with spin $\pm 1/2$ at the point $\{w_j\}_{j=1\cdots n^{\uparrow/\downarrow}}$ is:

$$\Psi^H = \langle\prod_i^{n^\uparrow}\Phi_{qh}^\uparrow(w_i)\prod_i^{n^\downarrow}\Phi_{qh}^\downarrow(w_i)\ \prod_i\Phi_e^\uparrow(z_i)\prod_i\Phi_e^\downarrow(z_i)\rangle\,. \tag{2.39}$$

Moore-Read state

The basics idea for explaining the plateau at $\nu = 5/2$ is that bosonic degrees of freedom realize the fluid, as introduced in section 1.2.4. At the level of RCFT, the clustering of electrons [14, 4, 30, 63] can be implemented by use of the Ising CFT [47, 48]. Indeed the correlation function of Majorana fermions is given by a Pfaffian that reproduces the $p-$waves superconductor results of section 1.2.4. Another way to understand the clustering is through the OPE $\psi\psi \sim I$, implying that the wave function does not vanish

when two electrons are brought together. The inclusion of the standard $\widehat{U(1)}$ CFT for the charge leads to consider the RCFT Ising $\times \widehat{U(1)}$; the electron field is [14]:

$$\Phi_e(z) = \psi(z) e^{i\sqrt{\frac{2M+2}{2}}\varphi_c(z)}, \qquad M \text{ odd}; \tag{2.40}$$

it is the simple current of the RCFT. The numerical factor at the exponent gives Fermi statistics (Bose statistics of M even). The wave function is obtained substituting this $\Phi_e(z)$ in (2.34); the ground state wave function is factorized in two parts:

$$\Psi_{MR}(\{z\},\{\bar{z}\}) = \text{Pf}\left[\frac{1}{z_i - z_j}\right] \prod_{i<j} (z_i - z_j)^{M+1}. \tag{2.41}$$

This wave function describes fluids with $\nu = 2 + \frac{1}{M+1}$. Among all the possible products of primary fields of the two factors of the RCFT, the physical fields must be local with respect to the electron field [64]: the possible ones are

$$e^{i2n\frac{1}{\sqrt{2(2M+2)}}\varphi_c}, \qquad \psi e^{i2n\frac{1}{\sqrt{2(2M+2)}}\varphi_c}, \qquad \sigma e^{i(2n+1)\frac{1}{\sqrt{2(2M+2)}}\varphi_c}. \tag{2.42}$$

These are the quasiparticles of the theory. Their wave functions was found in [58, 65]. From the wave functions, the braiding properties of quasiparticle can be recovered [30, 58, 65]: they are non-Abelian anyons owing to the non trivial fusion $\sigma\sigma \sim I + \psi$.

Read-Rezayi states

The Moore-Read state can be generalized to describes clustering of k electrons, $k > 2$. A wave function $\Psi(\{z\})$ is clustered of order k if $\Psi(\{z\}) = \Psi'(\{z\}) \prod_{i<j}(z_i - z_j)^{M'}$ and if $\Psi'(\{z\}) \neq 0$ for $i \leq k$ particles at the same position [64]. Here Ψ' is symmetric under the exchange of particles and M' is an integer. States with this property are zero-energy eigenvalues of the following $(k+1)$-body repulsive model Hamiltonian:

$$\hat{H} = |V| \sum_{i_1<i_2\cdots<\imath_k} \delta^2(z_1 - z_2)\delta^2(z_3 - z_2)\cdots\delta^2(z_{k-1} - z_k)\delta^2(z_{k+1} - z_k). \tag{2.43}$$

Read and Rezayi understood [66] that k clustering property is encoded in the $\mathbb{Z}_k$ parafermionic CFT defined by the coset $\text{PF}_k = \widehat{SU(2)}_k/\widehat{U(1)}_{2k}$ [47, 52] (for $k = 2$ the Ising model is recovered). Indeed the basic parafermionic field ψ_1 obeys the OPE $\psi_1^k \sim I$ and carries a $\mathbb{Z}_k$ Abelian charge. The RCFT for these Hall fluids is $\text{PF}_k \times \widehat{U(1)}$ and the electron fields is:

$$\Phi_e(z) = \psi_1(z)\ e^{i\sqrt{\frac{kM+2}{k}}\varphi_c(z)}, \qquad M \text{ odd}. \tag{2.44}$$

The basic quasiparticles is described by the following field,

$$\Phi_{qh}(z) = \sigma(z)_1\ e^{i\frac{1}{\sqrt{(kM+2)k}}\varphi_c(z)}, \tag{2.45}$$

where $\sigma(z)_1$ is the one spin field of the PF_k and possess non-Abelian fusion rules. More details on the parafermion theory can be found in section 3.2.1 and in [30, 47, 52]. The wave function for these states in absence of quasiparticles are computed in [66, 67] and in presence of quasiparticles [58]. The filling fraction for these fluids are $\nu = 2 + \frac{k}{kM+2}$. The braiding of quasiparticles are computed in [65].

2.6 Edge states and RCFT

As discussed before, the low-energy physics of the QHE can be described in term of static quasiparticles in the bulk and edge excitations at the boundary of the systems. The CS-RCFT connection indeed presents these two sides of the QHE systems that can be both described by RCFT. In this thesis, the second aspect of the edge dynamics will be analyzed in details and described by means of partition functions. In this section, we briefly introduce this description and the direct derivation of the edge dynamics for integer filling.

Edge dynamics in IQHE

The CFT description of edge excitations can explicitly derived for $\nu = 1$ as follows. The II quantization of electron in the LLL is considered and higher LLs and Coulomb interactions are neglected. The field operator can be written as:

$$\hat{\Psi}(x,t) = \sum_{l>0} \eta_{0,l}(x)\hat{a}_{1,l}e^{-iE_l t}, \qquad \eta_{0,l}(x) = e^{-\frac{|z|^2}{2}}\frac{z^l}{\sqrt{l!}}\,, \tag{2.46}$$

and $\hat{a}_{0,l}$ are fermionic destruction operators. In the ground state all the eigenstates with momenta $l < \bar{l}$ are occupied, the density is a constant on a disk with radius $R \simeq \bar{l}^{1/2}$ and vanishing outside ($\ell_B = 1$). The small perturbations are described by the current that is different from zero only in the vicinity of R and perpendicular to the radius.

The effect of the boundary can be implemented in the Hamiltonian by a confining potential that lifts the degeneracy near the boundaries [1, 62]. The linear expansion of the confining potential near the boundary, i.e for $l \sim \bar{l}$, gives rise to a massless relativistic dispersion relation for the excitations: $E_l \sim E_{\bar{l}} - \frac{v}{R}(l - \bar{l} - \mu)$. These gapless edge excitations are described by the $\widehat{U(1)}$ CFT. There are two type of excitations: neutral particle-hole excitations and charge ones, the latter correspond to the motion of electrons from the deep interior to the edge. The velocity v and the chemical potential μ are phenomenological inputs.

This low-energy approximation for excitations near the boundary goes trough all the quantities of the second-quantized theory of electron in LLL [62]. The result is the $\widehat{U(1)}$ CFT of one chiral Weyl fermion with Neveu-Schwarz boundary condition. The field operators also reduces to the Weyl fermion field in the CFT, as follows [62]

$$\hat{\Psi}(Re^{i\vartheta},t) = e^{i\alpha}\sum_{l=\bar{l}+n} \hat{a}_{o,n}\; f_n(R)\frac{1}{R}e^{in(\vartheta - \frac{v}{R}t)}\,, \tag{2.47}$$

where $f_n(R)$ is approximately constant for $|n| \ll \bar{l}$, such that the radial dependence is frozen. The angular and time dependence are characteristic of a chiral fermionic conformal field that is defined on the spatial-time cylinder made by the edge and the time direction. This boundary manifold $\partial\mathcal{M} = \partial Y \times \mathbb{R}$ is described by the Euclidean complex coordinate $z = e^{w/r}$ where $w = v\tau + iR\vartheta$. Therefore the RCFT of the edge excitations is naturally defined on the cylinder. All these properties are encoded in the second CS-RCFT relation discussed before for a manifold $Y \times \mathbb{R}$ with boundary.

Edge theories summary

We sum up the main points of the connection between RCFT and QHE edge. The edge modes of Hall fluids are in correspondence with representations of Virasoro algebra; the RCFTs are associated to a chiral algebras $\widehat{\mathfrak{a}}$ [47, 48, 68], whose irreducible representations are labeled by the highest-weights $\lambda \in P^k$ (the set P^k depends on $\widehat{\mathfrak{a}}$).

The excitations in Hall fluids are charged, therefore $\widehat{\mathfrak{a}}$ contain a charge sub-algebra $\widehat{U(1)}$ factor; the latter is responsible to the conservation of the electric current j^{em}_μ [20, 30].

The CFT/QHE [14] relations attributes to all the quasiparticles in the fluids a primary field in the CFT. The descendants are connected with the particle-hole excitations at the boundary. Between all these fields at least one must have fermionic characteristics: Abelian fusion rules, Fermi statistics and integer charge. The finite number of independent elementary excitations suggests that CFT is a RCFT, and we will analyzed these cases only*. The presence of a minimal fractional charge implies that $\widehat{U(1)}$ bosons must be compatified on a finite radius p. Therefore the CFTs will be:

$$\widehat{\mathfrak{a}} = \widehat{\mathfrak{g}} \otimes \widehat{U(1)}_p \,, \tag{2.48}$$

for some Affine algebra (or coset) $\widehat{\mathfrak{g}}$ [64]. This is the general theory that describes wave function at the plateaus.

General primary fields of a composite CFT in (2.48) are express as the product,

$$\Phi_i = V^{\ell_i} e^{i\alpha_i \varphi_c} \,, \tag{2.49}$$

where V^{ℓ_i} are fields relate to the highest weight ℓ_i of $\mathfrak{g}$ with conformal dimension h^{ℓ_i}, φ_c is the bosonic field for the charge modes. The total number of such fields is $p|P^k_+|$, where $|P^k_+|$ is the number of primary fields in $\widehat{\mathfrak{g}}$. The following convention is used: the Abelian index (Abelian quantum number) is a subscripts, the non-Abelian index a superscript. The electron field is denoted by:

$$\Phi_e = V^{\ell_e} e^{i\alpha_e \varphi} \,. \tag{2.50}$$

*Non rational theories are considered in [12].

Chapter 3

Modular Invariant partition function in QHE

In this chapter the study of partition functions for edge excitations of quantum Hall states is developed. They are found in the geometries of the annulus and the disc where they enjoy the symmetry under modular transformations [69]. Partition function provide a complete identification of the Hilbert space of excitations and can be used to describe experiments searching non-Abelian statistics (analyzed in the next chapter).

Modular invariant partition functions were obtained in [69, 70, 71, 72] for the Abelian hierarchical and non-Abelian Read-Rezayi states; in section 3.2, we provide the expressions for the other non-Abelian states in the second Landau level for $2 < \nu < 3$ (these results was obtained in [73]). These are the non-Abelian spin-singlet states (NASS), introduced in [15] and further developed in [58], the charge-conjugates of Read-Rezayi's states ($\overline{\mathrm{RR}}$) [74], the Bonderson-Slingerland (BS) hierarchy built over the Pfaffian state [75], and Wen's $SU(n)$ non-Abelian fluids (NAF) [76], the $SU(2)$ case in particular. These states and their corresponding RCFT are listed in Fig. 3. These states in the second LL are receiving a lot of attention for the application to Topological Quantum Computation.

In general, the RCFT for non-Abelian states are of the type $\widehat{U(1)} \times \widehat{\mathfrak{g}}$, the Abelian part $\widehat{U(1)}$ accounts for the charge of excitations and the non-Abelian part is characterized by the Affine symmetry algebra $\widehat{\mathfrak{g}}$ or the coset $\widehat{\mathfrak{g}}/\widehat{\mathfrak{h}}$ [47, 52]. The parameters specifying the first part (compactification radius, charges and filling fractions) are determined by the standard requirements on the charge and statistics of the electron and its relative statistics with respect to the other excitations [77]; in some cases, further conditions are suggested by the physics of the specific Hall state [67].

In this chapter, we show that the construction of partition functions of non-Abelian Hall states is completely straightforward. Indeed, starting from the two choices of: i) the conformal field theory $\widehat{\mathfrak{g}}$ of the neutral non-Abelian part of excitations, and ii) of Abelian field representing the electron, the charge and statistics of all excitations can be self-consistently found without any further physical input. This implies a non-trivial pairing between the sectors of the neutral and charged RCFTs, that actually follows

from the requirement of modular invariance of the partition function on the annulus geometry [69]. We point out that the choices of the neutral algebra and the neutral part of the electron field fix, almost uniquely, all the characteristics of the fluid, including ν.

Our approach to QHE by CFT is complementary to the one proposed by Moore and Read [14]: our goal is to determine if a given chiral algebra $\widehat{\mathfrak{g}}$ can describe QH fluids and then obtain the corresponding physical properties. Since the partition function is a characterizing quantity of the RCFT [47, 56], it is fundamental to know its expression for each the state.

Let us stress that in this thesis we describe Hall states by means of Rational CFTs and exploit the modular invariance of their partition functions; we do not discuss other approaches involving non-rational theories, that could relevant for the Jain hierarchical states in particular [12, 13, 67].

We start with some general considerations on the partition function for QH edges states and use two well understood cases as examples, the Laughlin [69] and the Read-Rezayi states [67, 72].

RR	NAFF	$\overline{\text{RR}}$	BS	NASS
$\nu = 2 + \frac{k}{kM+2}$	$\nu = 2 + \frac{m}{mM+k\ell^2}$	$\nu = 2 + \frac{2}{kM+2}$	$\nu = 2 + \frac{n}{(2p-1)n+1}$	$\nu = 2 + \frac{2k}{2kM+3}$
$\widehat{U(1) \otimes PF_k}$	$U(1) \otimes SU(m)_k$	$U(1) \otimes \overline{SU(2)}_k$	$U(1) \times SU(M)_1 \otimes \mathbb{Z}_2$	$U(1) \otimes \frac{SU(3)_k}{U(1)^2}$

Figure 3.1: Non-Abelian fluids considered in this thesis and their effective conformal field theories.

3.1 Partition functions for Hall fluids

3.1.1 Annulus geometry

Partition functions are best defined for the Hall geometry of an annulus (see Fig. 3.2(a)), to which we add a compact Euclidean time coordinate for the inverse temperature β. This space geometry allows for the measure of the Hall current and is equivalent to the bar geometry (corresponding to $R \to \infty$), while enjoying some special symmetries. The disk geometry (Fig. 3.2(b)), describing isolated Hall droplets, can be obtained from the annulus by shrinking the inner radius to zero.

As space-time manifold, the annulus at finite temperature has the topology: $\mathcal{M} = S^1 \times S^1 \times I$, where I is the finite interval of the radial coordinate. The boundary $\partial\mathcal{M}$, corresponds to two copies of a space-time torus $S^1 \times S^1$ made by the circle boundary and compact Euclidean time. The edge excitations are chiral and anti-chiral waves on the outer (R) and inner (L) edges, respectively [35]. In the RCFT approach, the two edges modes correspond to two components (holomorphic and anti-holomorphic) of the Affine algebra. The torus geometry enjoys the symmetry under modular transformations acting on the two periodic coordinates and basically exchanging the space and time

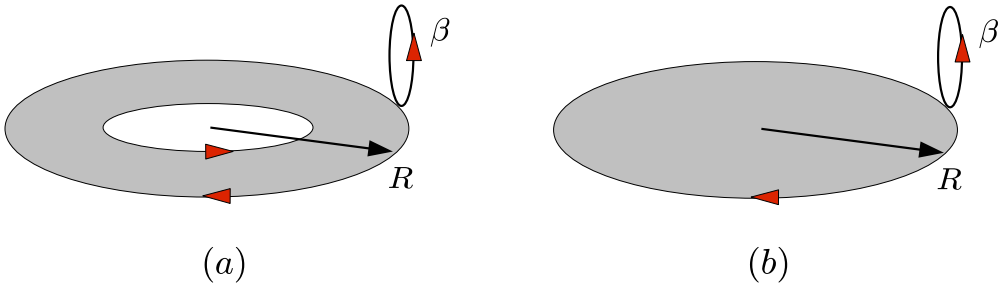

Figure 3.2: The (a) annulus and (b) disk geometries.

periods. The partition functions should be invariant under this geometrical symmetry that actually implies several physical conditions on the spectrum of the theory [69, 72].

3.1.2 The partition functions

In the CFTs description, the Hamiltonian and momentum of the modes on the edges are the conformal dimension and spin of the conformal fields,

$$H = \frac{v_R}{R_R}\left(L_0^R - \frac{c}{24}\right) + \frac{v_L}{R_L}\left(\overline{L}_0^L - \frac{c}{24}\right) + \text{ const.}, \qquad J = L_0^R - \overline{L}_0^L \ . \tag{3.1}$$

The coupling of edge modes and the potential difference V_0 between the two boundaries is given by $V_0\left(Q^L - Q^R\right)$, where $Q^{L\ (R)}$ are the electric charge of the modes. This coupling must be added to the Hamiltonian in (3.1).

The partition function of the conformal theory, already described in section (2.2), is rewritten in a more suitable notation as follows:

$$\mathrm{Z}_{\text{annulus}}\left(\tau,\zeta\right) \ = \ \mathcal{K}\ \mathrm{Tr}\ \left[\mathrm{e}^{i2\pi\left(\tau\left(L_0^L - c/24\right) - \overline{\tau}\left(L_0^R - c/24\right) + \zeta Q^L + \overline{\zeta} Q^R\right)}\right] \ , \tag{3.2}$$

where $\mathcal{K}$ is a normalization. The real and imaginary parts of τ are respectively given by the "torsion" η and the inverse temperature β, times the Fermi velocity v; the parameter ζ is proportional to the chemical potential μ and electric potential difference between the edges V_o as follows:

$$i2\pi\tau = -\beta\ \frac{v + i\eta}{R} \ , \qquad i2\pi\zeta = -\beta\left(V_o + i\mu\right) \ . \tag{3.3}$$

Starting with the partition function as in (2.10), the coupling with the external potential generates a no vanishing imaginary part for ζ. The grand canonical partition functions of edge modes is the partition function for the Affine algebra [47]. The chemical potential is introduced only for the electric charge since it is does note couple to the neutral modes (for spin-singlet states, a coupling between "spin" and external transverse magnetic field can also be introduced). The operators Q_L and Q_R are the charge operator that are proportional to the zero mode of the $\widehat{U(1)}$ charge algebra.

In general, charged and neutral modes can propagate with different velocities v_c and v_n, respectively: in this case, the expression of the total energy $\left(v\left(L_0 - c/24\right)\right)$ should

be replaced by,

$$v_c \left[L_0^{\widehat{U(1)}} - c^{\widehat{U(1)}}/24 + \frac{v_n}{v_c} \left(L_0^{\widehat{\mathfrak{g}}} - c^{\widehat{\mathfrak{g}}}/24 \right) \right] , \tag{3.4}$$

on both edges, where the Virasoro operators are relative to the two factors of the theory $\widehat{U(1)} \times \widehat{\mathfrak{g}}$. The conformal spin takes a contribution from both the CFT: $J = (L_0^{\widehat{U(1)}} + L_0^{\widehat{\mathfrak{g}}})^L - (L_0^{\widehat{U(1)}} + L_0^{\widehat{\mathfrak{g}}})^R$. If the neutral modes propagate in the opposite direction with respect to the charge mode as in the case of $\overline{\mathrm{RR}}$, their contribution to the energy (spin) does not change (take a minus). In the following, we shall momentarily choose a symmetric Hamiltonian for the two edges by adjusting the velocities of propagation of excitations, $v_L/R_L = v_R/R_R$.

As described in section 2.2, the Hilbert space of edge modes decomposes in representations whose states are summed in the characters θ_λ: in these notations, the partitions function can be written as follows:

$$Z_{\text{annulus}} \;=\; \sum_{\lambda,\mu \in P^k \times P^k}^{N} \mathcal{N}_{\lambda,\mu}\, \theta_\lambda(\tau,\zeta)\; \overline{\theta_\mu^c(\tau,\zeta)} \; . \tag{3.5}$$

In this equation, the bar denotes complex conjugation and the suffix (c) is the charge conjugation C, acting by: $Q \to -Q$, $\theta \to \theta^c$. The inner (resp. outer) excitations are described by θ_λ (resp. θ_μ^c), according to the definition (3.2).

The unknown quantities in (3.5) are the coefficients $\mathcal{N}_{\lambda,\mu}$ and and the function θ_λ. The coefficients are positive integer numbers $\mathcal{N}_{\lambda,\mu}$ giving the multiplicities of sectors of excitations, will be fixed by imposing modular invariance and some physical requirements. The form of θ_λ will be determined from the characters of the neutral and charged CFTs by self-consistency finding their coupling and selection rules; a crucial role is played by the physical properties of the electron field in the theory. This construction is described in section 3.1.4.

The partition function describes the degrees of freedom living on the boundaries of the disk, but their global properties should describe the systems of electrons. Therefore global excitations, paired between the two edges, have fermionic properties. Accordingly, the partition function must have four modular symmetries: S, T^2, U and V. The former two have been already discussed in section 2.2.1, with T instead of T^2. Let us describes them in detail:

- T^2: The global excitations are electrons, that carry the electric current in and out of the system: thus, excitations on both edges should combine among them to form global fermionic states with half integer spin, $2\left(L_0^L - L_0^R\right) \in \mathbb{Z}$. At the level of the partition function this condiction is realized by the symmetry,

$$T^2 : \qquad Z(\tau+2,\zeta) \equiv \mathrm{Tr}\, \left[\cdots \mathrm{e}^{\, i2\pi\; 2\left(L_0^L - L_0^R\right)} \right] = Z(\tau,\zeta) \; . \tag{3.6}$$

  In systems with electron excitations the condition T (integer spins) cannot be imposed. This implies a weaker modular invariance under: actually, S and T^2 generate a subgroup of the modular group, $\Gamma_\theta \subset \Gamma$ [47].

- U: The boundaries of the annulus are connected with external conductors. Thus the global charge must be a integer, $Q^L + Q^R \in \mathbb{Z}$, (if no quasiparticles are present in the bulk). This corresponds to the following conditions on the charge spectrum,

$$U: \qquad Z(\tau, \zeta + 1) \equiv \mathrm{Tr}\left[\cdots \mathrm{e}^{\,i2\pi\left(Q^R + Q^L\right)}\right] = Z(\tau, \zeta) \ , \tag{3.7}$$

  Thus, fractionally charged excitations at one edge must pair with complementary ones on the other boundary. Consider, for example, a system at $\nu = 1/3$ and add one electron to it: it can split into pairs of excitations with, $(Q^L, Q^R) = (1/3, 2/3), (0, 1), (2/3, 1/3), (1, 0)$. The different splittings are related one to another by tuning the electric potential V_o in (3.1)

- V: The potential at the edges can be varied by adding localized magnetic flux inside the annulus; the addition of one flux quantum leads to a symmetry of the spectrum, as first observed by Laughlin [2]. This is actually realized by the transformation $V_o \to V_o + 1/R$ corresponding to $\zeta \to \zeta + \tau$. The corresponding invariance of the partition function is,

$$V: \qquad Z(\tau, \zeta + \tau) = Z(\tau, \zeta) \ . \tag{3.8}$$

  This transformation is called "spectral flow", because it amounts to a drift of each state of the theory into another one [3].

3.1.3 Example: Laughlin fluids

The simplest example of Laughlin fluids, with $\nu = 1/p$ is used to show how the requirement of modular invariance fixes all the data of the $\widehat{U(1)}$ CFT [69]. This CFT has the following spectrum [62]:

$$Q = \frac{n}{p} \ , \qquad J = L_0 = \frac{n^2}{2p} \ , \qquad n \in \mathbb{Z} \ , \ p = 1, 3, 5, \ldots \ . \tag{3.9}$$

Each value of (Q, L_0) is the weight of a highest-weight representation of the $\widehat{U(1)}$ algebra, which contains a tower of neutral excitations with quantum numbers $(Q, L_0 + k)$, $k > 0$ integer (the descendant states) [47]. The $\widehat{U(1)}$ characters are:

$$Ch(Q, L_0) \ = \ \mathrm{Tr}|_{\widehat{U(1)}} \left[\mathrm{e}^{i2\pi(\tau(L_0 - c/24) + \zeta Q)}\right] \ = \ \frac{q^{L_0}\ w^Q}{\eta(q)} \ , \tag{3.10}$$

where η is the Dedekind function,

$$\eta(q) = q^{1/24} \prod_{k=1}^{\infty} \left(1 - q^k\right) \ , \qquad q = \mathrm{e}^{i2\pi\tau} \ , \quad w = \mathrm{e}^{i2\pi\zeta} \ . \tag{3.11}$$

Any conformal field theory with $c \geq 1$ contains an infinity of Virasoro and $\widehat{U(1)}$ representations [47]. The characters (3.10) should be regrouped into characters θ_λ of an extended algebra to obtain a finite-dimensional unitary representations of the modular

groups Γ_θ as required in RCFT. The modular conditions (T^2, S, U, V) fix how to achieve this: using the condition U, we can first collect $\widehat{U(1)}$ representations on one edge which have integer spaced charges $Q^L = \lambda/p + \mathbb{Z}$, p integer, and then combine them with the corresponding sums on the other edge. The Virasoro dimensions are given by Eq.(3.9); the charge unit $1/p$ is left free and is related to the normalization of ζ. The sums of $\widehat{U(1)}$ characters having integer spaced charge give the characters θ_λ of the extended algebra (3.5), which carry a finite-dimensional representation of Γ_θ [56]. These θ_λ are the theta functions with rational characteristics $\Theta\left[\begin{smallmatrix} a \\ b \end{smallmatrix}\right]$:

$$\begin{aligned} \theta_\lambda &= \mathrm{e}^{-\frac{\pi}{p}\frac{(\mathrm{Im}\ \zeta)^2}{\mathrm{Im}\ \tau}}\ \frac{1}{\eta}\ \Theta\begin{bmatrix} \lambda/p \\ 0 \end{bmatrix}(\zeta|p\tau) \\ &= \mathrm{e}^{-\frac{\pi}{p}\frac{(\mathrm{Im}\ \zeta)^2}{\mathrm{Im}\ \tau}}\ \frac{1}{\eta}\ \sum_{k\in\mathbb{Z}}\ \mathrm{e}^{i2\pi\left(\tau\frac{(pk+\lambda)^2}{2p}+\zeta\left(\frac{\lambda}{p}+k\right)\right)}\ , \end{aligned} \tag{3.12}$$

in this expression, the sum over the charge values $Q^L = \lambda/p + \mathbb{Z}$, $\lambda = 1, 2, \ldots, p$ is manifest. The non-analitic prefactor will be explained later. In the future we use the notation $K_\lambda(\tau, \zeta, p) \equiv \eta^{-1}\Theta\left[\begin{smallmatrix} \lambda/p \\ 0 \end{smallmatrix}\right](\zeta|p\tau)$. The transformations T^2, S, U, V of these generalized characters are as follows [47, 69]:

$$T^2: \qquad \theta_\lambda(\tau+2,\zeta) = \mathrm{e}^{i2\pi\left(\frac{\lambda^2}{p}-\frac{1}{12}\right)}\theta_\lambda(\tau,\zeta)\ , \tag{3.13}$$

$$S: \qquad \theta_\lambda\left(-\frac{1}{\tau},-\frac{\zeta}{\tau}\right) = \frac{\mathrm{e}^{i\frac{\pi}{p}\mathrm{Re}\ \frac{\zeta^2}{\tau}}}{\sqrt{p}}\ \sum_{\lambda'=0}^{p-1}\ \mathrm{e}^{i2\pi\frac{\lambda\lambda'}{p}}\ \theta_{\lambda'}(\tau,\zeta)\ , \tag{3.14}$$

$$U: \qquad \theta_\lambda(\tau,\zeta+1) = \mathrm{e}^{i2\pi\lambda/p}\ \theta_\lambda(\tau,\zeta)\ , \tag{3.15}$$

$$V: \qquad \theta_\lambda(\tau,\zeta+\tau) = \mathrm{e}^{-i\frac{2\pi}{p}\left(\mathrm{Re}\ \zeta+\mathrm{Re}\ \frac{\tau}{2}\right)}\theta_{\lambda+1}(\tau,\zeta)\ . \tag{3.16}$$

The non-trivial $S-$transformations can be proven by using the Poisson resummation formula. These transformations show that the characters θ_λ carry a unitary representation of the modular group Γ_θ, which is projective for $\zeta \neq 0$ (the composition law is verified up to a phase).

The corresponding sums of $\widehat{U(1)}$ representations for the other edge are given by $\bar{\theta}_{\bar{\lambda}}$ carrying charge $Q^R = -\bar{\lambda}/p + \mathbf{Z}$. The U condition (3.7) is applied to Z in the form (3.5) and it requires that left and right charges satisfy $\lambda = \bar{\lambda}$ mod p. The unique (the proof can be found in [69]) solution is $\lambda = \bar{\lambda}$, which also satisfies the (T^2, S, V) conditions, leading to the invariant:

$$Z_{annulus} = \sum_{\lambda=1}^{p}\ \theta_\lambda\ \bar{\theta}_\lambda\ . \tag{3.17}$$

This is the annulus partition function for the $c = 1$ edge theories we were after. It yields the multiplicities of representations $\mathcal{N}_{\lambda,\bar{\lambda}} = \delta^{(p)}_{\lambda,\bar{\lambda}}$, and still depends on two free parameters, p and ζ, which are determined by further physical conditions:

- The normalization of ζ, i.e. of the charge unit, is determined self-consistently as follows. Among the transformations (3.16), V is the only one sensitive to rescaling $\zeta \to a\zeta$, with a integer: we fix $a = 1$ by requiring that the minimal spectral flow $\zeta \to \zeta+\tau$ carry the minimal amount of fractional charge $(1/p)$ from one edge to the other, $\theta_\lambda(\zeta + \tau) \to \theta_{\lambda+1}(\zeta)$. This corresponds to the definition of the (fractional) charge in the Laughlin thought experiment [3]. Moreover, the amount of displaced charge per unit of flux is a measure of the Hall conductivity: we conclude that (3.17) describes the Hall effect at filling fractions $\nu = 1/p$.

- Within the spectrum of charges and fractional spins of Z (3.17), there should be electron states on each edge which have unit charge and odd statistics, $2J = 1 \mod 2$. From (3.9) one can see that this requirement fixes p to be an odd integer. Therefore, these partition functions describe the Laughlin plateaus $\nu = 1, 1/3, 1/5, \ldots$

- One can also verify that all the excitations have integer monodromies with respect to the electrons:
$$J[n_e] + J[n] - J[n_e + n] \in \mathbb{Z} \ , \tag{3.18}$$
where $(n_e = p, n)$ denote the integer labels in (3.9) for the electron and a generic excitation, respectively.

Let us add more comments about the main result of this section, Eqs.(3.17),(3.12). The non-holomorphic prefactor added to the characters in (3.12) is the constant term in the Hamiltonian (3.1), appropriately tuned to have the spectrum:

$$E_{n_L,n_R} = \frac{1}{R}\frac{1}{2p}\left[(n_L + RV_o)^2 \ + \ (n_R - RV_o)^2\right] \ , \tag{3.19}$$

whose minimum is independent of the the value of V_o. Actually, this is necessary for the invariance of Z under the spectral flow, and it amounts to adding a capacitive energy to the edges equal to $E_c = RV_o^2/2p$. This prefactor also appears in the quantization of the Chern-Simons theory on the space torus, in the measure for the wave-functions inner product [35].

A more explicit form of the partition function (3.17) is,

$$Z = \frac{\mathrm{e}^{-\dfrac{2\pi(\mathrm{Im}\ \zeta)^2}{p\ \mathrm{Im}\ \tau}}}{|\eta|^2} \sum_{\lambda=0}^{p-1} \sum_{k,\bar{k}\in\mathbb{Z}} q^{\frac{(pk+\lambda)^2}{2p}} \bar{q}^{\frac{\left(p\bar{k}+\lambda\right)^2}{2p}} w^{\frac{pk+\lambda}{p}} \bar{w}^{\frac{p\bar{k}+\lambda}{p}} \ . \tag{3.20}$$

This expression is *not* the same as the well-known partition function of a real bosonic field compactified on a rational circle of radius $R_c = r/2s$ [47],

$$Z_B = \frac{1}{|\eta|^2} \sum_{n,m\in\mathbb{Z}} q^{\frac{1}{2}\left(\frac{n}{2R_c} + mR_c\right)^2} \bar{q}^{\frac{1}{2}\left(\frac{n}{2R_c} - mR_c\right)^2} \ . \tag{3.21}$$

Indeed, after setting $\zeta = 0$, Z and Z_B would be equal for $R_c = 1/p$, which would require p *even*. Therefore, the RCFT of the Laughlin plateaus is an *odd* modification of the rational compactified boson, which is only invariant under the subgroup Γ_θ of the modular group.

The partition function in Eq. (3.17) is the diagonal partition function of the extended algebra. The field that extend the algebra is the electron field, the unique primary field that is local with respect to all the others. The same method can be applied for Jain's states [69] corresponding to the Abelian multicomponent theory $\widehat{U(1)}^m$ for $\nu = \frac{m}{2sm\pm1}$.

For more general QH states whose conformal algebra is given by the product $\widehat{U(1)} \times \widehat{\mathfrak{g}}$, a more detailed constructive method for obtaining the spectrum and the partition function is necessary. We should focus on the role of the electron field as the field that extends the maximal chiral algebra of the RCFT [14, 47].

3.1.4 Physical conditions for the spectrum

The construction of RCFTs for quantum Hall states, both Abelian and non-Abelian, has been relying on a set of conditions for the spectrum of charge and statistics that implement the properties of electron excitations [77]; they should have:

A) integer charge;

B) Abelian fusion rules with all excitations;

C) fermionic statistics among themselves (half-integer spin);

D) integer statistics with all other excitations (integer exponent of mutual exchange).

The charge operator is $\hat{Q} = \frac{\mathsf{c}}{2\pi} \oint \mathrm{d}z \partial\varphi_c$, condition (A) fix the normalization constant,

$$\mathsf{c} = \alpha_e^{-1} \,. \tag{3.22}$$

The (B) and (D) conditions characterize the operator-product expansion of the conformal field $\Phi_e(z)$, representing the electron, with the field $\Phi_i(w)$ of a quasiparticle: for $z \to w$, this is,

$$\Phi_e(z)\ \Phi_i(w) \sim (z-w)^{h_{ei}}\ \ \Phi_{e\times i}(w) \ . \tag{3.23}$$

The mutual statistics exponents is given by the conformal dimensions,

$$h_{ei} = -h_e - h_i + h_{e\times i} \ , \tag{3.24}$$

respectively of: the electron field, the i-th quasiparticle and their fusion product, $\Phi_{e\times i} = \Phi_e \times \Phi_i$. In general, excitations are made of a neutral part, described by a non-trivial RCFT $\widehat{\mathfrak{g}}$, and by a charged part (Luttinger liquid, i.e. a $\widehat{U(1)}$ RCFT) [47]: the fields in the above formulas are made of neutral and charged parts, and their dimensions h have contributions from both of them. The requirement of integer statistics of the electron with all excitations, $h_{ei} \in \mathbb{Z}$, is motivated by the properties of many-body wave functions (describing, e.g. states with a quasiparticle of i-th type), that are described by conformal blocks of the same RCFT for edge excitations (*c.f.* chapter 2.5).

The condition of Abelian fusion rules restricts to one the number of terms in the r.h.s. of the operator product expansion (3.23): indeed, if there were more terms, all the corresponding h_{ei} exponents would need to be simultaneously integer, a condition generically impossible to achieve. Even if it were satisfied, this would lead to a degeneracy of n-electron wave functions and to a unacceptable degenerate ground state. Non-Abelian fusion rules and associated degeneracies (the quantum dimensions d_a) are possible for quasiparticles but not for electrons (within the RCFT description, at least [78]).

Let us anticipate some results of the following analysis of the A-D condictions on non-Abelian Hall states. The point (B) imposes the neutral algebra $\widehat{\mathfrak{g}}_k$ to have at least one simple current (V^{ℓ_e} in in eq. (2.50)) to be associated to the electron field. Condition (C) fixes the possible values of α_e^2 in Eq. (2.50): that depend on the algebra $\widehat{\mathfrak{g}}_k$ that we are considering. In general, in this procedure two integers $\hat{p}$ and $p = \hat{p}p'$ emerge and they determine $\alpha_e^2 = \frac{\hat{p}}{p'}$ (α_e is defined in Eq. (2.50)). According to the relations between QHE and RCFT, from the ground state, *i.e.* from the correlation function of electron fields, the filling fraction $\nu = 2 + \frac{p'}{\hat{p}}$ is also obtained. This procedure shows that the choice of $\widehat{\mathfrak{g}}$ fixes $\hat{p}$, p' and thus ν.

The last point (D) imposes to consider only fields that are local with respect to the electron, *i.e.* $h_{ei} \in \mathbb{Z}$, and are primary fields with respect to the maximal extended algebra. This establishes a selection rule coupling the values of α_i and the ℓ_i weight of $\widehat{U(1)}$ and $\widehat{\mathfrak{g}}$ parts, respectivelly. Other fields in the original theory made by arbitrary combinations of those of the $\widehat{U(1)}$ and $\widehat{\mathfrak{g}}$ RCFT are not connect with physical excitations. In all cases that we will consider, the possible values of charge and conformal dimension of the charge sector, match with the spectrum of a compatified chiral boson on a circle with radius $\sqrt{p}$ [47, 62], up to rescaling the chemical potential by a factor p'.

3.1.5 Electron field as simple current and modular invariance

The RCFT description of Hall fluids suggests to relate the quasiparticles with primary fields of the maximal extended algebra. The corresponding characters are sums of product of characters:

$$\chi^{\ell}(\tau) K_q(\tau, p'\zeta, p)\,, \tag{3.25}$$

where χ^{ℓ} and K_q are the characters of $\widehat{\mathfrak{g}}$ and $\widehat{U(1)}_p$ with highest weight ℓ and q, respectively, whose values are related by a selection rule.

The physical fields Φ_i can be devided in equivalence classes, one class contains all the fields obtained by adding any number of electron to a given quasiparticles, $\Phi_{e^b \times i} = (\Phi_e)^b \Phi_i$. The conformal dimension (charge) of fields in the same classes differ by a half integer (integer) and the monodromy properties of these fields are the same. There is at least one such class for each value of fractional charge. The representative of a class is chosen to be the field with smaller electric charge. The identity field (I) and the electron field (Φ_e) belong to the same class.

The equivalence classes are representations of the algebra extended by the electrons fields [14]. The CFT gives the standard method to obtain the characters and therefore

the partition function for an extended algebra [47, 79, 68], where the field (current) generating the algebra is a simple current introduced in section 2.2.2.

In the following, we show that the electron conditions (A)-(D) can be re-derived from the requirement of modular invariance of the partition function. We find that, upon choosing the RCFT for the neutral part of excitations and identifying the field representing the electron, the modular conditions are sufficient to self-consistently determine the charge and statistics spectrum, as well as the filling fraction*, without the need of additional physical hypotheses.

Let us compare (A)-(D) with the modular conditions introduced in the previous section for Laughlin states. The condition (A) is clearly the same as the U modular invariance (3.7), whose solution is the extended character θ_λ (3.5), that resums electron excitations added to the λ quasiparticle.

The condition (B) of Abelian fusion rules of the electron has a natural correspondent in RCFT, where a field with such property is called a "simple current" J ($\equiv \Phi_e$). The notion of simple current was introduced for orbifold theories, as we now briefly recall [47, 79].

The action of the simple current is indicated by $J \times \Phi_i = \Phi_{J(i)} (\equiv \Phi_{e\times i})$; it implies an Abelian discrete symmetry in the theory that is generated by $\exp(2i\pi Q_J)$, with:

$$Q_J(\Phi_i) = h_J + h_i - h_{J(i)} \qquad \text{mod } 1. \tag{3.26}$$

This charge is the exponent for the monodromy discussed in (3.24) and is conserved in the fusion rules. The fields Φ_i can be organized in orbits, each orbit containing the fields generated by the repeated fusion with the simple current. The simple current and its powers generate an Abelian group by fusion that is called the "center" $\mathcal{G}$ of the conformal field theory.

The modular invariant partition function can be obtained by the orbifold construction corresponding to modding out the symmetry associated to the simple current. The result has the general form [79]:

$$Z = \sum_{\text{orbits } a|\ Q_J(a)=0} |\mathcal{S}_a| \left| \sum_{J\in\mathcal{G}/\mathcal{S}_a} \chi_{J(i_a)} \right|^2 = \sum_a |\theta_a|^2 ; \tag{3.27}$$

in this equation, a labels the orbits, i_a is a representative point on each orbit, and $|\mathcal{S}_a|$ is the order of the stabilizer $\mathcal{S}_a$ of the orbit a, i.e. the subgroup of $\mathcal{G}$ acting trivially on any element i in a. The proof of the general expression (3.27) is not trivial and it involves the symmetry of the S matrix under the J action: $S_{i,J(k)} = S_{i,k} \exp(2i\pi Q_J(i))$. The modular invariants (3.27) can be considered as diagonal invariants with respect to the basis of the extended chiral algebra, whose characters are θ_a. In the QHE case, the stabilizer is trivial and the J action has no fixed points, owing to the additivity of the physical charge carried by the electron [80]. We recognize in (3.26),(3.27), the (D) condition (3.24) derived from QHE wave functions.

* And the spin parts, for non-polarized Hall fluids.

In the cases that are considered, in this work the sum of characters $\chi_{J(i_a)}$ in (3.27), denoted by θ_a^ℓ, look like:

$$\theta_a^\ell = \sum_{b=0}^{p'-1} \chi^{J^b \ell}(\tau) K_{a+b\hat{p}}(\tau, x\zeta, p)\,, \tag{3.28}$$

where the (a, ℓ) are the quantum number of the representative of the class. The characters (3.28) are the sum of all the physical primary fields that are obtained by the fusion with some electrons (*i.e.* they differ by the addition of electrons on the edge). The number of independent characters is equivalent to the topological order [69] and it is $p|P_k^+|/(p'^2)$ (for BS and NASS there is some difference that are reported in the following).

Let us further analyze the solution (3.27); the T^2 invariance of the extended characters for the ground state and a-th quasiparticles, respectively θ_0 and $\overline{\theta}_a$, implies:

$$2\ h_e = M\ , \qquad 2\ h_{e\times i} - 2\ h_i = N\ , \qquad M, N \text{ integers.} \tag{3.29}$$

The condition (C) of half-integer electron spin requires M to be odd, i.e the even case is excluded for physical reasons (although sometimes allowed for bosonic fluids). Therefore, we should consider algebra extensions by half-integer spin currents, as in the case of the Neveu-Schwarz sector of supersymmetric theories [47].

In conclusion, we have re-derived the standard physical conditions (A)-(D) on Hall excitations from modular invariance of RCFT partition functions. They have been found to be diagonal invariants for extended symmetry algebras that are obtained in the orbifold construction through simple currents (in the present case without fixed points) [79].

In the following analysis of non-Abelian Hall fluids, we shall find that the (A)-(D) conditions (i.e. modular invariance) straightforwardly determine the charge and statistics spectrum of excitations, for a given choice of neutral RCFT and electron field (simple current). These results are relevant for model building: in the literature, the derivation of the theory pertaining to a given plateau often involves a combination of technical arguments and physical arguing, that might suggest a certain degree of arbitrariness in the construction of the theory, which is however not present.

We remark that the neutral RCFT may possess more than one simple current that could be used as electron field, although a preferred choice may exist, e.g. the lowest-dimensional field. This cannot be considered as an ambiguity of the construction, because the choice of electron field is part of the definition of the theory: different electrons correspond to different Hall states, with different charge spectra, filling fraction etc, all quantities being determined self-consistently.

Another possibility for RCFTs with two simple currents is that of using both of them simultaneously for building a modular invariant with further extended symmetry, but its physical interpretation remains to be understood.

3.1.6 Disk geometry

From the annulus partition function (3.17), we can deduce the disk partition function by letting the inner radius to vanish, $R_L \to 0$ (see Fig. 3.2(b)). To this effect, the variable $\overline{\tau}$ in $\overline{\theta}_\lambda$ should be taken independent of τ: Im $\tau \neq -$Im $\overline{\tau}$, $v_R/R_R \neq v_L/R_L$. The annulus partition function is no longer a real positive quantity but remains modular invariant, up to irrelevant global phases. In the limit $R_L \to 0$, the $\overline{\theta}_\lambda$ are dominated by their $|q| \to 0$ behavior: therefore, only the ground state sector remains in (3.17), leading to $\overline{\theta}_\lambda \to \delta_{\lambda,0}$, up to zero-point energy contributions. We find: $Z^{(0)}_{\rm disk} = \theta_0$. If, however, there are quasiparticles in the bulk with charge, $Q_{\rm Bulk} = -a/q$, the condition of total integer charge selects another sector, leading to:

$$Z^{(\lambda)}_{\rm disk} = \theta_\lambda \ . \tag{3.30}$$

Therefore, the disk partition functions are given by the chiral generalized characters θ_λ, whose index is selected by the bulk boundary conditions. The set of functions is modular covariant, i.e. it carries a unitary finite-dimensional representation of the modular group, as shown by (3.16).

These partition functions describe the edge physics of isolated Hall droplets with static bulk quasiparticles. Note that each sector has a specific lower-state energy that has been discarded in (3.30): indeed, it is difficult to compare edge energies of different sectors in the disk geometry, because they depend on the external work for adding gapful bulk quasiparticles and other environmental effects [62].

3.2 Building partition functions for the SLL

In this section we obtain the partition functions for non-Abelian states that have been proposed to describe plateaus with $2 < \nu < 3$: Read-Rezayi states [66], the Wen non-Abelian fluids (NAF) [76], the anti-Read-Rezayi states ($\overline{\rm RR}$) [74], the Bonderson-Slingerland hierarchy (BS) [75], and finally, the non-Abelian spin-singlet state (NASS) [15][58]. All these states have been considered as phenomenologically interesting in the recent literature searching for signatures of non-Abelian statistics in the quantum Hall effect. The filling that are consider in the work are reported in the Fig. 3.

From the technical point of view, non-Abelian states can be built out of the $\widehat{U(1)}_p$ charged part and a neutral part given by any RCFT that possess at least one "simple current" [47], a field with Abelian fusion rules that can be identified as the electron excitation. However, only a limited number of such constructions have received support by $(2+1)$-dimensional microscopic physics, that is based on wave-functions and analytic/numerical study of spectra searching for corresponding incompressible states.

3.2.1 Read-Rezayi states

In the following, the conditions (A)-(D) will be illustrated by rederiving the spectrum and partition functions [67] [72] of Read-Rezayi states [66] with filling fractions:

$$\nu = 2 + \frac{k}{kM+2} \ , \qquad k = 2, 3, \ldots , \quad M = 1, 3, \ldots \tag{3.31}$$

The Read-Rezayi theory is based on the neutral $\mathbb{Z}_k$ parafermion theory (PF_k) with central charge $c = 2(k-1)/(k+2)$, that can be described by the standard coset construction $\mathrm{PF}_k = \widehat{SU(2)}_k/\widehat{U(1)}_{2k}$ [52]. Form the coset, we find that neutral sectors are characterized by a pair quantum numbers for the representations of the algebras in the numerator and denominator: these are (ℓ, m), equal to twice the $SU(2)$ spin and spin component, respectively ($m = \ell \bmod 2$).

The dimensions of parafermionic fields ϕ^ℓ_m are given by:

$$\begin{aligned} h^\ell_m \ &= \ \frac{\ell(\ell+2)}{4(k+2)} - \frac{m^2}{4k} \ , \\ &\qquad \ell = 0, 1, \ldots , k, \qquad -\ell < m \leq \ell, \quad \ell = m \bmod 2 \ . \end{aligned} \tag{3.32}$$

The $\mathbb{Z}_3$ parafermion fields are shown in Fig. 3.3: the coset construction implies that the m charge is defined modulo $2k$ [52]; indeed, the fields are repeated once outside the fundamental (ℓ, m) domain (3.32) by the reflection-translation, $(\ell, m) \to (k-\ell, m+k)$,

$$\phi^\ell_m = \phi^{k-\ell}_{m-k} \ , \qquad \ell = 0, 1, \ldots , k, \qquad l < m \leq 2k - l \ , \tag{3.33}$$

also called "field identification" [81].

The fusion rules are given by the addition of the $\widehat{SU(2)}_k$ spin and $\widehat{U(1)}_{2k}$ charge:

$$\phi^\ell_m \cdot \phi^{\ell'}_{m'} = \sum_{\ell''=|\ell-\ell'|}^{\min(\ell+\ell', 2k-\ell-\ell')} \phi^{\ell''}_{m+m' \bmod 2k} \ . \tag{3.34}$$

The fields in the theory are called: parafermions, $\psi_j = \phi^0_{2j}$, $j = 1, \ldots , k-1$; spin fields, $\sigma_i = \phi^i_i$; and other fields. The parafermions have Abelian fusion rules with all the fields; among themselves, these are: $\psi_i \times \psi_j = \psi_n$, with $n = i + j \bmod k$. The basic parafermion ψ_1 represents the neutral component of the electron in the Read-Rezayi states: the fusion $(\psi_1)^k = I$, describes the characteristic clustering of k electrons in the ground state-wave function [66].

The excitations of the full theory are found by attaching $\widehat{U(1)}$ vertex operators to the parafermion fields: for the electron and a generic quasiparticle, we write,

$$\Phi_e = e^{i\alpha_0\varphi} \ \psi_1 \ , \qquad \Phi_i = e^{i\alpha\varphi} \ \phi^\ell_m \ , \tag{3.35}$$

with triplets of quantum numbers $(\alpha_0, 0, 2)$ and (α, ℓ, m), respectively. The mutual statistics exponent (3.24) is,

$$h_{ei} = \frac{(\alpha+\alpha_0)^2 - \alpha^2 - \alpha_0^2}{2} + h^\ell_{m+2} - h^\ell_m - h^0_2 \ . \tag{3.36}$$

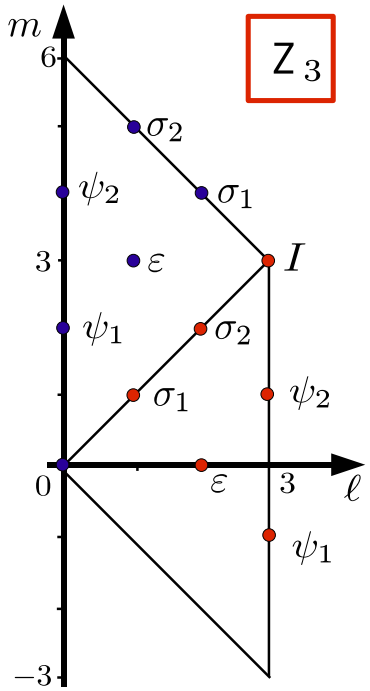

Figure 3.3: Diagram of $\mathbb{Z}_3$ parafermion fields with field symbols

Upon substituting (3.32), the conditions (D) reads:

$$(D) \ : \ \alpha\alpha_0 - \frac{m}{k} = N, \qquad \text{integer.} \tag{3.37}$$

In particular, for the electron with itself, we find $\alpha_0^2 - 2/k = M$ integer; in combination with the condition (C) of half-integer electron spin,

$$(C) \ : \ 2h_e = 2h_2^0 + \alpha_0^2 = 2 + M, \qquad \text{odd integer,} \tag{3.38}$$

it determines,

$$\alpha_0^2 = \frac{2 + kM}{k}, \qquad M \text{ odd integer.} \tag{3.39}$$

The electric charge Q of excitations is proportional to the $\widehat{U(1)}$ charge, $Q = \mu\alpha$: the constant μ is fixed by assigning $Q = 1$ to the electron, i.e. $\mu = 1/\alpha_0$ ((A) condition).

In conclusion, the (A)-(D) conditions determine the charge and spin (i.e. half statistics) of excitations in the Read-Rezayi theory as follows:

$$Q = \frac{\alpha\alpha_0}{\alpha_0^2} = \frac{Nk + m}{2 + Mk} = \frac{q}{2 + Mk} \ , \tag{3.40}$$

$$J = h_m^\ell + \frac{1}{2}Q^2\alpha_0^2 = h_m^\ell + \frac{q^2}{2k(2 + kM)} \ . \tag{3.41}$$

The excitations are characterized by triplets of integer labels (q, ℓ, m), where q is the charge index. From the Abelian part of conformal dimensions (3.41), we find that

the Luttinger field is compactified into p sectors (cf. (3.12)), $p = k(2 + kM)$, and is indicated by $\widehat{U(1)}_p$; the charge index q is thus defined modulo p. We write $p = k\hat{p}$, where $\hat{p} = 2 + kM$ is the denominator of the fractional charge; moreover, equation (3.40) shows that q is coupled to the $SU(2)$ spin component m by the selection rule:

$$q = m \mod k \ , \qquad (q \mod \hat{p} = (kM + 2) \ , \quad m \mod 2k) \, . \tag{3.42}$$

We thus recover the $\mathbb{Z}_k$ "parity rule" of Ref. [67] that constraints charge and neutral quantum numbers of Read-Rezayi quasiparticle excitations. Earlier derivations of this rule were based on some physical conditions, such as a relation with a "parent Abelian state", that were useful as motivations but actually not necessary (see, however, section 4.1.1). The present derivation shows that the relevant information is the type of RCFT for neutral excitations and the identification in this theory of the field ψ_1 representing the electron.

As outlined in the previous section, the U symmetry (3.7) requires to put each basic anyon together with its electron excitations, leading to sectors of charge $Q = \lambda/p + \mathbb{Z}$ described by the RCFT extended character θ_λ as in (3.12). The addition of an electron changes the integer labels of excitations as follows:

$$(q, m, \ell) \ \rightarrow \ (q + \hat{p}, m + 2, \ell) \ . \tag{3.43}$$

Therefore, the extended characters θ_λ of the theory $PF_k \otimes \widehat{U(1)}_p$ are made of products of characters of the charged and neutral parts, whose indices obey the parity rule (3.42) and are summed over according to (3.43). The charged characters are given by the functions $K_q(\tau, k\zeta; k\hat{p})$ introduced earlier in (3.12), with parameters chosen to fit the fractional charge and the Abelian conformal dimension in (3.40). The $\mathbb{Z}_k$ parafermionic characters are denoted by $\chi^\ell_m(\tau; 2k)$ and have rather involved expressions; actually it is enough to know their periodicities,

$$\begin{aligned} \chi^\ell_m &= \chi^\ell_{m+2k} = \chi^{k-\ell}_{m+k} \ , \quad m = \ell \bmod 2, \\ \chi^\ell_m &= 0 \qquad\qquad\qquad\quad m = \ell + 1 \bmod 2 \ , \end{aligned} \tag{3.44}$$

and modular transformation:

$$\begin{aligned} \chi^\ell_m \left(-1/\tau; 2k\right) &= \frac{1}{\sqrt{2k}} \sum_{\ell'=0}^{k} \sum_{m=1}^{2k} e^{-i2\pi \frac{mm'}{2k}} \ s_{\ell,\ell'} \ \chi^{\ell'}_{m'}(\tau; 2k) \ , \\ s_{\ell,\ell'} &= \sqrt{\frac{2}{k+2}} \ \sin\left(\frac{\pi(\ell+1)(\ell'+1)}{k+2}\right) \ . \end{aligned} \tag{3.45}$$

As recalled in Appendix B.4, this transformation can be obtained from the coset construction $PF_k = \widehat{SU(2)}_k / \widehat{U(1)}_{2k}$ [52].

The extended characters are thus given by products $K_q \chi^\ell_m$, with $q = m \bmod k$ and $\ell = m \bmod 2$: adding one electron to the earlier product gives the term $K_{q+\hat{p}} \chi^\ell_{m+2}$; by

continuing to add electrons until a periodicity is found, one obtain the expressions †,

$$\begin{aligned} \theta_a^\ell &= \sum_{b=1}^{k} K_{a+b\hat{p}}(\tau, k\zeta; k\hat{p})\ \chi^\ell_{a+2b}(\tau; 2k)\ , \\ & \quad a = 0, 1, \ldots, \hat{p}-1,\ \hat{p} = kM+2, \\ & \quad \ell = 0, 1, \ldots, k, \\ & \quad a = \ell \bmod 2, \end{aligned} \tag{3.46}$$

that reproduce the charge and statistics spectrum (3.40), (3.41).

The expression (3.46) corresponds to the following solution of the parity rule (3.42):

$$\begin{aligned} & q = a + b\hat{p}, \qquad a = 1, \ldots, \hat{p}, \qquad b = 1, \ldots, k\ , \\ & m = a + 2b\ , \end{aligned} \tag{3.47}$$

(note $\hat{p} = 2 \bmod k$). The other solution $m = k + a + 2b \bmod 2k$ would lead to the same expressions with shifted index, $\theta_a^{k-\ell}$, owing to the field identification of parafermion fields $(\ell, m) \sim (k-\ell, m \pm k)$.

The θ_a^ℓ characters have the periodicity, $\theta^\ell_{a+\hat{p}} = \theta_a^{k-\ell}$, that explains the ranges of indices indicated in (3.46); the dimension of the basis of θ_a^ℓ characters is therefore given by $\hat{p}(k+1)/2$, in agreement with the value of the topological order of Read-Rezayi states [66] [67]. Moreover, the V transformation of these characters reads, $\theta_a^\ell(\zeta+\tau) \sim \theta(\zeta)^{k-\ell}_{a+k}$, showing that the charge $\Delta Q = k/\hat{p}$ is created by adding one flux quantum: we thus recover the value of the filling fraction $\nu = k/(Mk+2)$ with M odd.

The final step is to find the modular transformations of θ_a^ℓ, that is given by [72] (see Appendix A):

$$\theta_a^\ell(-1/\tau) = \delta^{(2)}_{a,\ell}\ \frac{1}{\sqrt{\hat{p}}} \sum_{a'=1}^{\hat{p}} \sum_{\ell'=0}^{k}\ e^{-i2\pi \frac{aa'M}{2\hat{p}}}\ s_{\ell,\ell'}\ \theta^{\ell'}_{a'}(\tau), \tag{3.48}$$

where the delta modulo two tells that $\theta_a^\ell(-1/\tau)$ vanishes for $a = \ell + 1 \bmod 2$ (we also disregard the global phase $\propto \mathrm{Re}\ (\zeta^2/\tau)$ acquired by the characters). In Appendix A, the check of the unitarity of the S matrix confirms that the extended characters θ_a^ℓ form an independent basis.

We remark that the coupling of neutral and charged parts by the $\mathbb{Z}_k$ parity rule and the sum over electron excitations amounts to a projection in the full $K_\lambda \chi^\ell_m$ tensor space to a subspace of dimension $1/k^2$ smaller: this reduction by a square factor is a standard property of S transformations (i.e. discrete Fourier transforms). We also note that the S matrix is factorized into charged and neutral parts, where the latter is the naive expression for the $\widehat{SU(2)}_k$ part, although the sectors are not factorized at all, as shown by the extended characters θ_a^ℓ.

Finally, the annulus partition function of Read-Rezayi states is given by the diagonal sesquilinear form,

$$Z^{\mathrm{RR}}_{\mathrm{annulus}} = \sum_{\ell=0}^{k} \sum_{\substack{a=0 \\ a=\ell \bmod 2}}^{\hat{p}-1} \Big|\ \theta_a^\ell\ \Big|^2\ , \tag{3.49}$$

† Hereafter, we disregard the non-analytic prefactor of K for ease of presentation.

that solves the (S, T^2, U, V) conditions of section 2.2.

For example, the expression of the $k = 2$ Pfaffian state is as follows. The $\mathbb{Z}_2$ parafermions are the three fields of the Ising model: $\phi_0^0 = \phi_2^2 = I$, $\phi_1^1 = \phi_3^1 = \sigma$ and $\phi_2^0 = \phi_0^2 = \psi$, of dimensions $h = 0, 1/16, 1/2$, respectively. For $\nu = 5/2$, i.e. $M = 1$ in (3.31), the Pfaffian theory possesses 6 sectors. The partition function is:

$$\begin{aligned} Z_{\text{annulus}}^{\text{Pfaffian}} &= |K_0 I + K_4 \psi|^2 + |K_0 \psi + K_4 I|^2 + |(K_1 + K_{-3})\,\sigma|^2 \\ &+ |K_2 I + K_{-2} \psi|^2 + |K_2 \psi + K_{-2} I|^2 + |(K_3 + K_{-1})\,\sigma|^2 \ . \end{aligned} \tag{3.50}$$

where the neutral characters are written with the same symbol of the field and the charged ones are, $K_\lambda = K_\lambda(\tau, 2\zeta; 8)$, $K_\lambda = K_{\lambda+8}$, with charge $Q = \lambda/4 + 2\mathbb{Z}$. The first square term in Z describes the ground state and its electron excitations, such as those in $K_4\psi$ with $Q = 1 + 2\mathbb{Z}$; in the third and sixth terms, the characters $K_{\pm 1}\sigma$ contain the basic quasiparticles with charge, $Q = \pm 1/4$, and non-Abelian fusion rules $\sigma \cdot \sigma = I + \psi$. The other three sectors are less familiar: the second one contains a neutral Ising-fermion excitation (in $K_0\psi$) and the 4th and 5th sectors describe $Q = \pm 1/2$ Abelian quasiparticles.

As in section 2.1, the partition function on the disk is given by the extended character θ_a^ℓ, with indices selected by the quasiparticle type in the bulk; if there are many of them, their indices are combined by using the fusion rules to find the edge sector (a, ℓ).

In conclusion, the annulus and disk partition functions completely determine the Hilbert space of edge excitations and the fusion rules through the Verlinde formula. Physical applications to current experiments will be describe in chapter 4.

3.2.2 $SU(2)$ non-Abelian fluids

Starting from the physical idea of breaking the electron excitation into k fermions called "partons", Block and Wen [76] considered the natural choice of RCFT with affine symmetry $\widehat{SU(m)}_k$ and the associated $SU(m)$ non-Abelian Chern-Simons theory. In such theories, there always are one or more simple currents. We shall limit ourselves to the simplest $SU(2)$ case, that has been recently considered in relation with the physics of second Landau level [44][82] and also serves as a starting point for other non-Abelian fluids.

We shall obtain the annulus partition function for the RCFT $\widehat{SU(2)}_k \otimes \widehat{U(1)}_p$. The $\widehat{SU(2)}_k$ theory is characterized by the primary fields ϕ^ℓ, for $\ell = 0, 1, \ldots, k$, with dimensions $h_\ell = \ell(\ell+2)/(4(k+2))$. The simple current is ϕ^k with $h_k = k/4$ and fusion rules given by (cf. (3.34)):

$$\phi^k \times \phi^\ell = \phi^{k-\ell} \ , \qquad 0 \le \ell \le k \ , \tag{3.51}$$

which realizes a $\mathbb{Z}_2$ parity among the neutral sectors. Following the steps outlined in section 2.2, we introduce the fields $\Phi_e = \phi^k \exp(i\alpha_0\varphi)$, $\Phi_i = \phi^\ell \exp(i\alpha\varphi)$ corresponding to the electron and to a quasiparticle excitation, respectively.

The condition (D) on the mutual statistics exponent (3.24) of these excitations and

of the electron with itself imply, respectively:

$$\alpha\alpha_0 = \frac{2N+\ell}{2} \ , \qquad \alpha_0^2 = \frac{2M+k}{2} \ , \qquad N, M \in \mathbb{Z}. \tag{3.52}$$

The charge and spin of excitations are therefore:

$$\begin{aligned} Q &= \frac{\alpha}{\alpha_0} = \frac{2N+\ell}{2M+k} = \frac{q}{2M+k} \ , \qquad M+k \ \text{ odd integer}, \\ J &= h^\ell + \frac{1}{2}Q^2\alpha_0^2 = \frac{\ell(\ell+2)}{4(k+2)} + \frac{q^2}{4(2M+k)} \ . \end{aligned} \tag{3.53}$$

In particular, the condition (C) of half-integer electron spin requires that $(M+k)$ is odd.

The $\widehat{U(1)}_p$ contribution to the J spectrum identifies the compactification parameter $p = 2\hat{p}$, with $\hat{p} = (2M+k)$ the fractional-charge denominator. A quasiparticle is characterized by the integer pair $(\ell, 2N+\ell)$ of $SU(2)$ spin and charge, that are constrained by the parity rule: $q = \ell \bmod 2$. The additions of one (two) electrons to a quasiparticle cause the following shifts (i.e. changes of sector):

$$(\ell, 2N+\ell) \ \rightarrow \ (k-\ell, 2N+\ell+\hat{p}) \ \rightarrow \ (\ell, 2N+\ell+2\hat{p}) \ , \tag{3.54}$$

that involves two non-Abelian sectors only.

Therefore, we are lead to consider extended characters θ_a^ℓ of the full theory, labeled by spin ℓ and charge a indices, that are made of products of charged characters, $K_q = K_q(\tau, 2\zeta; 2\hat{p})$ in the notation of (3.12), and $\widehat{SU(2)}_k$ characters $\chi^\ell(\tau)$, as follows:

$$\theta_a^\ell = K_a \ \chi^\ell + K_{a+\hat{p}} \ \chi^{k-\ell} \ , \qquad \begin{array}{l} a = 0, 1, \ldots, \hat{p}-1, \ \hat{p} = 2M+k, \\ \ell = 0, 1, \ldots, k, \\ a = \ell \bmod 2. \end{array} \tag{3.55}$$

Note that only two terms are needed in the sums, owing to the mentioned $\mathbb{Z}_2$ symmetry. As explained in section 2.2, the topological order of the $SU(2)$ NAF is given by the number of independent θ_a^ℓ characters: the symmetry $\theta_{a+\hat{p}}^{k-\ell} = \theta_a^\ell$ confirms the index ranges indicated in (3.55). Furthermore, the filling fraction can be obtained from the V transformation of K_a characters: in summary, the $SU(2)$ NAF fluids are characterized by the values,

$$T.O. = (k+1)\frac{2M+k}{2} \ , \qquad \nu = \frac{2}{2M+k} \ , \qquad M+k \text{ odd}. \tag{3.56}$$

The modular transformations of extended characters can be obtained by those of the components K_a and χ^ℓ introduced in earlier sections: the result is (see Appendix A):

$$\theta_a^\ell(-1/\tau) = \frac{1}{\sqrt{\hat{p}}} \sum_{a'=0}^{\hat{p}-1} \sum_{\ell'=0}^{k} \ \delta_{a,\ell}^{(2)} \ e^{i2\pi\frac{aa'}{2\hat{p}}} \ s_{\ell,\ell'} \ \delta_{a',\ell'}^{(2)} \ \theta_{a'}^{\ell'}(\tau), \tag{3.57}$$

where $s_{\ell,\ell'}$ is the $\widehat{SU(2)}_k$ S-matrix (3.45). The S-matrix of the full theory is again factorized in Abelian and non-Abelian parts (up to details) and is unitary.

In conclusion, the annulus partition function is given by the diagonal combination of extended characters,

$$Z^{\rm NAF}_{\rm annulus} = \sum_{\ell=0}^{k} \sum_{\substack{a=0 \\ a=\ell \bmod 2}}^{\hat{p}-1} \left| \theta^\ell_a \right|^2 , \tag{3.58}$$

with ranges of parameters given by (3.55). Each individual θ^ℓ_a is the partition function on the disk geometry in presence of a specific bulk excitation.

3.2.3 Anti-Read-Rezayi fluids

It has been recently proposed [74] that a particle-hole conjugate of the $M = 1$ Read-Rezayi fluids could be realizable in the second Landau level, with filling fractions $\nu - 2 = 1 - k/(k+2) = 2/(k+2)$. In particular, for $\nu = 5/2$ the Pfaffian state may compete with its conjugate state. The fluid of RR holes inside the $\nu = 3$ droplet possesses an additional edge, leading to the CFT $\overline{SU(2)_k/U(1)_{2k} \otimes U(1)_p} \otimes \widehat{U(1)}$. The Luttinger liquids on edges of opposite chirality interact through impurities and re-equilibrate: the result of this process was shown to lead to the $\overline{SU(2)_k} \otimes \widehat{U(1)}_p$ edge theory [74] for the so-called anti-Read-Rezayi state ($\overline{\rm RR}$).

The partition function of this theory can be obtained as in the NAF case of the previous section, with little modifications due to the different chirality of the neutral sector. The electron and quasiparticle fields are given by $\Phi_e = \overline{\phi^k} \exp(i\alpha_0\varphi)$ and $\Phi_i = \overline{\phi^\ell} \exp(i\alpha\varphi)$, respectively (note that ϕ^k is the unique simple current of the $\widehat{SU(2)}_k$ theory).

In the mutual statistics exponent, the chiral and antichiral conformal dimensions should be subtracted leading to the conditions,

$$\alpha\alpha_0 = \frac{2N-\ell}{2} , \qquad \alpha_0^2 = \frac{2M+k}{2} , \qquad N, M \in \mathbb{Z}. \tag{3.59}$$

The charge and spin of excitations are therefore:

$$\begin{aligned} Q &= \frac{\alpha}{\alpha_0} = \frac{2N-\ell}{2M+k} = \frac{q}{2M+k} , \qquad M \ \text{ odd} \\ J &= -h^\ell + \frac{1}{2}Q^2\alpha_0^2 = -\frac{\ell(\ell+2)}{4(k+2)} + \frac{q^2}{4(2M+k)} . \end{aligned} \tag{3.60}$$

In particular, the condition (C) of half-integer electron spin requires that M is odd.

The $\widehat{U(1)}_p$ compactification parameter is $p = 2\hat{p}$, where $\hat{p} = (2M+k)$ is the denominator of the fractional charge. A quasiparticle is characterized by the integer pair $(\ell, 2N-\ell)$ of $SU(2)$ spin and charge, that are again constrained by $q = \ell \bmod 2$.

Following the same steps of the NAF case (cf. (3.54), (3.55)), we obtain the extended characters θ^ℓ_a,

$$\theta^\ell_a = K_a\, \overline{\chi^\ell} + K_{a+\hat{p}}\, \overline{\chi^{k-\ell}} , \qquad \begin{array}{l} a = 0, 1, \ldots, \hat{p}-1, \ \hat{p} = 2M+k, \\ \ell = 0, 1, \ldots, k, \\ a = \ell \bmod 2, \end{array} \tag{3.61}$$

that are products of charged characters $K_q = K_q(\tau, 2\zeta; 2\hat{p})$, of same period $p = 2(2M+k)$ as in the NAF case, and conjugate $\widehat{SU(2)}_k$ characters.

The values of topological order and filling fractions of $\overline{\rm RR}$ fluids are given by the NAF expressions (3.56),

$$T.O. = (k+1)\frac{2M+k}{2} \ , \qquad \nu = \frac{2}{2M+k} \ , \quad M \text{ odd}; \tag{3.62}$$

only the parity of M is different. The $M = 1$ case mentioned at the beginning is recovered.

The modular transformations of $\overline{\rm RR}$ (3.61) are the same as in the NAF case (3.57), because the $\widehat{SU(2)}_k$ S-matrix is real and thus not affected by conjugation. The annulus partition function is finally given by:

$$Z^{\overline{\rm RR}}_{\rm annulus} = \sum_{\ell=0}^{k} \sum_{\substack{a=0 \\ a=\ell \bmod 2}}^{\hat{p}-1} \Big| \ \theta^\ell_a \ \Big|^2 \ . \tag{3.63}$$

3.2.4 Bonderson-Slingerland hierarchy

In Ref. [75], the authors considered the realization of hierarchical Hall states in the second Landau level, that are build over the Pfaffian $\nu = 5/2$ state. In the Jain construction [1], the wave functions are given by $\Psi = \Delta^{2p}\chi_n$, where χ_n is relative to n filled Landau levels and Δ^{2p} is an even power of the Vandermonde factor, leading to the filling fraction $\nu = n/(2pn+1)$. The (projected) Jain wave function, interpreted within the Haldane-Halperin hierarchical construction, can be transposed into the second Landau level, and give rise to the Bonderson-Slingerland wave functions of the form $\Psi = {\rm Pf}(1/(z_i - z_j))\Delta^M\chi_n$, with filling fractions $\nu - 2 = n/(nM+1)$, with M odd.

From earlier studies of edge excitations of Jain states [77], [69], we know that the associated CFT has central charge $c = n$ and is Abelian with extended symmetry $\widehat{SU(n)}_1 \otimes \widehat{U(1)}$: this theory is described by a specific n-dimensional charge lattice that includes the $SU(n)$ root lattice. The Bonderson-Slingerland hierarchy is thus realized by the CFT $\widehat{U(1)}_p \otimes \widehat{SU(n)}_1 \otimes$ Ising, where the last two factors are neutral. The respective conformal dimensions are [47] [72]:

$$\begin{array}{lll} \widehat{U(1)}_p & : & h_\alpha = \frac{\alpha^2}{2} \ , \\ \widehat{SU(n)}_1 & : & h_\beta = \frac{\beta(n-\beta)}{2n} \ , \qquad \beta = 0, 1, \ldots, n-1, \\ \text{Ising} & : & h_m = 0, \ \frac{1}{16}, \ \frac{1}{2} \ , \quad m = 0, 1, 2. \end{array} \tag{3.64}$$

The electron and quasiparticle excitations are made by triplets of fields,

$$\Phi_e = \rho_1 \ \phi^0_2 \exp(i\alpha_0\varphi) \ , \qquad \Phi_i = \rho_\beta \ \phi^\ell_m \exp(i\alpha\varphi) \ . \tag{3.65}$$

In this equation, we indicated the $\widehat{SU(n)}_1$ fields by ρ_β, with β mod n, and the Ising fields by ϕ^ℓ_m in the notation of section 2.3. The index ℓ in ϕ^ℓ_m can be omitted because it is determined by m: indeed, the three Ising fields, the identity, the parafermion and the spin are, respectively, $\phi^0_0 = I$, $\phi^0_2 = \psi$ and $\phi^1_1 = \sigma$, with periodicities, $\phi^0_{m+4} = \phi^0_m$

and $\phi^1_{m+2} = \phi^1_m$. The electron excitation is associated to the parafermion, obeying $\psi \times \psi = 1$, and to the $\widehat{SU(n)}_1$ field with smallest charge $\beta = 1$ (with Abelian fusion rules over β modulo n) [72]. The other fusion rules with the parafermion field are given by $\psi \times \psi = I$ and $\sigma \times \psi = \sigma$.

The excitations are thus associated with triplets (α, β, m), where the index β is mod n and m is mod 4 (2) if even (odd). The condition of integer statistics with the electron $(\alpha_0, 1, 2)$ should be independently computed for the three Ising sectors $m = 0, 1, 2$, leading to conditions that can be summarized into:

$$\alpha\alpha_0 = \frac{2nN + 2\beta + n\delta_{m,1}}{2n} \ , \quad \alpha_0^2 = \frac{nM+1}{n} \ , \qquad N, M \text{ integers.} \tag{3.66}$$

The resulting spectrum is,

$$\begin{aligned} Q &= \frac{2nN + 2\beta + n\delta_{m,1}}{2nM+2} = \frac{q}{2nM+2} \ , \\ J &= \frac{\beta(n-\beta)}{2n} + h_m + \frac{q^2}{4n(2nM+2)} \ . \end{aligned} \tag{3.67}$$

This spectrum identifies the number of $\widehat{U(1)}$ sectors and the value of the charge denominator, $p = 2n\hat{p}$ and $\hat{p} = 2nM + 2$, respectively. The parity rules relating the neutral and charge sectors are:

$$\begin{aligned} q &= 2\beta \qquad\quad \text{mod } 2n, \ m \text{ even}, \\ q &= 2\beta + n \qquad \text{mod } 2n, \ m \text{ odd}. \end{aligned} \tag{3.68}$$

In particular, the condition on half-integer electron spin requires that M is odd.

As in the previous cases, the extended characters should resum the spectra obtained by adding any number of electrons to each anyon: in the Bonderson-Slingerland states, the addition of one electron amount to the following index shifts,

$$(q, \beta, m) \ \rightarrow \ (q + \hat{p}, \beta + 1, m + 2) \ . \tag{3.69}$$

Therefore, we are led to consider the extended characters,

$$\begin{aligned} \theta_{q,m} &= \sum_{b=1}^{2n} K_{q+b\hat{p}}\,(\tau, 2n\zeta; 2n\hat{p}) \ \Theta_{q/2+b} \ \chi^0_{m+2b}, \qquad m = 0, 2, \\ \theta_{q,m} &= \sum_{b=1}^{2n} K_{q+b\hat{p}+n}\,(\tau, 2n\zeta; 2n\hat{p}) \ \Theta_{q/2+b} \ \chi^1_m, \qquad m = 1, \end{aligned} \tag{3.70}$$

where q is even. In this equation the factors $K_a = K_{a+p}$ and $\chi^\ell_m = \chi^\ell_{m+4}$ denote the $\widehat{U(1)}$ and $\mathbb{Z}_2$ parafermion characters introduced earlier, respectively, and the $\Theta_\beta = \Theta_{\beta+n}$ are the $\widehat{SU(n)}_1$ characters described in [72]. From the periodicity property $\theta_{q+\hat{p},m} = \theta_{q,m+2}$, the identity of sectors $m = 1 \sim 3$, and the V transformation of K characters, we obtain the following values for the topological order and filling fraction of the Bonderson-Slingerland states:

$$T.O. = 3(nM+1), \qquad \nu = 2 + \frac{n}{nM+1}, \qquad M \text{ odd}, \tag{3.71}$$

that reduce to those of the Pfaffian state in the $n = 1$ case.

Owing to the fact that $(n, nM+1) = 1$, a representative set of the $(nM+1)$ values of the charge q in the extended characters can be chosen to be $q = 2an$, $a = 0, 1, \ldots, nM$, leading to the characters:

$$\begin{aligned}
\theta_{a,0} &= \sum_{b=1}^{2n} K_{2an+b\hat{p}}\,(\tau, 2n\zeta; 2n\hat{p})\ \Theta_b \left(I\ \delta^{(2)}_{b,0} + \psi\ \delta^{(2)}_{b,1} \right), \qquad m = 0, \\
\theta_{a,1} &= \sum_{b=1}^{2n} K_{(2a+1)n+b\hat{p}}\,(\tau, 2n\zeta; 2n\hat{p})\ \Theta_b\ \sigma\ , \qquad m = 1, \\
\theta_{a,2} &= \sum_{b=1}^{2n} K_{2an+b\hat{p}}\,(\tau, 2n\zeta; 2n\hat{p})\ \Theta_b \left(\psi\ \delta^{(2)}_{b,0} + I\ \delta^{(2)}_{b,1} \right), \qquad m = 2, \\
& \qquad a = 0, 1, \ldots, nM.
\end{aligned} \tag{3.72}$$

where we rewrote the Ising characters with the same symbols of the fields.

The annulus partition function is therefore given by the diagonal combination of these characters,

$$Z^{\rm BS}_{\rm annulus} = \sum_{a=0}^{nM} \mid \theta_{a,0} \mid^2 \ + \ \mid \theta_{a,1} \mid^2 \ + \ \mid \theta_{a,2} \mid^2 \ . \tag{3.73}$$

In particular, the expression earlier found for the Pfaffian state (3.50) is recovered for $n = M = 1$.

As before, the final step is to verify that this set of extended characters is closed under S modular transformation, that is unitarily represented. As discussed in Appendix A in more detail, the transformation of Ising characters is particularly simple in the following basis,

$$\begin{aligned}
&\widetilde{\chi}_m = \left\{ \frac{I+\psi}{\sqrt{2}}, \sigma, \frac{I-\psi}{\sqrt{2}} \right\}, \\
&\frac{1}{\sqrt{2}} \left(I\left(-\tau^{-1}\right) + \psi\left(-\tau^{-1}\right) \right) = \frac{1}{\sqrt{2}} \left(I(\tau) + \psi(\tau) \right), \\
&\sigma\left(-\tau^{-1}\right) = \frac{1}{\sqrt{2}} \left(I(\tau) - \psi(\tau) \right).
\end{aligned} \tag{3.74}$$

The full S matrix in this basis turns out to be:

$$S_{(a,m),(a',m')} = \frac{e^{i2\pi \frac{aa'n}{nM+1}}}{\sqrt{nM+1}} \begin{pmatrix} 1 & 0 & 0 \\ 0 & 0 & e^{i2\pi a'n/2(nM+1)} \\ 0 & e^{i2\pi an/2(nM+1)} & 0 \end{pmatrix}, \tag{3.75}$$

that is unitary and again factorized in neutral and charged parts, up to details.

3.2.5 Non-Abelian spin-singlet states

The main physical idea of this proposal is that of generalizing the clustering property of the Read-Rezayi states to spinful electrons: namely, of requiring that the ground-state

wave function does not vanish when $n_\uparrow$ electrons with spin up and $n_\downarrow$ with spin down are brought to the same point, with $n_\uparrow,\ n_\downarrow \leq k$[15]. In terms of CFT operator product expansion, we need two species of parafermions, $\psi_\uparrow, \psi_\downarrow$, that obey $(\psi_\uparrow)^k = (\psi_\downarrow)^k = I$. This possibility is offered by the generalized parafermions that are obtained by the coset construction $\widehat{SU(3)}_k/\widehat{U(1)^2}$, first discussed in [81]. Let us recall their main features.

The $\widehat{SU(3)}_k/\widehat{U(1)^2}$ parafermion fields ϕ^Λ_λ are characterized by the pair of $SU(3)$ weights (Λ, λ), that belong to the two-dimensional lattice generated by the positive fundamental weights μ_1, μ_2, with scalar products $(\mu_1, \mu_1) = (\mu_2, \mu_2) = 2/3$ and $(\mu_1, \mu_2) = 1/3$. The dual lattice is generated by the positive roots α_1, α_2, with $(\alpha_1, \alpha_1) = (\alpha_2, \alpha_2) = 2$ and $(\alpha_1, \alpha_2) = -1$, i.e. $\alpha_1 = 2\mu_1 - \mu_2$ and $\alpha_2 = -\mu_1 + 2\mu_2$. The weight Λ takes values inside the so-called truncated Weyl chamber, $\Lambda\ \in P^+_k$, while λ is a vector of the weight lattice P quotiented by the k-expanded root lattice Q , $\lambda \in P/kQ$. In more detail, we have the following values of the weights (Λ, λ) and integer labels $(n_1, n_2, \ell_1, \ell_2)$:

$$\begin{array}{ll} \phi^\Lambda_\lambda \equiv \phi^{n_1,n_2}_{\ell_1,\ell_2}, & \\ \Lambda = n_1\mu_1 + n_2\mu_2, & 0 \leq n_1, n_2,\ n_1 + n_2 \leq k, \\ \lambda = \ell_1\mu_1 + \ell_2\mu_2, & (\ell_1, \ell_2) \bmod (2k, -k), (k, -2k), \\ & n_1 - n_2 = \ell_1 - \ell_2 \mod 3. \end{array} \tag{3.76}$$

The last condition in this equation states that the $SU(3)$ triality of two weights is the same, $(\Lambda - \lambda) \in Q$. Another trivalent condition is the so-called coset field identification [81], saying that the following labellings are equivalent:

$$\phi^{n_1,n_2}_{\ell_1,\ell_2} = \phi^{k-n_1-n_2,n_1}_{\ell_1+k,\ell_2} = \phi^{n_2,k-n_1-n_2}_{\ell_1,\ell_2+k}\ . \tag{3.77}$$

The number $k^2(k+1)(k+2)/6$ of parafermion fields is easily determined from these data: the product of the independent Λ values is $(k+1)(k+2)/2$, that of the λ's ones is $3k^2$ (from the areas of lattice fundamental cells $|k\alpha_1 \wedge k\alpha_2|/|\mu_1 \wedge \mu_2|$), while the two conditions account for a factor $1/9$.

Within this theory, the two fundamental parafermions are $\psi_\uparrow = \phi^0_{\alpha_1}$ and $\psi_\downarrow = \phi^0_{-\alpha_2}$, which have Abelian fusion rules with all fields: actually, the lower index λ of ϕ^Λ_λ belongs to an Abelian charge lattice and is thus additive modulo kQ, leading to the fusion rules $\phi^\Lambda_\lambda \times \phi^0_{\alpha_i} = \phi^\Lambda_{\lambda+\alpha_i \bmod kQ}$. (The choices of root sign in the definition of the fundamental parafermions will be relevant in (3.82).)

The conformal dimension of parafermion fields are given by [52],

$$h^\Lambda_\lambda = \frac{(\Lambda, \Lambda + 2\rho)}{2(k+3)} - \frac{|\lambda|^2}{2k}\ , \tag{3.78}$$

where $\rho = \mu_1 + \mu_2$ is half the sum of positive roots and $|\lambda|^2 = (\lambda, \lambda)$; finally, the central charge of the theory is $c = 8k/(k+3)$.

The excitations of the NASS state are characterized by two Abelian quantum numbers, the charge Q and the intrinsic spin S (not to be confused with the orbital J, equal to half the statistics). The full description is based on the RCFT $\left(\widehat{SU(3)}_k/\widehat{U(1)^2}\right) \otimes \widehat{U(1)}_n \otimes \widehat{U(1)}_p$: in the following, we shall determine the spin and charge compactification

parameters (n,p) and the selection rules relating the (S,Q) values to the non-Abelian weights (Λ,λ) by extending the conditions (A)-(D) for physical excitations of section 2.2. The NASS quasiparticles are described by parafermion fields and vertex operators with α and β charges for electric charge and spin, respectively:

$$\Psi_i = \phi^{\Lambda}_{\lambda}\ e^{i\alpha\varphi}\ e^{i\beta\varphi'}\ ; \tag{3.79}$$

in particular, the two electron fields are,

$$\Psi^{\uparrow}_e = \phi^0_{\alpha_1}\ e^{i\alpha_0\varphi}\ e^{i\beta_0\varphi'}\ , \qquad \Psi^{\downarrow}_e = \phi^0_{-\alpha_2}\ e^{i\alpha_0\varphi}\ e^{-i\beta_0\varphi'}\ . \tag{3.80}$$

The conditions of integer statistics of each excitation with the two electrons read:

$$\begin{aligned} &\alpha\alpha_0 + \beta\beta_0 + h^{\Lambda}_{\lambda+\alpha_1} - h^{\Lambda}_{\lambda} - h^0_{\alpha_1} \in \mathbb{Z}\ , \\ &\alpha\alpha_0 - \beta\beta_0 + h^{\Lambda}_{\lambda-\alpha_2} - h^{\Lambda}_{\lambda} - h^0_{-\alpha_2} \in Z\ ; \end{aligned} \tag{3.81}$$

from the conformal dimensions (3.78), one finds that the weight Λ does not enter in these conditions. We now analyze the various cases of mutual statistics in turn: for the electrons with/among themselves, we obtain,

$$\alpha_0^2 - \beta_0^2 = \frac{1}{k} + N, \qquad \alpha_0^2 + \beta_0^2 = \frac{2}{k} + N'; \tag{3.82}$$

for the electrons with a quasiparticle with labels $(\ell_1,\ell_2,\alpha,\beta)$, they are,

$$2\alpha\alpha_0 = M + M' + \frac{\ell_1-\ell_2}{k}, \qquad 2\beta\beta_0 = M - M' + \frac{\ell_1+\ell_2}{k}\ , \tag{3.83}$$

with N, N', M, M' integers.

Applying these quantization conditions, we obtain the spectrum:

$$\begin{aligned} Q &= \frac{\alpha}{\alpha_o} = \frac{(M+M')k+\ell_1-\ell_2}{3+2kN} = \frac{q}{3+2kN}, \qquad N \text{ odd}, \\ S &= \frac{\beta}{2\beta_o} = \frac{(M-M')k+\ell_1+\ell_2}{2} = \frac{s}{2}, \\ J &= h^{\Lambda}_{\lambda} + \frac{\alpha^2+\beta^2}{2} = h^{\Lambda}_{\lambda} + \frac{q^2}{4k(3+2kN)} + \frac{s^2}{4k}\ . \end{aligned} \tag{3.84}$$

In these equations, the condition of electron intrinsic spin $S = \pm 1/2$ has fixed $N = N'$ (i.e. $\beta_0^2 = 1/2k$), and that of half-integer orbital spin J has selected N odd.

From the spectrum, we identify the compactification parameters for s and q,

$$s \mod n = 2k, \qquad q \mod p = 2k\hat{p},\ \hat{p} = 3+2kN, \tag{3.85}$$

and the parity rules,

$$\ell_1 = \frac{s+q}{2} \mod k, \qquad \ell_1 = \frac{s-q}{2} \mod k, \tag{3.86}$$

that also imply $s = q \bmod 2$. In summary, a quasiparticle is characterized by the integer labels $(\Lambda,\lambda,q,s) \equiv (n_1,n_2;\ell_1,\ell_2;q,s)$ obeying these parity rules and further constrained by triality, $n_1 - n_2 = \ell_1 - \ell_2 = q \bmod 3$.

The addition of electrons to a quasiparticles causes the following index shifts:

	$\Delta\ell_1$	$\Delta\ell_1$	Δq	Δs
$+\psi^{\uparrow}$	2	-1	$\hat{p}$	1
$+\psi^{\downarrow}$	1	-2	$\hat{p}$	-1

(3.87)

The extended characters are thus obtained by products of Abelian characters, $K^{(Q)} = K(\tau, 2k\zeta; 2k\hat{p})$, $K^{(S)} = K(\tau, 0; 2k)$, for charge and intrinsic spin, respectively, and of parafermion characters $\chi^{\Lambda}_{\lambda}(\tau)$, summed over electron excitations:

$$\theta^{\Lambda}_{q,s} = \sum_{a,b} K^{(Q)}_{q+(a+b)\hat{p}}\, K^{(S)}_{s+a-b}\, \chi^{n_1,n_2}_{\ell_1,\ell_2} \ , \tag{3.88}$$

where the values of (ℓ_1, ℓ_2) are constrained by the parity rules (3.86).

Further specifications/conditions on the expression (3.88) are the following:

i) the (a, b) ranges are fixed by checking the periodicity of the summand; upon inspection, the ranges a, b mod $2k$ are surely periodic, but also shifts by $(a, b) \to (a + k, b + k)$ and $(a, b) \to (a + k, b - k)$ maps the sums into themselves: thus, we can take $a = 1, \ldots, k$ and $b = 1, \ldots, 2k$.

ii) The parity rule (3.86) has 3 solutions for $\lambda \in P/kQ$, i.e. for (ℓ_1, ℓ_2) mod $(2k, -k), (k, -2k)$; these are,

$$\begin{pmatrix} \ell_1 \\ \ell_2 \end{pmatrix} = \begin{pmatrix} \frac{s+q}{2} \\ \frac{s+q}{2} \end{pmatrix}, \quad \begin{pmatrix} \frac{s+q}{2} + k \\ \frac{s+q}{2} \end{pmatrix}, \quad \begin{pmatrix} \frac{s+q}{2} \\ \frac{s+q}{2} + k \end{pmatrix}. \tag{3.89}$$

However, using the field identifications (3.77), these three solutions can be traded for Λ changes and should not be considered as independent. We thus obtain:

$$\theta^{\Lambda}_{q,s} = \frac{1}{2} \sum_{a,b=1}^{2k} K^{(Q)}_{q+(a+b)\hat{p}}\, K^{(S)}_{s+a-b}\, \chi^{\Lambda}_{\frac{s+q}{2}+2a+b, \frac{s-q}{2}-a-2b} \ . \tag{3.90}$$

iii) Independent values of (q, s) indeces, $q = s$ mod 2, are found by checking the periodicities of $\theta^{\Lambda}_{q,s}$; we find that:

$$\theta^{\Lambda}_{q,s+2} = \theta^{\Lambda}_{q,s} \ , \qquad \theta^{n_1,n_2}_{q+\hat{p},s+1} = \theta^{k-n_1-n_2,n_1}_{q,s} \ . \tag{3.91}$$

Therefore, the intrinsic spin index is not independent and can be taken to be $s = 0$ (1) for q even (odd), while the charge range is $q = 1, \ldots, \hat{p} = 3 + 2kN$.

The number of independent extended NASS characters is given by the values of q and Λ constrained by triality, $n_1 - n_2 = q$ mod 3. We obtain,

$$T.O. = (3 + 2kN)\frac{(k+1)(k+2)}{6}, \qquad \nu = \frac{2k}{2kN+3} \ , \quad N \text{ odd}, \tag{3.92}$$

where the filling fraction follows from the V transformation of $K^{(Q)}$.

In conclusion, the NASS partition function on the annulus geometry is,

$$Z^{\rm NASS}_{\rm annulus} = \sum_{q=1}^{2kN+3} \sum_{\substack{s=0,1 \\ s=q \ \mathrm{mod}\ 2}} \sum_{\substack{0\le n_1+n_2\le k \\ n_1-n_2=q \ \mathrm{mod}\ 3}} \left| \ \theta^{n_1,n_2}_{q,s} \ \right|^2 \ . \tag{3.93}$$

The modular transformation of the NASS characters is derived in Appendix A and reads:

$$\theta^{\Lambda}_{q,s} = \delta^{(2)}_{q,s}\ \delta^{(3)}_{n_1-n_2,q} \sum_{q'=1}^{\hat{p}} \sum_{\substack{s'=0,1 \\ s'=q' \bmod 2}} \sum_{\Lambda' \in P_k^+} \frac{1}{\sqrt{\hat{p}}}\ e^{-i2\pi \frac{qq'N}{2\hat{p}}}\ \delta^{(2)}_{q',s'}\ s_{\Lambda,\Lambda'}\ \theta^{\Lambda'}_{q',s'}\ , \tag{3.94}$$

where $s_{\Lambda,\Lambda'}$ is the $\widehat{SU(3)}_k$ modular S-matrix.

The $k = 2$, $M = 1$ case.

Let us discuss the simplest NASS state with $k = 2$ and $M = 1$, corresponding to $\nu = 4/7$. There are 8 parafermionic fields,

$$\begin{aligned} I = \Phi^{0,0}_{0,0}, \quad \psi_1 = \phi^{0,0}_{2,-1}, \quad \psi_2 = \phi^{0,0}_{-1,2} = \phi^{0,0}_{1,-2}, \quad \psi_{12} = \Phi^{0,0}_{1,1} = \Phi^{0,0}_{3,-3}, \\ \sigma_\downarrow = \Phi^{0,1}_{0,1} = \Phi^{1,1}_{2,-1}, \quad \sigma_\uparrow = \Phi^{1,0}_{1,0} = \Phi^{1,1}_{-1,2}, \quad \sigma_3 = \Phi^{1,1}_{1,1}, \quad \rho = \Phi^{1,1}_{0,0}, \end{aligned} \tag{3.95}$$

that are also written in the notation of Ref. [58].

There are 14 sectors in the theory, and corresponding extended characters $\theta^{\Lambda}_{\lambda}$, that are made of the parafermion characters χ^{Λ}_{λ} combined with Abelian characters $K^{(Q)}_m K^{(S)}_s$, with m mod $p = 28$ and s mod 4; quasiparticles have charge $m/7 + 4\mathbb{Z}$ and intrinsic spin $s/2 + 2\mathbb{Z}$. The partition function (3.93) can be rewritten:

$$\begin{aligned} &Z^{\rm NASS}_{annulus}(k=2) \ = \\ &= \sum_{m=0,4,8,12,16,20,24} \left|\chi_I Q_{m,0} + \chi_{\psi_1} Q_{m+7,1} + \chi_{\psi_2} Q_{m+7,3} + \chi_{\psi_{12}} Q_{m+14,0}\right|^2 \\ &+ \sum_{m=0,4,8,16,20,24,26} \left|\chi_\rho Q_{m,0} + \chi_{\sigma\downarrow} Q_{m+7,1} + \chi_{\sigma_\uparrow} Q_{m+7,3} + \chi_{\sigma_3} Q_{m+14,0}\right|^2 , \end{aligned} \tag{3.96}$$

where we denoted,

$$Q_{m,s} = Q_{m+14,s+2} = K^{(Q)}_m K^{(S)}_s + K^{(Q)}_{m+14} K^{(Q)}_{s+2}\ . \tag{3.97}$$

The $m = 0$ term in the first sum contains the identity I and the two electron excitations made of ψ_1 and ψ_2 parafermions, obeying the fusions $(\psi_1)^2 = (\psi_2)^2 = I$ and also $\psi_1 \times \psi_2 = \psi_{12}$, leading to the forth term in that sector. The term $m = 8$ in the second sum contains the basic quasiparticle made of spin fields $\sigma_\uparrow, \sigma_\downarrow$, with smallest charge $Q = 1/8$ and spin $S = \pm 1/2$. The other terms are further quasiparticle excitations. Note that the division into extended characters is in agreement with the fusion subalgebras made by multiple fusing of ψ_1, ψ_2 with all the fields; the complete table of fusion rules can be found in [58].

Chapter 4

Physical applications

4.1 Introduction

The quantum Hall systems in the second Landau level are the most prominent candidates for observing non-Abelian anyons, and are receiving a lot of attention due to the proposal of Topological Quantum Computation [30, 40]. As discussed in chapter. 2 we expect that observed plateaus at some filling fractions realize the non-Abelian fluids presented in sections 1.2.4 and 3.2. The most stable $\nu = 5/2$ and $12/5$ are expected to be the Moore-Read or (anti-Moore-Read) and anti-Read-Rezayi fluids, respectively [30]. Some experimental indications and numerical simulations support these identifications. Direct experimental signatures of the non-Abelian statistics are actively studied.

The proposal of experimental quantities and signals of non-Abelian Hall fluids are of fundamental importance. In this chapter, we report our contributions in this direction [72, 73]. Most of the experimental data about QH matter come from transport experiments. The present proposals are interference experiments [4, 44, 83], measure of thermopower [84] and current conduction in the Coulomb Blockade regime [85]. These experiments measure some characteristics of non-Abelian anyons such as: braiding matrix, fusion rules, quantum dimensions (*i.e.* ground state degeneracy) and energy levels. All these informations are build in the partition function. Interference experiment with Anyons, introduced in section 1.5.2, are not further discussed in this thesis: more informations in this topic can be found in [4, 44, 83].

In Fig. 4.1 is drawn the geometry of the quantum Hall interferometer, namely a bar-shaped sample with two constrictions [83]. In this device, one can consider two opposite regimes of weak and strong backscattering of edge excitations at the constrictions: the interference of edge waves is best achieved in the weak backscattering limit (a), while the Coulomb blockade takes place for strong backscattering (b). In case (b), an isolated droplet of Hall fluid is formed and only electrons can tunnel into the droplet; this isolated droplet regime is experimentally more stable. For small droplets, electron tunneling is caused by the electric potential difference but is counterbalanced by the electrostatic charging energy of the isolate droplet, leading to conductance peaks at exact matching. This is the Coulomb blockade effect. One can observe characteristic peak patterns upon

varying: i) the area of the dot by means of a side modulation gate or ii) by tuning the magnetic field (a third possibility not discussed here could be charging an anti-dot engineered inside the droplet). The Coulomb blockade in quantum Hall droplets has been considered in [71, 73, 85, 86, 87, 88], where it was shown to provide interesting tests of the conformal field theory description. Indications of experimental feasibility have been recently reported [89].

In this chapter, we obtain the peak patterns of the Coulomb blockaded current. We use the disk partition function $Z^{(\lambda)}_{\rm disk}$, in Eq. (3.30), for describing the isolated Hall droplets; this resumes all excitations corresponding to adding electrons to the droplet within the λ sector of given fractional charge. We study the peak patterns in the (S, B) plane, corresponding to simultaneous changes of area and magnetic field, and discuss the bulk-edge relaxation (recombination) of neutral excitations.

In [72], we gave a detailed account of the Coulomb blockade in the Jain hierarchical states already presented in [71], as well as the results in two alternative theories for the same states. Then in [73], we discussed the case of non-Abelian states also at $T = 0$, extending the results [85, 86]. The peaks follow a periodic pattern with a modulation in the separations that is due to the presence of neutral excitations. In the recent literature, the partition functions of Abelian hierarchical and non-Abelian Read-Rezayi states were successfully employed to study this pattern also at $T > 0$ [88, 87]. Here we extend these analysis to the other non-Abelian fluids; we also point out that the thermal-activated off-equilibrium CB current can measure the degeneracies of neutral states and distinguish between different Hall states with equal peak patterns at zero temperature [82]. In this chapter we report the results of [73].

The partition function can be applied to the study of the thermodinamical properties of Hall fluids, see for example [90]. At $T = 0$ the thermal fluctuation vanish and the partition function contains only quantum effects. For example, the topological entanglement entropy $\gamma = \frac{1}{2}\log\left(\sum_a d_a^2\right)$ [91, 92] coincides with the $T = 0$ limit, of the thermal entropy. Another proposed signature of non-Abelian statistics that could be experimentally accessible [93] is the thermopower, namely the ratio of the thermal and electric gradients at equilibrium [84, 94]: this could measure the quantum dimension d_1 of the basic quasiparticle in the Hall fluid. We show that the thermopower can be easily described by the edge partition function, with the S modular matrix playing again an important role.

4.1.1 Relevant properties of the partition function

We first recapitulate the main features of partition functions discussed in the previous chapter, using a standard notation for all of them (inspired by the Read-Rezayi states). The partition function on the annulus is a sum of square terms:

$$Z_{\rm annulus} = \sum_{a,\ell} \left|\theta_a^\ell\right|^2 \ , \tag{4.1}$$

where a and ℓ are the Abelian and non-Abelian indices, respectively, possibly obeying some conditions. The total number of terms in the sum is equal to the topological order

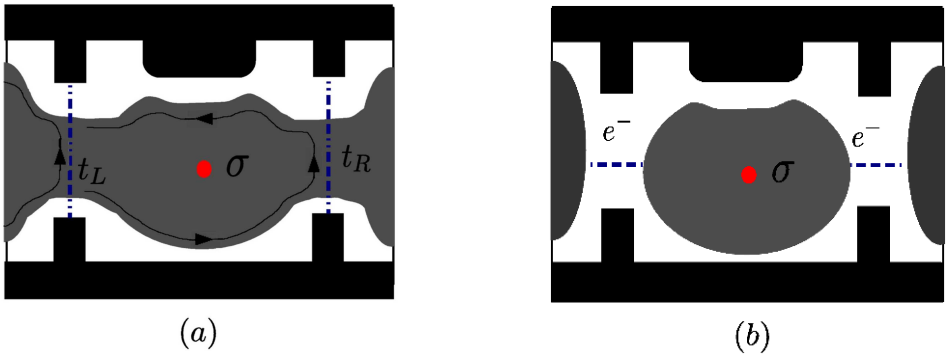

Figure 4.1: The quantum Hall interferometer: the electron fluid is drawn in the (a) weak and (b) strong backscattering limits.

of the Hall state. Each extended character takes the form,

$$\theta_a^\ell = K_a \chi_m^\ell + K_{a+\hat{p}} \chi_{m+\hat{m}}^\ell + \cdots \ , \tag{4.2}$$

where the Abelian indices (a, m) are related by a selection rule (parity rule) and the various terms in the sum describe the addition of electrons (quantum numbers $(\hat{p}, \hat{m})$) to the basic quasiparticle of that sector.

The extended characters transforms linearly under the modular S transformation,

$$\theta_a^\ell\,(-1/\tau) = \sum_{a',\ell'} S_{aa'}\ s_{\ell\ell'}\ \theta_{a'}^{\ell'}(\tau) \ , \tag{4.3}$$

where the total S-matrix is basically factorized into an Abelian phase, $S_{aa'} \sim \exp\left(i2\pi \frac{aa'N}{M}\right)$, and a less trivial non-Abelian part $s_{\ell\ell'}$ [79].

Finally, the expression of charged characters $K_a(\tau, n\zeta; n\hat{p})$ is well-known and given by the theta functions (3.12) with parameters defined in (3.3), while that of non-Abelian ones $\chi_m^\ell(\tau_n)$ is less explicit: nonetheless, the knowledge of their leading low-temperature behavior $\tau_n \to i\infty$ is usually sufficient. This is in general,

$$\chi_m^\ell(\tau_n) = d_m^\ell\ e^{i2\pi\tau_n\left(h_m^\ell - c/24\right)}[1 + \sum_{n\neq 0} d_{m,n}^\ell e^{2\pi\tau_n n}/d_{\Lambda,0}] \tag{4.4}$$

$$\sim d_m^\ell\ e^{i2\pi\tau_n\left(h_m^\ell - c/24\right)} \ , \qquad \text{Im}\ \tau_n = \frac{\beta}{2\pi}\frac{v_n}{R} \ . \tag{4.5}$$

In this equation, h_m^ℓ is the conformal dimension of the corresponding non-Abelian field and c is the central charge of the neutral CFT; d_m^ℓ is the multiplicity of the low-lying state in the sector, that is present in some theories. The integers $d_{m,n}^\ell$ are the number of descendants states at level n for the primary fields ϕ_m^ℓ. Note that we changed the modular parameter $\tau \to \tau_n$ to account for a different Fermi velocity v_n of neutral excitations.

Composite edge modes have two energies scales, since charged and neutral modes propagate at different velocities (one in the cases of Laughlin's fluids, three for BS and

NASS). It is useful to express these energy scales in terms of temperatures, as follows:

$$T_{ch(n)} = \frac{v_{ch(n)}}{2\pi k_B R} , \tag{4.6}$$

for charged (T_{ch}) and neutral (T_n) edge modes. Their typical values, for a small droplet with radius $R \sim 10\ \mu m$, are:

$$T_n = O\left(\frac{v_n}{R}\right) \sim 50\ mK , \qquad T_{ch} = O\left(\frac{v}{R}\right) \sim 250\ mK . \tag{4.7}$$

(The values of the two temperatures depend on the fluids and are not universal quantities.) The temperature axis is divided in three intervals, that will be analyzed separately and can be explored in experiments. For $T \ll T_n$ there are not thermal activated charge edge modes and a low temperature expansion of neutrals characters can be performed. In the range of temperature $T_n < T < T_{ch}$ the neutral edge modes are activated and a $T = 0$ expansion of charged characters can be used. The last possibility is the high temperature $T \gg T_{ch}$; where all the modes are excited. The role of the modular transformation (4.3) is fundamental, because it connects high and low temperatures. The upper limit of the temperature range is the gap:

$$T < T_{GAP} = 500\ mK ; \tag{4.8}$$

for larger temperatures, bulk excitations can be thermally activated and the CFT description is no longer valid; thus the third range $T > T_{ch}$ is note relevant for small droplets.

From the disk partition function, one obtains the thermal average of any quantity of the Hall droplets. For example, the edge charge,

$$\langle Q \rangle = -\frac{1}{\beta}\frac{\partial}{\partial V_o} \log \theta_a^\ell , \tag{4.9}$$

whose qualitative expression at low temperature is:

$$\langle Q \rangle_\ell = \frac{\sum_i\ i\ \delta_\beta\left(\sigma - \sigma_i^\ell\right)}{\sum_i \delta_\beta\left(\sigma - \sigma_i^\ell\right)} , \tag{4.10}$$

where the $\delta_\beta(x)$ is a Gaussian representation of the delta function with spread proportional to $1/\beta$. The spreads, are considered in [88] and are not discussed here.

4.2 Coulomb blockade conductance peaks

4.2.1 Coulomb blockade patterns at $T = 0$

The Coulomb blockade in quantum Hall droplets has been proposed as a probe of the structure of the edge states in [85, 72]. For $T = 0$ only the lowest energy state is relevant, therefore the charge inside the droplets is quantized.

We start from describing the Laughlin fluids and then analyze the non-Abelian fluids. The Coulomb blockade takes place when an electron tunnels in a small quantum dot:

the current cannot flow freely because the charging energy may overcame the work done by the electric potential,

$$\Delta E(n) = -neV + \frac{(ne)^2}{2C} , \qquad \Delta Q = -ne , \tag{4.11}$$

where C is the capacitance (very small for small droplets) and V the potential. It follows that tunneling is possible when the two terms compensate exactly, $\Delta E(n) = 0$, leading to isolated peaks in the current because the charge is quantized.

In QHE droplet of Fig. 4.1, the corresponding stationary condition for Coulomb blockade peaks is:

$$E_{S,B}(n+1) = E_{S,B}(n) , \tag{4.12}$$

where $E_{S,B}(n)$ are the energies for adding n electrons to the edge, that depend on external parameters such as the droplet area S and the magnetic field B.

The dependence on area deformations ΔS can be included in the charge edge spectrum (3.9) as follows [85]. The variation of the droplet area induces a deviation of the background charge $Q_{\rm bkg}$ with respect to its (vanishing) equilibrium value, yielding a contribution to the charge accumulated at the edge, $Q \to (Q - Q_{\rm bkg})$. The edge energies acquire a electrostatic contribution that can be derived near equilibrium by observing that, $E \propto (Q - Q_{\rm bkg})^2$. For the charge sector, we obtain:

$$E^c_{a,\sigma}(n) = \frac{v}{R}\frac{(a + pn - \sigma)^2}{2p} , \qquad \sigma = \frac{B\Delta S}{\phi_o} , \tag{4.13}$$

where σ is a dimensionless measure of area deformations and n is the integer part of the charge on the edge, alias the number of the electron. he Coulomb peaks are obtained by looking for degenerate energy values with $\Delta Q = n$, i.e. within the same fractional charge sector λ: in Fig. 4.2(a), we show the dependence of $E_{0,\sigma}(n)$ on σ: the degeneracy condition (4.12) is satisfied at the midpoints between two consecutive parabolas; there, the electrons can tunnel into the dot yielding the conductance peaks, see 4.2(a). The separation between two consecutive peaks is:

$$\Delta\sigma = p = \frac{1}{\nu} , \qquad \Delta S = \frac{e}{n_o} . \tag{4.14}$$

This result is consistent with the classical picture for which the change in the area precisely matches the value required for incorporating one electron at the average density n_o [85]. We now re-obtain the conductance peaks from the analysis of the disk partition function, illustrating the method that will be extensively used in the following sections [71, 72]. The disk partition function of Laughlin's states for $\nu = 1/p$ (3.30) including the area deformation reads, up to irrelevant factors:

$$\theta_\lambda = K_\lambda(\tau, \zeta; p) = \frac{1}{\eta}\sum_{n=-\infty}^{\infty} \exp\left[i2\pi\left(\tau\frac{(np + \lambda - \sigma)^2}{2p} + \zeta\frac{np + \lambda}{p}\right)\right] . \tag{4.15}$$

Consider the Hall droplet without quasiparticles in the bulk corresponding to $\lambda = 0$: from the character K_0 (4.15), we can extract the energies and charges of the electron

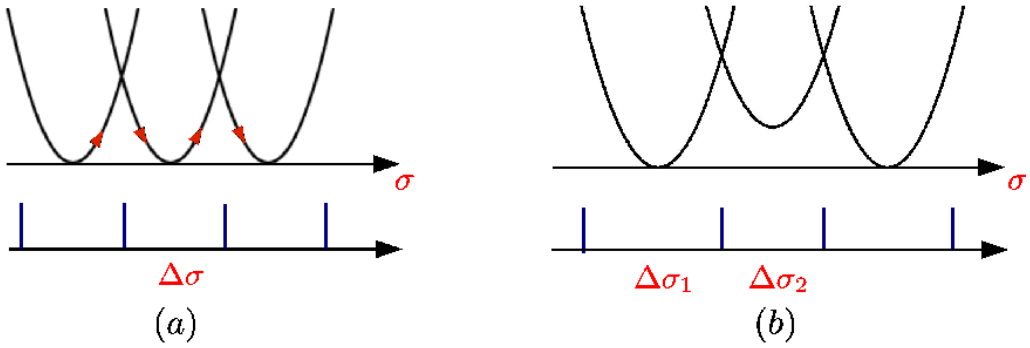

Figure 4.2: Energy levels as a function of the area deformation $\Delta\sigma$: (a) Laughlin states and (b) In presence of neutral modes.

excitations as the factors multiplying τ and ζ, respectively. Upon deformation of the dot area, the ground state energy, $E \sim \sigma^2/2p$, $Q = 0$, and that of the one-electron state, $E \sim (\sigma - p)^2/2p$, $Q = 1$, become degenerate at the midpoint $\sigma = p/2$, leading again to (4.14). In the presence of quasiparticles in the bulk with charge $Q = -\alpha/p$, one should repeat the analysis using the partition functions θ_α ((3.30)): one obtains the same peak separations, because the energies in the different λ sectors are related by global shifts of σ.

We see that the disk partition function is rather convenient for studying the Coulomb blockade: its decomposition into sectors clearly indicates the allowed electron transitions and considerably simplifies the analysis of more involved non-Abelian theories. In the latter cases, there are charged and neutral modes that are coupled in the sectors descried by θ_λ.

The neutral modes do not couple with the background charge and with magnetic field, thus their energies stay constant. The total energy of the edge modes, for fix bulk configurations and for a given charge can be read form the characters: the general structure is:

$$\begin{aligned} E_a^\Lambda(b,n,\sigma) =& v_c E^c_{\lambda,\sigma}(n) + \sum_i v_n^i E_n^i(a,b,\Lambda) + \cdots \\ =& v_c E^c_{\lambda,\sigma}(b+\hat{p}n) + v_n h^\ell_{a+2n} + \cdots , \end{aligned} \tag{4.16}$$

The dots indicate the additional terms for descendant states, that are not relevant because they are never excited at $T = 0$. The charged energy is a quadratic function in σ see Fig. 4.2. For each value of integer charge we have a different parabola whose minimum is at equidistant points. The contribution from the neutral energy translates the parabolas, see picture 4.2 (b), leading to a displaced position of the current peak as a function of σ. Therefore, the neutral sector of the theory implies a modulation of the peak distance that has a characteristic pattern.

The two energies in equation (4.12) must belong to in the same character because, as observed in the last section, the simple current corresponds to the addition of unit

of charge on the edge. In the following, we find the peaks patterns for all the fluids in the SLL. The pattern were originally derived in [85] for RR fluids and in [82, 86] for the other fluids BS, $\overline{\text{RR}}$, NASS ($k = 2$) and NAFF ($m = 2$). The use of the partition functions makes the derivation straightforwards since the selection rules for the addition of electrons to the excitations are build-in.

Read-Rezayi states

The analysis of conductance peaks under area variations ΔS can be obtained from the disk partition functions (3.46),

$$\begin{aligned} Z^{(a,\ell)}_{\text{disk}} &= \theta^\ell_a = \sum_{\beta=1}^{k} K_{a+\beta\hat{p}}(\tau, k\zeta; k\hat{p})\ \chi^\ell_{a+2\beta}(\tau; k)\ , \\ & a = 1, \dots, \hat{p} = (kM+2), \quad \ell = 0, 1, \dots, k, \quad a = \ell \bmod 2. \end{aligned} \tag{4.17}$$

As seen in the previous examples, each (ℓ, a) sector involves the parafermion fields of same ℓ value (along the vertical line in Fig. 3.3(b)), each one associated to charges mod $k\mathbb{Z}$. Therefore, adding one electron corresponds to going from $\beta \to \beta + 1$ in the corresponding sector θ^ℓ_a (4.17). The distance between the conductance peaks is given by:

$$\Delta\sigma^\ell_\beta = \sigma^\ell_{\beta+1} - \sigma^\ell_\beta = \frac{\hat{p}}{k} + \frac{v_n}{v}\left(h^\ell_{a+2\beta+4} - 2h^\ell_{a+2\beta+2} + h^\ell_{a+2\beta}\right)\ . \tag{4.18}$$

The peak distances are modulated by the energies of neutral parafermions h^ℓ_m through their discrete second derivative. This is constant, $\Delta^2 h^\ell_m = -2/k$, up to discontinuities at the boundaries of the domains in the (ℓ, m) plane, which are the diagonals, $\ell = \pm m$, m mod $2k$ (see Fig. 3.3(a).). Whenever $a+2\beta+2$ in (4.18) stays on one diagonal, the result is $\Delta^2 h^\ell_m = 1-2/k$; at the crossing of two diagonals, $(\ell, m) = (0, 0), (k, k)$, mod $(0, 2k)$, it reads $\Delta^2 h^\ell_m = 2 - 2/k$. Therefore, the peak patterns are the following,

$$\begin{aligned} \ell = 0, k \quad &: \quad \Delta\sigma = (\Delta + 2r, \Delta, \cdots, \Delta)\,, && (k) && \text{groups}, \\ \ell = 1, \dots, k-1 \quad &: \quad \Delta\sigma = (\Delta + r, \Delta, \cdots, \Delta + r, \Delta, \dots, \Delta)\,, && (\ell)(k-\ell) && \text{groups}, \\ & \Delta = \frac{1}{\nu} - \frac{v_n}{v}\frac{2}{k}\ , \qquad r = \frac{v_n}{v}\ . \end{aligned} \tag{4.19}$$

In these non-Abelian Hall states, the peak patterns depend on the number of basic σ_1 quasiparticles in the bulk: for ℓ of them, there are groups of ℓ and $(k-\ell)$ equidistant peaks separated by a larger gap, $\Delta + r$, $r = v_n/v$. The patterns are symmetric by $\ell \leftrightarrow (k-\ell)$ and depends on the other quantum number a only in the (irrelevant) starting point of the sequence. In particular, for the Pfaffian state ($k = 2$), the peaks group in pairs when the number of bulk quasiparticles is even, and are equidistant when it is odd, the so called "even-odd effect" [85]. The analysis of χ^ℓ_a characters also shows that there are no degenerate states in parafermionic excitations, and thus the Coulomb peaks have no multiplicities.

The peak patterns repeat periodically with period $\Delta\sigma = k/\nu = kM + 2$, apart from the case k even and $\ell = k/2$, where it is halved. The same results were found by

the direct analysis of parafermion Hilbert space in [85, 86]. The modulation of peak distances is equal to the ratio of velocities of neutral to charged excitations $v_n/v = r \sim 1/10$. Let us stress that this is a equilibrium phenomenon obtained by adiabatic variation of the Hamiltonian.

The peak pattern in the ground state sector of Read-Rezayi states is actually the same as in the Jain hierarchical Hall states see Appendix A.2 up to a factor of 2 in the neutral energies. However, the Abelian case is characterized by specific peak multiplicities and is independent of the sector, i.e. of bulk excitations.

In Ref. [82], it has been argued that the modulation of Coulomb peaks at $T = 0$ is not a signature of non-Abelian states, since similar or equal patterns can also be found in Abelian states that have non-trivial neutral excitations. Indeed, at $T = 0$ one is probing only the leading behavior (4.5) of the neutral characters χ^{ℓ}_{m}, that can be the same for different theories, Abelian and non-Abelian. For example, the Read-Rezayi states and the (331) Haldane-Halperin Abelian hierarchical fluids have this property.

One physical explanation of this fact was given in Ref. [67], where it was shown that the (331) state can be considered as a "parent" Abelian theory of the Read-Rezayi state, because the two theory possess the same k-th electron clustering property but it is realized through the addition of a k-fold quantum number, called e.g. "color". Since electrons of different color are distinguishable, their wavefunction needs not to vanish when k of them come close; this behavior can be achieved in a standard Abelian multicomponent theory specified by a charge lattice. In this setting, the Read-Rezayi state is re-obtained when electrons are made indistinguishable, i.e. when wave functions are antisymmetrized with respect to all electrons independently of the color.

In CFT language, such antisymmetrization amounts to a projection in the Hilbert space that does not change the sectors and selection rules over which the partition function is built; the neutral CFT undergoes a coset reduction, from the Abelian lattice with $\widehat{SU(k)}_1 \otimes \widehat{SU(k)}_1$ symmetry to the non-Abelian theory $\widehat{SU(k)}_1 \otimes \widehat{SU(k)}_1/\widehat{SU(k)}_2$, the latter being another realization of $\mathbb{Z}_k$ parafermions [67]. Therefore, the Abelian and non-Abelian fluids have the same form of the partition function, only the neutral characters are different: however, their leading behavior (4.5) is unaffected by the projection, leading to the same patterns of Coulomb peaks at $T = 0$. In conclusion, the presence of equal Coulomb peaks patterns in two different theories, Abelian and non-Abelian, is not accidental and it may suggest a physical mechanism behind it.

Bonderson Slingerland states

In these states the quantum number of excitations are the fractional charge (a) and the number of quasiparticles in the bulk respectively (ℓ). The computations of the peaks

patterns gives, for even number of bulk excitations,

$$\Delta\sigma_\beta = \frac{\hat{p}}{m} - \frac{v_n}{v_c}\frac{1}{m} \pm \frac{v_I}{v_c}\begin{cases} -1 & \beta \text{ even}, \\ +1 & \beta \text{ odd}, \end{cases} \qquad \beta = 0, \cdots m-2,\ \ell = 0,\ 2\,, \tag{4.20a}$$

$$\Delta\sigma_\beta = \frac{\hat{p}}{m} + \frac{v_n}{v_c}\frac{m-1}{m} \pm \frac{v_I}{v_c}\begin{cases} -1 & \beta \text{ even}, \\ +1 & \beta \text{ odd}, \end{cases} \qquad \beta = m-1,\ \ell = 0,\ 2\,. \tag{4.20b}$$

sign plus for $\ell = 0$. For a odd number of quasiparticles in the bulk the peaks patterns are:

$$\Delta\sigma_\beta = \frac{\hat{p}}{m} - \frac{v_n}{v_c}\frac{1}{m}, \qquad \beta = 0, \cdots m-2,\ \ell = 1\,, \tag{4.20c}$$

$$\Delta\sigma_\beta = \frac{\hat{p}}{m} + \frac{v_n}{v_c}\frac{m-1}{m}, \qquad \beta = m-1,\ \ell = 1\,. \tag{4.20d}$$

Also the BS states present the odd/even effect in the modulations of the peaks [85, 86]. Noticed that the modulation of the peaks is a sum of contributions of the Jain's and MR's modulations. The pattern of the packs has period m in general, but for m odd and even number of elementary quasiparticles in the bulk the period is $2m$.

Non-Abelian fluids

We report the peaks pattern for Wen's $SU(2)$ non-Abelian fluids (NAF) [76]. In these case the each sector is label by a neutral label ℓ and fractional charge a. The distance between β and $\beta + 1$ peaks are:

$$\Delta\sigma_\beta = \frac{\hat{p}}{m} \pm \frac{v_n}{v_c}(\ell - k/2), \qquad \ell = 0, \cdots k \tag{4.21}$$

where the plus (minus) sign in the formula (4.21) is for β odd (even). Noticed that the period is 2 as we expected since there are two terms in the characters. The modulation depend on the quasiparticles in the bulk.

Anti Rear-Rezayi state

In these cases the computations of the peaks pattern is very simple the results is,

$$\Delta\sigma_\beta = \frac{\hat{p}}{m} - \pm\frac{v_n}{v_c}\frac{2\ell - k}{2}\,, \tag{4.22}$$

where the sign plus is for the distance between packs $\ell \mapsto k-\ell \mapsto \ell$. We noticed that the patterns has period 2. The pattern for RR have a different period respect to the charge conjugate one. This means that in the anti-RR we have not the $k-$clusters phenomena. Indeed the new periodicity is govern by the $\mathfrak{su}(2)$ symmetry.

4.2.2 Coulomb blockade patterns for $T > 0$ at equilibrium

Temperature $T \leq T_n$

For non-vanishing temperature, a new feature [71, 72, 88] is associated to the multiplicity factor d_m^ℓ in the leading behavior of the neutral characters (4.5): if $d_m^\ell > 1$, the electron entering the droplet finds more than one available degenerate state. The presence of level multiplicities does not influence the $T = 0$ peak pattern, but is observable for $T > 0$. Indeed at equilibrium for $T \simeq 0$, the probability of one-electron tunneling under parametric variation of the Hamiltonian is either one (at degeneracy) or zero (off degeneracy), thus the presence of more than one available empty state is not relevant. Inclusion of a small finite-size energy splitting among the d_m^ℓ states does not substantially modify the peak shape.

On the other hand, for $T > 0$ these multiplicities lead to a displacement of the peak centers, as follows [88]:

$$\sigma_i^\ell \to \sigma_i^\ell + \frac{T}{T_{ch}} \log \left(\frac{d_{a+2i}^\ell}{d_{a+2i+2}^\ell} \right) , \tag{4.23}$$

as is clear by exponentiating the d_m^ℓ factor into the energy in the expression of the characters (4.5). The effect is observable for $T \leq T_n$ by increasing the experimental precision. In particular, the multiplicities and the associated peak displacements are present in the (331) states (due to color multiplicity) and absent in the Read-Rezayi states, thus providing a difference in the Coulomb peaks of these two theories for $T > 0$ [88].

The level multiplicities of the other non-Abelian states are found by the leading expansion of the respective neutral characters:

$$\begin{array}{lll} d^\ell = (\ell + 1) \ , & \chi^\ell \sim d^\ell \ q^{h^\ell - c/24} \ , & SU(2) \text{ NAF and } \overline{\text{RR}} \ , \\ d_\beta = \binom{n}{\beta} \ , & \Theta_\beta \sim d_\beta \ q^{\beta(n-\beta)/2n - n/24} \ , & SU(n) \text{ BS and Jain} \ , \\ d_m^\ell = d_\lambda^\Lambda = 1 \ , & & \text{RR and NASS.} \end{array}$$

The peak displacements are particularly interesting when they can be used to distinguish between competing theories with same filling fraction and $T = 0$ Coulomb peak pattern. In the case of the Jain hierarchical states, one can test the multiplicities of states predicted by the multicomponent $\widehat{SU(n)}_1 \otimes \widehat{U(1)}$ Abelian theories versus the $W_{1+\infty}$ minimal models possessing no degeneracy, as discussed in [12][78]. The peak pattern including displacements of the $\widehat{SU(n)}_1 \otimes \widehat{U(1)}$ theory are, for $\nu = n/(2sn \pm 1)$:

$$\begin{aligned} \Delta\sigma_i &= \frac{1}{\nu} - \frac{v_n}{v}\frac{1}{n} + \frac{T}{T_{ch}} \log \frac{(i+1)(n-i+1)}{i(n-i)} \ , \qquad i = 1, \ldots, n-1, \\ \Delta\sigma_n &= \frac{1}{\nu} + \frac{v_n}{v}\frac{n-1}{n} + \frac{T}{T_{ch}} \log \frac{1}{n^2} \ . \end{aligned} \tag{4.24}$$

The $W_{1+\infty}$ minimal models possess the same pattern without the temperature dependent term for $T < T_n$.

Another interesting case is the competition between the Pfaffian state at $\nu = 5/2$ and its particle hole conjugate state $\overline{\text{RR}}$, possessing multiplicities due to its $SU(2)$

symmetry, as indicated in (4.24). Let us discuss this point in some detail. The Coulomb peak distances in the $\overline{\rm RR}$ states, parameterized by (ℓ, a), $a = \ell \bmod 2$ (cf. (3.61)), have period two for any k and their expressions including the shift due to level multiplicity are, for $\nu = 2/(2M + k)$:

$$\begin{aligned} \Delta\sigma_a^\ell &= \frac{1}{\nu} + (-1)^a \left[\frac{v_n}{v} \frac{2\ell - k}{2} + 2\frac{T}{T_{ch}} \log\left(\frac{k - \ell + 1}{\ell + 1} \right) \right], \\ & \qquad \ell = 0, 1, \ldots, k. \end{aligned} \tag{4.25}$$

In particular, for $\nu = 5/2$ ($k = 2$) there is the so-called even/odd effect [85] for both the RR, the $\overline{\rm RR}$ and (331) states (no modulation for $\ell = 1$, pairwise modulation for $\ell = 0, 2$). The peak shifts are present in the last two theories for $\ell = 0$, but are absent in the Pfaffian state. It follows that the observation of a temperature dependent displacement in the position of paired peaks could support both the (331) and the anti-Pfaffian of the $\nu = 5/2$ plateau as the correct theory.

Temperature $T_n < T < T_{ch}$

At higher temperatures, in the region $T_n < T < T_{ch}$, the Boltzmann factors relative to higher neutral excitations can be of order one and can contribute beyond the leading $T \to 0$ term in (4.5). As observed in [87], it is convenient to perform the S modular transformation on the neutral characters $\chi(\tau_n)$, $\tau_n \to -1/\tau_n \sim iT/T_n$, and expand them for $\tau_n \to 0$.

We use again the Read-Rezayi case as an example: after $S-$transformation of the neutral characters (3.45), we keep the first leading three terms, and obtain:

$$\begin{aligned} \chi_m^\ell(\tau_n) &\sim \frac{1}{\sqrt{2k}} \left(s_{\ell 0}\ \chi_0^0\left(\frac{-1}{\tau_n}\right) + s_{\ell 1}\ e^{-i\pi m/k}\ \chi_1^1\left(\frac{-1}{\tau_n}\right) + s_{\ell 1}\ e^{i\pi m/k}\ \chi_{-1}^1\left(\frac{-1}{\tau_n}\right) \right) \\ &\sim s_{\ell 0} \left(1 + \frac{s_{\ell 1}}{s_{\ell 0}} e^{-i(2\pi/\tau_n)h_1^1}\ 2\cos\left(\frac{\pi m}{k}\right) \right) \\ &\sim s_{\ell 0}\ e^{D_m^\ell}\ , \qquad\qquad \tau_n \to 0. \end{aligned} \tag{4.26}$$

In this limit, the extended characters (3.46) become:

$$\theta_a^\ell \sim \sum_{b=1}^{k} K_{a+b\hat{p}}(\tau)\ s_{\ell 0}\ e^{D_{a+2b}^\ell}\ , \tag{4.27}$$

where,

$$D_{a+2b}^\ell = e^{-4\pi^2 h_1^1 T/T_n}\ 2\cos\frac{\pi(\ell+1)}{k+2}\ 2\cos\frac{\pi(a+2b)}{k}\ . \tag{4.28}$$

The distance between Coulomb peaks in RR states for $T > T_n$ is therefore given by (cf. (4.18)):

$$\Delta\sigma_i^\ell = \frac{1}{\nu} - \frac{T}{T_{ch}} e^{-4\pi^2 h_1^1 T/T_n}\ 8\cos\frac{\pi(\ell+1)}{k+2}\cos\frac{\pi(a+2i)}{k}\left(\cos\frac{2\pi}{k} - 1\right). \tag{4.29}$$

Although exponentially small, this temperature effect is full-fledged non-Abelian, since it involves the ratio $s_{\ell 1}/s_{\ell 0}$ of components of the S-matrix for neutral states; such ratios

also appears in other non-Abelian effects, including the Fabry-Perot interference phase [44].

The corresponding correction terms for the other non-Abelian Hall states are, as follows:

$$SU(n)\text{ Jain}: \qquad D_b = e^{-4\pi^2 h_1 T/T_n}\ 2n\ \cos\frac{2\pi b}{n}\ , \tag{4.30}$$

$$SU(2)\text{ NAF and }\overline{\text{RR}}: \qquad D_a^\ell = e^{-4\pi^2 h^1 T/T_n}\ (-1)^a\ 4\cos\frac{\pi(\ell+1)}{k+2}\ , \tag{4.31}$$

$$\begin{aligned} SU(n)\times\text{Ising BS}: \qquad & D_{a,m} = e^{-4\pi^2 h_1 T/T_{SU(n)}}\ 2n\ \cos\frac{2\pi a}{n} + \\ & + \begin{cases} (-1)^{a+m/2}\sqrt{2}\ e^{-\pi^2 T/(4T_{\text{Ising}})}, & m=0,2, \\ -e^{-2\pi^2 T/T_{\text{Ising}}}, & m=1. \end{cases} \end{aligned} \tag{4.32}$$

In all these expressions, we used the notations introduced earlier in the respective description in chapter 3; $T_{SU(n)}$ and T_{Ising} are proportional to the neutral edge velocities of the corresponding terms in the BS theory. We remark that the difference between the Jain (Abelian) (4.30) and Read-Rezayi (non-Abelian) (4.28) correction is precisely due to the neutral S-matrix term.

The corresponding $T > T_n$ Coulomb peak separations are,

$$\begin{aligned} &SU(n)\text{ Jain}: \\ &\qquad \Delta\sigma_i = \frac{1}{\nu} - \frac{T}{T_{ch}} e^{-4\pi^2 h_1 T/T_n}\ 4n\cos\frac{2\pi i}{n}\left(\cos\frac{2\pi}{n} - 1\right), \\ &\text{NAF and }\overline{\text{RR}}: \\ &\qquad \Delta\sigma_i^\ell = \frac{1}{\nu} - \frac{T}{T_{ch}} e^{-4\pi^2 h^1 T/T_n}(-1)^i\ 16\cos\frac{\pi(\ell+1)}{k+2}, \\ &SU(n)\times\text{Ising BS}: \\ &\qquad \Delta\sigma_i^m = \frac{1}{\nu} - \frac{T}{T_{ch}} e^{-4\pi^2 h_1 T/T_{SU(n)}}\ 4n\cos\frac{2\pi i}{n}\left(\cos\frac{2\pi}{n} - 1\right) + \\ &\qquad\qquad + \begin{cases} (-1)^{i+m/2} 4\sqrt{2}\ e^{-\pi^2 T/(4T_{\text{Ising}})}, & m=0,2, \\ 0, & m=1. \end{cases} \end{aligned} \tag{4.33}$$

Let us finally discuss the Coulomb blockade for temperature $T > T_{ch}$ [87]. The Coulomb peaks could be similarly predicted from the partition function by performing the S transformation on both τ_n and τ. However, the experimental values of T_{ch} for small droplets are comparable to the bulk gap Δ of Hall states in the second Landau level, such that the CFT description is doubtful for these temperatures.

4.2.3 Peak patterns in the (S, B) plane

We now analyze the peak patterns in the (S, B) plane, i.e. by simultaneous change of area and magnetic field. Let us first discuss ΔB changes at $\Delta S = 0$: from section 3.1, we recall that varying the field causes a chiral anomaly and a drift of all charges in the theory. The addition of one flux quantum, $\delta = S\Delta B/\phi_o = 1$ modifies the charged

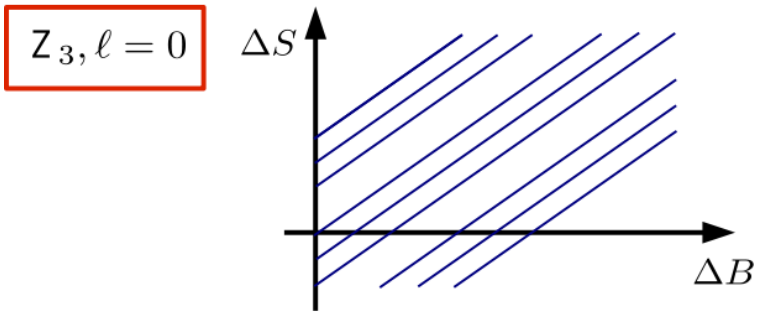

Figure 4.3: Coulomb peaks in the area (S) and magnetic field (B) plane.

characters in the disk partition functions (4.17) by $K_\lambda(\tau, k\zeta; q) \to K_{\lambda+k}$, i.e. by a charge equal to the filling fraction. The spectral flow of Read-Rezayi sectors is therefore:

$$\theta_a^\ell \;\to\; \theta_{a+k}^{k-\ell} = \theta_{a-2-(M-1)k}^\ell \;. \tag{4.34}$$

Namely, the sector ℓ goes into itself with a shift of the a index: the peak pattern already found for S variations at $\Delta B = 0$ repeats itself at $\Delta B = \phi_o/S$ with an upward translation (see Fig. 4.2.3). This continues for $\delta = 2, \ldots$: eventually the sector ℓ goes to the $(k - \ell)$ one, with the same pattern, and then back to itself.

This B dependence actually holds in full generality: the peaks only depend on the combined variation $(\sigma - \delta)$. The magnetic field does not couple to that neutral characters, that are unchanged; since they determine the peak modulations, the pattern remains the same. The only effect is a rigid shift of the ΔS peak pattern at $\Delta B = 0$.

In general, a magnetic flux induces a localized charge excitation inside the Hall droplet, but this has to combine with a neutral excitation to form a physical state: in non-Abelian states, there might be several possibilities. The result of the present analysis is that neutral parts are not created and the ℓ sector does not change: there is a drift of states within the same sector or the conjugate $(k-\ell)$. One could naively think that $\Delta B > 0$ would create the lowest charge quasiparticle σ_1, but this would require a transition $(\Delta\ell, \Delta m) = (1, 1)$ that cannot be induced in isolated droplets within the relativistic CFT description. Maybe it could be realized by engineering a anti-dot inside the disk and by charging it, if further non-relativistic effects are taken into account [85].

In conclusion, the peak patterns in the (S, B) plane are not different from those on the S axis. In ref. [89], it was observed that, for $\nu > 2$, increasing B causes a depletion of electrons in the second Landau level, that go into available states in the first level; this is another effect that rigidly translate upwards the peak patterns in the B plane, i.e. it is of the same sign as the spectral flow described here.

4.2.4 Bulk-edge relaxation

In reference [86], a mechanism for relaxation of edge excitations has been proposed. While the electric charge is locally conserved at the edge, the neutral charge is (expected

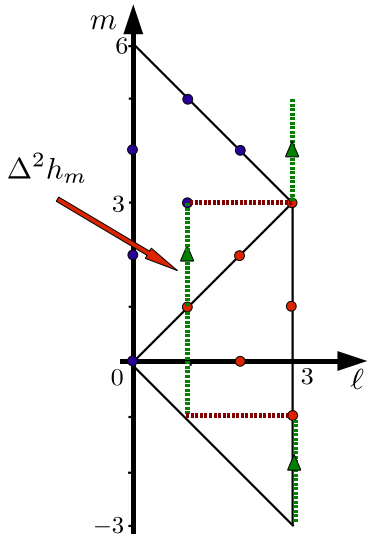

Figure 4.4: Zig-zag path connecting the $\mathbb{Z}_3$ parafermion fields involved in the evaluation of Coulomb peaks with relaxation: the read segments are relaxation transitions.

to be) only globally conserved: therefore, a (slow-time) process can be conceived in which neutral excitations at edge and bulk fuse together thus achieving a lower energy state at the edge. In this mechanism, the electron added at the boundary decays into another excitation with same charge but different neutral content. This process is possible whenever the theory possess two or more excitations with same electric charge but different neutral parts, among which the relaxation transition can take place.

In non-Abelian theories, there are necessarily many-to-one combinations of neutral and charged parts. Consider the following example of fusion rules:

$$\phi_1 \cdot \phi_2 = \psi + \psi' \ . \tag{4.35}$$

Both ϕ_1, ϕ_2 fields contain charged and neutral components, and electric charge is conserved: thus, the fields ψ, ψ' have same electric charge but different neutral parts. A possible relaxation at the edge is, $\psi \to \psi'$, by absorption of one neutral bulk excitation, call it ε, via the fusion, $\psi \cdot \varepsilon = \psi' + \cdots$. It is rather natural to expect that the ε field exists in the theory.

In the Read-Rezayi states, the parafermionic parts can change as follows: the m quantum number should stay fixed because it is related to the charge by the $\mathbb{Z}_k$ parity rule, thus ℓ can change by an even integer: the minimal value is $(\Delta\ell, \Delta m) = (\pm 2, 0)$. These transitions should reduce the value of the edge energy, i.e. of h^ℓ_m. The plot in Fig. 4.5 shows that the smallest values are found on the diagonals $m = \pm\ell \bmod 2k$: therefore, the peak patterns are analyzed starting from the low-lying states $(\ell, m = \pm\ell)$.

Let us consider for example the initial state $(\ell, m) = (1, 1)$, as drawn in the parafermion diagram of Fig. 4.2.4. The first peak is found by comparing with the energy levels of the next term in the same $\ell = 1$ sector, i.e in θ^1_1, which is $(1, 3)$ (joined by a green line in Fig.

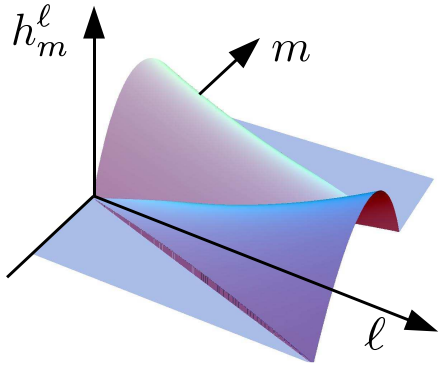

Figure 4.5: Conformal dimension h^ℓ_m of parafermion fields.

4.2.4); then the higher energy of the latter allows the relaxation, $(1,3) \to (3,3)$, (red line), bringing to the $\ell = 3$ sector. The next peak is therefore obtained by comparing $(3,3)$ to $(3,-1)$, followed by the relaxation $(3,-1) \to (1,-1)$; the next peak compares $(1,-1)$ with $(1,1)$ and so on.

Therefore, the peak patterns with relaxation are obtained by comparing points in the (ℓ, m) plane that are reached by zig-zag walking along the diagonals, that correspond to minimal edge energies (Fig. 4.2.4). The relaxations are achieved by fusing the edge fields with the $(\ell, m) = (2,0)$ parafermion that is always present in the spectrum (higher $\Delta\ell$ transitions have larger energies and are never reached). The peak distances $\Delta\sigma$ are computed as in section 4.2:

$$\Delta\sigma = \sigma^{\ell\pm2}_{\beta+1} - \sigma^\ell_\beta = \frac{\hat{p}}{k} + \frac{v_n}{v}\left(h^{\ell\pm2}_{2\beta+4} - h^{\ell\pm2}_{2\beta+2} - h^\ell_{2\beta+2} + h^\ell_{2\beta}\right) \ , \tag{4.36}$$

where the $\ell \pm 2$ point is along the zig-zag path. These derivatives are independent of ℓ and their values are already known: the separations $\Delta\sigma$ acquire the extra contribution v_n/v when the midpoint $m = 2\beta + 2$ stays on a diagonal.

The resulting peak patterns are the following,

$$\begin{array}{lll} k \text{ even, any } \ell: & \left(\frac{k}{2}\right)\ \left(\frac{k}{2}\right) & \text{groups,} \\ k \text{ odd, any } \ell: & \left(\frac{k+1}{2}\right)\ \left(\frac{k-1}{2}\right) & \text{groups.} \end{array} \tag{4.37}$$

They do not depend on the (starting) ℓ value; in particular, the even-odd effect in the Pfaffian state doe not take place in presence of bulk-edge relaxations. Form the experimental point of view, relaxations could take place on long time scales, and thus be controlled [86].

Let us remark that in the Jain hierarchical states of section 3, bulk-edge relaxations corresponding to change of sectors θ_a (A.12) are not possible, because any charge component, K_λ, appears only once in the spectrum (cf.(A.13)), so it is uniquely coupled to a neutral part.

The peak pattern in presence of relaxation can be computed for all the fluids by use of the corresponding versions of equation (4.36). In general these pattern give a less

clear signal of the statistics of the excitations, with respect to that without relaxation [82].

4.3 $T > 0$ off-equilibrium.

In this section we discuss the $T > 0$ Coulomb blockade in presence of a finite potential ΔV_o between the Hall droplet and left (L) and right (R) reservoirs, leading to a steady flow of electrons through the droplet. This setting resembles a scattering experiment and is sensible to the multiplicity of edge states d_a^ℓ discussed before.

We shall study the problem within the phenomenological approach of the Master Equation of Ref. [95], that was successfully applied to studying the fluctuations of the CB current in a quantum dot, in particular its suppression due to Fermi statistics when the transmission rates are not too small. Clearly, a more precise analysis of off-equilibrium physics would need the knowledge of the finite-temperature real-time current-current correlation function that is beyond the scopes of this work.

The starting point of [95] is the evolution equation of the semiclassical density matrix ρ, $d\rho/dt = M\rho$, where M is the matrix of transition rates. The latter can be written in the basis of states with definite electron number n inside the dot: its components are the rates Γ_{ij} that can be computed by the Fermi golden rule and have the following factor for ideal-gas statistics:

$$\gamma(\varepsilon) = \frac{\varepsilon}{1 - e^{-\beta\varepsilon}} \ , \tag{4.38}$$

where $\varepsilon = E_i - E_f$ is the energy of one-particle transitions. This expression has two natural limits:

$$\gamma(\varepsilon) \sim \begin{cases} \varepsilon \ , & \beta\varepsilon \gg 1, \\ |\varepsilon| \ e^{-\beta|\varepsilon|} \ , & \varepsilon < -T \ , \end{cases} \tag{4.39}$$

showing the $T \to 0$ phase-space enhancement for allowed electron transition and the distribution of thermal-activated forbidden transitions, respectively.

The transition rates for one electron entering ($n \to n+1$) or leaving ($n \to n-1$) the dot, coming from the (L) or (R) reservoirs are respectively given by [95]:

$$\Gamma^{\mathrm{L(R)}}_{n\to n\pm1} = \frac{1}{e^2 R_{\mathrm{L(R)}}} \ \gamma\left[\phi e \left(V - V_{\mathrm{L(R)}}\right) - E_C\right] \ , \tag{4.40}$$

where $R_{\mathrm{L(R)}}$ and $V_{\mathrm{L(R)}}$ are the resistance and potential levels of the reservoirs, and V is the dot potential (here we assume $V_L - V = V - V_R = \Delta V_o$). In the case of Hall droplets, the Coulomb energy E_C should be replaced by the difference of edge energies $\Delta E_\sigma = E_\sigma(Q+1) - E_\sigma(Q)$ (4.13), including neutral parts, that are obtained from the CFT partition function as seen before (we also set $e = 1$ in the following).

Among the different regimes considered in [95], that of $T < \Delta V_o < \Delta E_\sigma$ is the most relevant for our purposes: this is the situation of thermal-activated CB conduction, where few electrons can enter the droplet from the left by thermal jumps and then quickly get out to the right. The rate for the combined process is:

$$\Gamma = \Gamma^L_{n\to n+1}\Gamma^R_{n+1\to n} \sim \left((\Delta E_\sigma)^2 - (\Delta V_o)^2\right) \ e^{-\beta(\Delta E_\sigma - \Delta V_o)}, \tag{4.41}$$

and the time interval between the peaks is $\Delta t \sim 1/\Gamma$.

The main observation in this section is the following: if the Hall states possess multiplicities d_a^ℓ (4.24) for edge electron states, the corresponding transition rates are amplified accordingly:

$$\Gamma \ \rightarrow \ d_a^\ell \, \Gamma. \tag{4.42}$$

Therefore, a real-time experiment of peak rate can provide a direct test of edge multiplicities, and be useful to distinguish between Hall states with otherwise equal CB peak patters. Clearly, the formula (4.41) depends on several unknown and state-dependent phenomenological parameters, such as reservoir-droplet couplings. Nevertheless, the qualitative signal should be detectable: upon parametric variation of σ one can find the points of level matching $\sigma = \sigma_i$, where $\Delta E_\sigma \rightarrow 0$ and the rate Γ saturates. From these points, one can tune σ at the midpoints in-between and test the formula (4.41) of thermal activated CB conduction with less uncertainty. The signal is more significant if the values of d_a^ℓ change considerably from one σ interval to the following (as e.g. for $SU(n) \times U(1)$ Jain states with $d_a = \binom{n}{a}$).

4.4 Thermopower measurements and $T = 0$ entropies

Quasiparticles with non-Abelian statistics are characterized by degenerate energy levels that are due to the multiplicity of fusion channels [4]. Their wave functions, described by Euclidean RCFT correlators in the plane, form multiplets whose dimension can be obtained by repeated use of the fusion rules reported in Eq. (2.21). The number of terms obtained by fusing n quasiparticles of a-th type is given by Eq. (2.27) is d_a^{n-1} (for $n \ \rightarrow \ \infty$) where d_a is the so-called quantum dimension (not to be confused with other multiplicities discussed in the previous sections). This result is obtained in sections 2.2.2 and 2.3.

From the thermodynamical point of view, the presence of $n_{qp} \gg 1$ quasiparticles in the system implies a quantum entropy at $T = 0$,

$$S_a(T = 0) \sim n_{qp} \log (d_a) \ , \tag{4.43}$$

that is "unexpected" because the state is completely determined (gapped, fixed control parameters, fixed quasiparticle positions, etc.).

This entropy can be obtained from the RCFT partition function described in this paper, that encodes all the low-energy physics of static bulk quasiparticles and massless edge excitations. Let us consider an isolated droplet of Hall fluid, i.e. the disk geometry, and compute the entropy first for one quasiparticle and then for many of them.

The disk partition function for a quasiparticle of type a in the bulk is given by the generalized character $\theta_a(\tau)$ (cf. (3.30) and section 2.1), owing to the condition of global integer charge, $Q_{\rm bulk} + Q_{\rm edge} \in \mathbb{Z}$. The $T = 0$ entropy is a many-body effect that manifests itself in the thermodynamic limit; therefore, we should first send $R \rightarrow \infty$ and then $T \rightarrow 0$, i.e. expand the partition function for $\tau \rightarrow 0$ [47]. Upon performing the $\mathcal{S}$ modular transformation (of both neutral and charged parts), we obtain the leading

behavior, $\theta_a(\tau) \sim \mathcal{S}_{a0}\ \theta_0(-1/\tau) \sim \mathcal{S}_{a0} \exp(i2\pi c/(24\tau))$, and compute the entropy:

$$S_a(T \to 0) = \left(1 - \tau \frac{d}{d\tau}\right) \log \theta_a \sim \log \frac{\mathcal{S}_{a0}}{\mathcal{S}_{00}} - \log \frac{1}{\mathcal{S}_{00}}, \tag{4.44}$$

The first contribution indeed reproduces the entropy for one non-Abelian quasiparticle, $S_a = \log d_a$; note that the Abelian part of the $\mathcal{S}$-matrix cancels out (e.g. $\mathcal{S}_{0a}^{(\text{Abelian})} = 1/\sqrt{\hat{p}}$, $\forall a$, in the Read-Rezayi state) and one obtains the quantum dimension (2.27).

The last term in (4.44) is the (negative) boundary contribution to the entropy, that is also present without quasiparticles; it involves the "total quantum dimension", $\mathcal{D} = 1/\mathcal{S}_{00} = \sqrt{\hat{p}}\sqrt{\sum_a d_a^2}$ [92], where the sum extends over all quasiparticles, and receives a contribution from the Abelian part. Note that a single quasiparticle is not usually associated to a bulk entropy, as described at the beginning of this section, because multiple fusion channels only appear for $n_{pq} \geq 4$ quasiparticles. On the other hand, from the topological point of view, the edge divides the infinite system in two parts, interior and exterior, with the edge keeping track of the missing part [92].

The entropy for several quasiparticles in the bulk can be obtained from the corresponding disk partition function; for two quasiparticles, for example, this is obtained by fusing the two particles and summing over the resulting edge sectors, as follows:

$$Z_{aa} = \sum_b N_{aa}^b\ \theta_b(\tau)\ . \tag{4.45}$$

In general, the repeated fusion of several particles reproduces the computation of the bulk entropy contribution (2.27), leading again to $S \sim n_{qp} \log(d_a)$.

Several aspects of the non-Abelian entropy have been discussed in [91][92]; here we deal with the proposal of observing it in thermopower measurements [84], that could be feasible [93]. Let us consider the annulus geometry and introduce both an electric potential difference ∇V_o and a temperature gradient ∇T between the two edges. The electric current takes the form:

$$\mathbf{J} = -\sigma \cdot \nabla V_o - \alpha \cdot \nabla T\ , \tag{4.46}$$

where σ, α are the electric and Peltier conductivity tensors. The thermopower (or Seebeck coefficient) is defined as the tensor, $S_{\text{Seebeck}} = \sigma^{-1} \cdot \alpha$, i.e. the ratio of transport coefficients pertaining to the two gradients [94].

Here we consider the case of exact compensation between the gradients, such that the current vanishes, $\mathbf{J} = 0$. In this case, the thermopower component in the annulus geometry is given by:

$$S_{\text{Seebeck}} = \frac{\alpha}{\sigma} = -\ \frac{\Delta V_o}{\Delta T}\ = \frac{S}{eN_e}\ . \tag{4.47}$$

In the last part of this equation, we also wrote the desired relation, that the thermopower is equal to the entropy per electron [94][84].

In the following, this result is recovered by adapting the near-equilibrium description by Yang and Halperin [84] to our setting. We consider a small variation of the grand-canonical potential,

$$d\Omega = -SdT - N_e(d\mu + e\ dV_o), \tag{4.48}$$

involving both the chemical μ and electric V_o potentials coupled to the N_e electrons. Note that Eq. (4.48) takes the non-relativistic form because we are describing bulk effects related to adding the quasiparticles. For vanishing current, the gradients induce an excess of charge at the edges that is equivalent to the pressure effect considered in [84]. Therefore, from the definition (4.46) and the grand-canonical potential (4.48), we can express the two conductivities in terms of second derivatives (implying the Maxwell relations), as follows:

$$\sigma = -\frac{\partial Q}{\partial V_o} = e^2 \frac{\partial^2 \Omega}{\partial \mu^2} = -e^2 \frac{\partial N}{\partial \mu} \ , \qquad \alpha = -\frac{\partial Q}{\partial T} = e \frac{\partial^2 \Omega}{\partial \mu \partial T} = -e \frac{\partial S}{\partial \mu} \ . \tag{4.49}$$

Upon taking their ratio, the result (4.47) is recovered for S linear in the number of electrons, as shown momentarily.

From the experimental point of view, quasiparticles of smaller charge ($a = 1$) are induced in the system by varying infinitesimally the magnetic field from the center of the plateau $B = B_o$. In the diluted limit, ν remains constant and the number of quasiparticles n_{qp} and of electrons can be related as follows:

$$n_{qp} = \frac{e(B - B_o)}{e^* B_o} \ N_e \ . \tag{4.50}$$

The entropy associated to the non-Abelian quasiparticles is given by partition function as explained before: in the annulus geometry, its expression for $T \to 0$ is given by the one-edge expression, e.g. (4.45), multiplied by the ground-state contribution for the other edge $\overline{\theta(\tau)}_0$. The result is again given by (4.43) up to a constant.

Finally, the value of the thermopower is found by taking the ratio (4.47) of the entropy over the total electron charge [84]:

$$S_{\text{Seebeck}} = \left| \frac{(B - B_o)}{e^* B_o} \right| \log(d_1) \ . \tag{4.51}$$

Upon measuring the two gradients $\nabla T, \nabla V_o$ near the center of the plateau, one can observe a characteristic V-shaped behavior of S_{Seebeck} signaling the non-Abelian state [93]; other sources of entropy are under control in the gapped state.

In conclusion, we have shown that the RCFT partition function of edge excitations is useful to obtain the $T = 0$ entropies associated to non-Abelian quasiparticles.

Chapter 5

Conclusion

In this thesis, the methods of Rational Conformal Field Theories were applied to the quantum Hall effect, where they provide the low-energy effective-theory description. In this approach, the partition function is a quantity of fundamental importance [47, 56]. The main results of this work were: a straightforward method to obtain the partition functions on non-Abelian Hall states, and the determination of experimental signatures on non-Abelian statistics from these functions. In particular, we analyzed the states in the second Landau level: the Read-Rezayi (RR) and anti-Read-Rezayi ($\overline{\text{RR}}$) states, the Bonderson-Slingerland (BS) hierarchy, the Wen non-Abelian fluids (NAF) and the Ardonne-Schoutens non-Abelian spin-singlet states (NASS). The RCFTs considered are of the type $\widehat{U(1)} \times \widehat{\mathfrak{g}}$, where $\widehat{\mathfrak{g}}$ are Affine algebras or cosets of them $(\widehat{\mathfrak{g}}/\widehat{\mathfrak{h}})$, which describe the neutral part of the edge modes: this is the relevant part for non-Abelian anyons.

In the chapters 1 and 2 we introduced some general topics; in particular, at the end of chapter 2 we reported the conditions that a RCFT must fulfil to describe a QH fluid.

In chapter 3 we described the method to derive the partition function for the annulus geometry; the starting point is to choose the neutral part of the edge theory and the neutral part of the electron field Φ_e. In general, the electron field must be a spin one-half simple current in the RCFT and the charge operator must be normalized in such a way that Φ_e has charge one. In order to obtain the partition function, only the primary fields that are local with respect to the electron field must be taken into account (integer relative statistics with the electron); this condition couples in a non-trivial way the sectors of neutral and charged CFTs, *i.e.* introduce a selection rule among the respective quantum numbers. The sectors of the full theory are equivalence classes containing the states that can be obtained by repeated fusion with the electron. The extended characters are given by the sum of the characters of $\widehat{U(1)} \times \widehat{\mathfrak{g}}$ of primary fields in these equivalence classes; finally, the partition function is diagonal in the basis of these extended characters. For the SLL, the sectors are usually labeled by two kinds of quantum number: a, giving the fractional charge and ℓ, specifying the non-Abelian quantum number.

The partition function is completely determined by imposing the invariance under modular transformations with group Γ_θ. Its generators are: S, T^2, U and V, that can be seen to express natural symmetries in Hall fluids. The invariance under Γ_θ permits

to apply Verlinde's formula: therefore, the closure of the algebra, the fusion rules and the topological order can be derived [69]. We also show that the geometrical modular invariance conditions are completely equivalent to the physical requirements on the spectrum and the properties of electron excitations.

The modular invariant partition function provides a complete definition of the Hilbert space of edge modes and its decomposition into sectors. The derivations of Z is (almost) unique when the conformal initial data ($\widehat{\mathfrak{g}}$) are given and the electron field is specified (Φ_e).

In chapter 4 we used the partition functions to obtain informations about possible signals of non-Abelian statistics. First, we reported the computations of the Coulomb peaks patterns at $T = 0$ for the RR, $\overline{\text{RR}}$, BS, and NAF non-Abelian fluids; in the case of NASS fluids, these are known for $k = 2$ [86] and may be derived also for general k from the partition function. As observed in [82], the patterns measure the low-lying energy levels, so they give partial informations on the excitations that cannot distinguish between Abelian and non-Abelian states. Indeed, we remark that the patterns are equal in some cases where the non-Abelian state can be obtained from an Abelian one by projection [71]. Another case of projection is discussed in appendix A.2 for Jain's states.

Next, the peaks patterns are computed at finite temperature. For $T < T_n$ (the energy scale of neutral modes) the peaks are shifted by a temperature dependent contribution due to the multiplicity factor of the neutral modes. This provides richer information about the neutral modes than the $T = 0$ pattern and, by increasing the experimental precision, it may help to distinguish different proposed effective theories for the same filling fraction ν. In particular, these experiments may be used to understand if $\nu = 5/2$ is either in the Moore-Read or in the anti-Moore-Read and (331) universality class. The modulations of the peaks are also computed in the range of temperature $T_n < T < T_c$ (the energy scale of charged modes). In this range, the modulations depend on the modular matrix $\mathcal{S}_{a,b}$ that is a fundamental quantity characterizing the non-Abelian statistics of excitations.

Furthermore, in the thesis we propose that the multiplicities of the neutral modes could be seen in an experiment of Coulomb-peak time-rate off-equilibrium, *i.e.* at finite bias $V_0 > 0$. The partition function is also used to compute the thermopower that gives experimental access to the entropy of non-Abelian quasi-particles, *alias* measure their so-called quantum dimension.

The partition function of Wen's $SU(m)$ non-Abelian fluids (NAF) for $m > 2$ and of the spin-charge separated states [16] are not reported in this thesis. For the former, we have obtained the partition functions as well the peaks patterns, but have not reported here because they are not of particular phenomenological interest. For the spin-charge separated states the partition function has also been obtained.

We remark that our method of construction of partition functions can be applied to propose other (non-Abelian) edge theories for QH states, as *e.g.* the ADE solution [55] of modular invariant partition function was applied to classify the critical points in 2D. As discussed also in [57], other non-Abelian models can be obtained by the orbifold

technique.

In conclusion, we have observed several analogies between the entanglement and the thermodynamic entropies of non-Abelian Hall states. The numerical simulations also support such relation [96]. We think that an analysis of this point within the methods of RCFT presented in this thesis could be particularly interesting.

Appendix A

Hierarchical states

In this appendix we report the computation of the partition functions for Hierarchical states [73] and the computations of the peak pattern obtained in [71, 72].

The multi-component generalization of the Abelian theory of the Laughlin case (discussed in sections 1.2.1, 2.5.1 and 3.1.3) is obtained as follows [77]: the electron fluid is assumed to have m independent edges, each one described by a Luttinger liquid, altogether yielding the $\widehat{U(1)}^{\otimes m}$ Affine algebra [47]. Its representations are labeled by a vector of (mathematical) charges $r_a, a = 1, \ldots, m$, which spans an m-dimensional lattice, $\vec{r} = \sum_i \vec{v}^{(i)} n_i$, $n_i \in \mathbb{Z}$, that is the closed set for the addition of charge vectors (the Abelian fusion rules). The physical charge is a linear functional of $\vec{r}$ and the Virasoro dimension is a quadratic form, both parameterized by the metric of the lattice, $K^{-1}_{ij} = \vec{v}^{(i)} \cdot \vec{v}^{(j)}$. The spectrum is reported in Eq. (1.13). In these expressions, K is an arbitrary symmetric matrix of couplings, with integer elements, odd on the diagonal, due to requirement that the spectrum contains m electron-like excitations [77]. The vector $\vec{t}$ can be set to, $\vec{t} = (1, \ldots, 1)$, in a standard basis [77]. The spectrum (1.13) is very general due to the many free parameters in the K matrix: these can actually be chosen to reproduce the results of all known hierarchical constructions of wave functions [2].

The prominent Jain hierarchical states [1], with filling fraction $\nu = m/(2ms \pm 1)$, $m, s = 2, 3, \ldots$, where shown to correspond to the matrices $K_{ij} = \pm\delta_{ij} + s\, C_{ij}$ [77], how explained in section 1.3. The Jain spectrum is:

$$Q = \frac{1}{2ms \pm 1} \sum_{i=1}^{m} n_i \ , \qquad L_0 = \pm\frac{1}{2}\left(\sum_{i=1}^{m} n_i^2 - \frac{2s}{m2s \pm 1} \left(\sum_{i=1}^{m} n_i \right)^2 \right) \ . \tag{A.1}$$

(Let us first disregard the case with the minus signs, corresponding to antichiral neutral excitations). The spectrum (A.1) is rather peculiar because it contains $m(m-1)$ *neutral* states with unit Virasoro dimension, $(Q, L_0) = (0, 1)$. By using a bosonic free field construction, one can show that these are chiral currents $J_{\vec{\beta}}$, that can be labeled by the simple roots of $SU(m)$ and generate the $\widehat{U(1)} \otimes \widehat{SU(m)}$ Affine algebra at level one ($c = m$) [77, 12].

The annulus partition functions for multicomponent Luttinger liquids were obtained in [69]: we recall their expressions, first for general K-matrix theories and then for the Jain hierarchy.

As in the previous section, the U modular condition is the most relevant one. In order to solve it, we first group the states with integer-spaced charges in the K lattice (1.13). These are clearly parameterized by $\vec{n} = K\vec{\ell} + \vec{\lambda}$, with $\vec{\ell} \in \mathbb{Z}^m$. Since K is an integer matrix, there is a finite number of $\vec{\lambda}$ values (the sectors of the RCFT), belonging to the quotient of the $\vec{n}$ lattice by the $\vec{\ell}$ lattice:

$$\vec{\lambda} \in \frac{\mathbb{Z}^m}{K\ \mathbb{Z}^m} \ . \tag{A.2}$$

As in section 3.1.3, the $\widehat{U(1)}$ characters in each sector sum up into m-dimensional generalization of the theta functions (3.12):

$$\theta_{\vec{\lambda}} = \frac{\mathrm{e}^{-\pi\, t^T K^{-1} t\, \frac{(\mathrm{Im}\,\zeta)^2}{\mathrm{Im}\,\tau}}}{\eta(q)^m} \times \sum_{\vec{\ell}\,\in\,\mathbb{Z}^m} \mathrm{e}^{i2\pi\left[\frac{\tau}{2}\left(K\vec{\ell}+\vec{\lambda}\right)^T K^{-1}\left(K\vec{\ell}+\vec{\lambda}\right) + \zeta\, \vec{t}^T\left(\vec{\ell}+K^{-1}\vec{\lambda}\right)\right]} . \tag{A.3}$$

Their T^2, S, U, V transformations are straightforward generalizations of (3.16) and can be found in [69]: again, the characters (A.3) carry a finite-dimensional unitary projective representation of the modular group. The dimension of representation is $|\det K|$ from (A.2) and matches the Wen topological order.

The U invariance of the annulus partition function, written as a sesquilinear form of the characters (A.3), implies the equation $t^T K^{-1}(\vec{\lambda} + \vec{\mu}) \in \mathbb{Z}$ for the left and right weights. Its solutions depend on the specific form of K; here, we shall only discuss the diagonal solution, $\vec{\lambda} + \vec{\mu} = 0$, that also solves the other (T^2, S, V) conditions (more details in [69]). Therefore, the modular invariant partition function is obtained replacing (A.3) in (3.17) :

In the Jain hierarchical case, the $\widehat{SU(m)}$ symmetry, the neutral CFT, can be used to rewrite sums of $(m-1)$-dimensional $\widehat{U(1)}$ characters into generalized characters pertaining to representations of this extended symmetry: indeed, all states in the $(m-1)$-dimensional sectors have integer-spaced dimensions. The $\widehat{SU(m)}$ representations and characters were described in Ref.[97]: there are m highest weight representations, corresponding to completely antisymmetric tensor representations of the $SU(m)$ Lie algebra. They are characterized by an additive quantum number modulo m, the so-called m-ality, $\alpha = 1, \ldots, m$: thus, the $\widehat{SU(m)}$ fusion rules are isomorphic to the $\mathbb{Z}_m$ group. Since the $\widehat{SU(m)}$ excitations are neutral, we shall need their characters for $\zeta = 0$, denoted by $\chi_\alpha(\tau, 0)$: they clearly obey $\chi_\alpha(\tau, 0) = \chi_{\alpha \pm m}(\tau, 0)$. The Virasoro dimension of $\widehat{SU(m)}$ representations is:

$$h_\alpha = \frac{\alpha(m-\alpha)}{2m} \ , \qquad \alpha = 0, \ldots, m-1 \ , \tag{A.4}$$

The explicit form of the $\widehat{SU(m)}$ characters will not be necessary in the following, but their leading $|q| \to 0$ behavior:

$$\chi_\alpha(\tau) \sim \binom{m}{\alpha} \exp\left[i2\pi\tau \frac{v_n}{v} \left(\frac{\alpha(m-\alpha)}{2m} - \frac{m-1}{24} \right) \right] + \cdots , \qquad \alpha = 0, 1, \ldots, m-1 \ . \tag{A.5}$$

In this expression we introduced a different Fermi velocity v_n for neutral edge excitations, whose experimental value is expected to be, $v_n \sim v/10$ [85].

The modular transformations of $\widehat{SU(m)}$ characters are reported in [69, 97], S is an Abelian transformation (a phases); while U, V do not act on neutral states.

Furthermore, the $\widehat{U(1)}$ states in $\widehat{U(1)} \otimes \widehat{SU(m)}$ theories can be described by the $\mathbb{Z}_p$ characters (3.12) of section 2.2, with free parameter p, $K_\lambda(\tau, \zeta; p)$, with $\lambda = 1, \ldots, p$. In summary, the modular invariance problem can be reformulated in the two-dimensional basis of $K_\lambda \chi_\alpha$ characters.

The Jain spectrum (A.1) can be rewritten in a basis that makes apparent the decomposition into $\widehat{U(1)}$ and $\widehat{SU(m)}$ sectors: upon substitution of,

$$n_1 = l + \sum_{i=2}^{m} k_i \pm \alpha \ , \qquad n_i = l - k_i \ , \ i = 2, \ldots, m \ , \tag{A.6}$$

where $l, k_i \in \mathbb{Z}$ and α is the $\widehat{SU(m)}$ weight, we find $\nu = \frac{2m}{ms \pm 1}$ and

$$Q = \frac{ml \pm \alpha}{2ms \pm 1} \ , \qquad L_0 = \frac{(ml \pm \alpha)^2}{2m(2ms \pm 1)} \pm \frac{\alpha(m-\alpha)}{2m} + \ r \ , \quad r \in \mathbb{Z} \ . \tag{A.7}$$

Consider these formulas with the upper signs, the other choice will be discussed later. One recognizes the $\widehat{SU(m)}$ contributions to L_0 (A.4), while the $\widehat{U(1)}$ part identifies the parameters of K_λ as $p = m\hat{p}$, $\hat{p} = (2ms + 1)$ and $\lambda = ml + \alpha \mod (m\hat{p})$; note that $\hat{p} = 1 \mod m$ and $\lambda = \alpha \mod m$, and that $\hat{p}, m$ are coprime numbers $(\hat{p}, m) = 1$. The normalization of ζ is chosen for K_λ (3.12) to reproduce the spectrum (A.7): this is, $K_\lambda(\tau, m\zeta; p)$.

The tensor characters $K_\lambda \chi_\alpha$ form a $(m^2\hat{p})$ dimensional basis on which the S transformation act as the $\mathbb{Z}_{m\hat{p}} \times \mathbb{Z}_m$ Fourier transform. The analysis of the spectrum shows that charged and neutral excitations are paired by the condition $\lambda = \alpha \mod m$ (this the consequence of the condition D of section 3.1.4): therefore, we should choose a subspace of tensor characters that obeys this condition and is closed under modular transformations. The dimension of this subspace is the topological order $\hat{p}$. A well-known trick to reduce the space of the discrete Fourier transform by a a square factor m^2 [55] is to consider the following m-term linear combinations of characters obeying $\lambda = \alpha \mod m$ [69],

$$\mathrm{Ch}_\lambda(\tau, \zeta) = \sum_{\beta=1}^{m} K_{\lambda+\beta\hat{p}}(\tau, m\zeta; m\hat{p}) \ \chi_{\lambda+\beta\hat{p} \bmod m}(\tau, 0) \ , \qquad \lambda = 1, \ldots, m\hat{p} \ . \tag{A.8}$$

These characters satisfy $\mathrm{Ch}_{\lambda+\hat{p}} = \mathrm{Ch}_\lambda$; thus, there are $\hat{p}$ independent ones, which can be chosen to be (due to $\hat{p} = 1 \mod m$):

$$\theta_a = \mathrm{Ch}_{ma} \ , \qquad a = 1, \ldots, \hat{p} \ , \qquad \hat{p} = ms + 1 \ . \tag{A.9}$$

They can be obtained as well by the extension of the initial algebra by the electron field.

One can check that these generalized characters θ_a carry a $\hat{p}$ dimensional representation of the modular transformations (T^2, S, U, V), with $S_{ab} \propto \exp(i2\pi\ mab/\hat{p})/\sqrt{\hat{p}}$ that gives Abelian fusion rules. The modular invariant annulus partition function is therefore the diagonal expression in these characters: $Z^{\widehat{U(1)}\times\widehat{SU(m)}}_{\rm annulus} = \sum_{a=1}^{\hat{p}}\ \theta_a\ \overline{\theta}_a$. Indeed, the characters θ_a can be shown to be equal to the $\chi_{\vec{\lambda}}$ in (A.3) for $K = 1 + sC$, once the corresponding $\widehat{U(1)}$ charges are identified [69].

The V transformation,

$$V\ :\ \theta_a(\tau, \zeta + 1) = \mathrm{e}^{-i2\pi\frac{m}{\hat{p}}\left(\mathrm{Re}\ \zeta + \mathrm{Re}\ \frac{\tau}{2}\right)}\ \theta_{a+1}(\tau, \zeta)\ , \tag{A.10}$$

shows that the minimal transport of charge between the two edges is m times the elementary fractional charge; this is the smallest spectral flow among the states contained in (A.8) which keeps β constant, namely which conserves the $\widehat{SU(m)}$ quantum number carried by the neutral excitations. The Hall current, $\nu = m/\hat{p}$, is thus recovered.

We now give the partition functions for Jain states with charged and neutral excitations of opposite chiralities on each edge, corresponding to $\nu = m/(ms-1)$ in (A.1) [69]. The chirality of the neutral excitations can be switched by a simple modification of the characters (A.8),

$$\mathrm{Ch}^{(-)}_{\lambda} = \sum_{\beta=1}^{m}\ K_{\lambda+\alpha\hat{p}}(\tau, m\zeta; m\hat{p})\ \overline{\chi}_{\lambda+\beta\hat{p}\ \mathrm{mod}\ m}\ , \qquad \lambda = 1, \ldots, m\hat{p} = m(ms-1)\ . \tag{A.11}$$

This gives again a representation of the modular group for $\hat{p} = ms - 1 > 0$. The U condition implies the partition function: $Z^{(-)}_{\rm annulus} = \sum_{a=1}^{\hat{p}}\ \mathrm{Ch}^{(-)}_{m\lambda}\overline{\mathrm{Ch}}^{(-)}_{m\lambda}$. that is modular invariant and reproduces the spectrum (A.1) for $\nu = m/(ms-1)$.

A.1 Coulomb peaks in hierarchical states

The following disk partition functions can be extracted from the annulus expressions (3.17),

$$Z^{\widehat{U(1)}\otimes\widehat{SU(m)}}_{\mathrm{disk},a} = \theta_a = \sum_{\beta=1}^{m} K_{ma+\beta\hat{p}}(\tau, m\zeta; m\hat{p})\ \chi_\beta(\tau)\ \ , \quad a = 1, \ldots, \hat{p}, \tag{A.12}$$

where $\hat{p} = ms + 1$. The novelty w.r.t. the Laughlin case of section 3.1, is that each sector contains combined charged and neutral excitations, that are described by the K_λ (4.15) and $\chi_\alpha(\tau)$ (A.5) characters, respectively. For example, in the $\nu = 2/5$ case, $(m = 2, \hat{p} = 5)$, there are two neutral characters that combine with ten charged ones to obtain the following five sectors:

$$\begin{aligned}
\theta_0 &= K_0(\tau, 2\zeta; 10)\ \chi_0 + K_5(\tau, 2\zeta; 10)\ \chi_1\ , \\
\theta_{\pm1} &= K_{\pm2}(\tau, 2\zeta; 10)\ \chi_0 + K_{5\pm2}(\tau, 2\zeta; 10)\ \chi_1\ , \\
\theta_{\pm2} &= K_{\pm4}(\tau, 2\zeta; 10)\ \chi_0 + K_{5\pm4}(\tau, 2\zeta; 10)\ \chi_1\ .
\end{aligned} \tag{A.13}$$

We now search for degeneracy of energy levels differing by the addition of one electron, $\Delta Q = 1$. Consider for definiteness the $\nu = 2/5$ case without any bulk quasiparticle, i.e. θ_0 above. From the expressions (4.15, A.12, A.13), one finds that the first term K_0 resumes all even integer charged excitations, while K_5 the odd integer ones. Therefore, the first conductance peak is found when the lowest energy state in K_0 χ_0, i.e. the ground state, with $E = (v_c/R)(2\sigma)^2/20$, $Q = 0$, becomes degenerate with the lowest one in K_5 χ_1, with $E = (v_c/R)(-5 + 2\sigma)^2/20 + v_n/4R$, $Q = 1$. The next peak occurs when the latter becomes degenerate with the first excited state ($Q = 2$) in K_0 χ_0, and so on. Note that in the previous energies we modified $\sigma \to 2\sigma$, (cf. (4.15)), in order to respect the flux-charge relation, $\Delta Q = \nu \Delta\phi/\phi_o$.

For general m values, the result can be similarly obtained by comparing the energies in consecutive pairs of terms, β and $\beta + 1$, in θ_0 (A.12). One finds:

$$\Delta\sigma_\beta = \sigma_{\beta+1} - \sigma_\beta = \frac{\hat{p}}{m} + \frac{v_n}{v}\left(h_{\beta+2} - 2h_{\beta+1} + h_\beta\right) \ . \tag{A.14}$$

where h_β are the $\widehat{SU(m)}$ dimensions (A.4). Since they are quadratic in β, the discrete second derivative in (A.14) is constant, except for one value at the border of the m period. This implies that there are groups of m equally spaced peaks, with a larger spacing between groups.

An important fact shown by the $\widehat{SU(m)}_1$ character (A.5), is that the low-lying neutral states occur with characteristic multiplicities $d_\beta = \binom{m}{\beta}$. This means that d_β degenerate states are simultaneously made available for the β-th electron to tunnel into the droplet. These multiplicities can be easily understood in a classical model of m superposed fluids, where the one-electron excitation is m times degenerate, the two-electron one is $m(m-1)/2$ times and so on.

Summarizing, in the Jain hierarchical states, $\nu = m/\hat{p}$, the peak pattern is the following: the separation $\Delta\sigma_k$ between the k-th and $(k+1)$-th peaks and the level multiplicity d_k read ($\sigma = B\Delta S/\phi_o$):

$$\begin{aligned} \Delta\sigma_k &= \frac{\hat{p}}{m} - \frac{v_n}{v}\frac{1}{m} \ , & d_k &= \binom{m}{k} \ , \ k = 1, \ldots, m-1, \\ \Delta\sigma_m &= \frac{\hat{p}}{m} + \frac{v_n}{v}\frac{m-1}{m} \ , & d_m &= 1 \ . \end{aligned} \tag{A.15}$$

The pattern repeats with periodicity m. It is independent of the presence of quasiparticles in the bulk, because the corresponding sectors, θ_a, $a \neq 0$, have linearly shifted energies w.r.t those of θ_0 (cf.(A.12)) [71]. Note that the bulk quasiparticles have the same multiplicities: for example, at $\nu = 2/5$ there are two quasiparticles with $Q = 1/5$ (cf. (A.13)). In presence of quasiparticles with multiplicity $\binom{m}{k-1}$, the sequence of peaks (A.15) starts from $\Delta\sigma_k$ (instead of $\Delta\sigma_1$) and goes on periodically. We remark that the results (A.15) can also be obtained from the analysis of the m-dimensional lattice of excitations (A.1), where the multiplicities d_k are found by counting the shortest vectors with integer charge k.

The multiplicities d_β of low-lying edge excitations could be experimentally observed in the Coulomb peaks at $T > 0$ and in the off equilibrium experiments described in Chapter 4.

We now consider the Jain hierarchical states with mixed chiralities, $\nu = m/(ms-1)$, described by the disk partition functions (A.11). These were obtained by the replacement, $\chi_\beta \to \overline{\chi}_\beta$, that does not affect the earlier discussion of energetics.

The dynamics of these m-composite edge theories was much discussed in the literature, starting from the experimental result [98]. Actually, the presence for $\nu = m/(ms-1)$ of neutral and charged excitations of opposite chiralities on the same edge may allow for destabilizing interactions, leading to edge reconstruction effects [99]. Several deformations of, or additions to the Luttinger liquid Hamiltonian, have been put forward; as these break the $\widehat{SU(m)}_1$ symmetry and possibly the conformal symmetry, they may lift the peak degeneracy. Therefore, it is interesting to find their predictions for the Coulomb peak patterns and compare with the present results of the m-component Abelian theory.

A.2 Coulomb peaks in alternative hierarchical theories

In this section we discuss the Coulomb peaks in two alternative theories of the Jain states: the $W_{1+\infty}$ minimal models [12], introduced by Trugenberger and some of the authors, and the three-fluid theory [100] by Fradkin and Lopez. Both theories:

i) possess a reduced number of currents and more generally less degrees of freedom w.r.t. the m component Luttinger theory;

ii) are not rational CFT, i.e. their partition function are not modular invariant. Nevertheless, these theories are projections of RCFTs and the partition function can be found by working out the reduction of degrees of freedom; the Coulomb blockade peaks are then found by the same methods as before.

We first discuss the minimal $W_{1+\infty}$ models [12]: these theories were introduced by exploiting the main geometrical feature of incompressible Hall fluids, which is the symmetry under area-preserving diffeomorphisms of the plane, the local coordinate transformations that keep the density constant [12]. The edge excitations can be seen as infinitesimal area-preserving deformations of the Hall droplet , and can be naturally described by the representations of the symmetry algebra. In the mathematical literature, this is called the $W_{1+\infty}$ algebra and its representations on the circle, i.e. on the edge CFT, have been completely classified [101].

The mathematical results are the following: for generic parameters, the $W_{1+\infty}$ representations are isomorphic to those of the multicomponent Luttinger theory and their m dimensional K lattices. However, for special lattices, there exist degenerate representations, with a reduced set of excitations: as shown in [12], these correspond one-to-one with the $\widehat{SU(m)}_1$ symmetric lattices of the Jain states discussed before. For these theories, it is thus possible to project out states of the Luttinger theory and obtain the minimal $W_{1+\infty}$ models made of irreducible representations only. The main features of these models are [12]:

i) the multiplicities due to the $SU(m)$ symmetry are completely eliminated; in particular, there is only one conserved $U(1)$ current, the electric current, a single electron state (not m) and no further degeneracies in the spectrum. The charges and conformal

dimensions are still given by the formulas (A.1), but the integer labels are constrained within the wedge,

$$n_1 \geq n_2 \geq \cdots \geq n_m \ ; \tag{A.16}$$

ii) the conformal symmetry is maintained, but the partition function is not modular invariant. The projection from the m component Luttinger liquid to the minimal models can be realized by introducing a non-local, $\widehat{SU(m)}$ breaking interaction in the Luttinger Hamiltonian, that commutes with Virasoro [78]. This term is diagonal in the $SU(m)$ basis and gives higher energies to the unwanted states; at infinite coupling the projection is realized leading to the $W_{1+\infty}$ minimal theory. The non-locality of the interaction term in the Hamiltonian explains the lack of modular invariance in these theories.

The conductance peaks in the minimal $W_{1+\infty}$ theories are easily obtained: since the projection preserves the structure of the Hilbert space of the ($c = m$) Luttinger theory, it does not modify the structure of disk partition functions (A.12), but only replaces the neutral characters χ_α by other expressions whose leading terms (A.5) have no multiplicity factors [102]:

$$\chi_\alpha^{W_{1+\infty}}(\tau) \sim \exp\left[i2\pi\tau\frac{v_n}{v}\left(\frac{\alpha(m-\alpha)}{2m} - \frac{m-1}{24}\right)\right] + \cdots , \qquad \alpha = 0, 1, \ldots, m-1 \ . \tag{A.17}$$

The absence of multiplicities can also be understood from the charge lattice (A.1) as due to the constraint (A.16). We conclude that the $W_{1+\infty}$ minimal models predict conductance peaks in Jain states with the same pattern (A.15) as the Luttinger theory but without any multiplicity.

The Lopez-Fradkin theory of Jain's states is a variant of the multicomponent Luttinger liquid and can be formulated in the charge lattice approach introduced before: all Jain states, $\nu = m/(ms+1)$, s even, are described by the same three-dimensional K matrix and charge vector t,

$$K = \begin{pmatrix} -s & 1 & o \\ 1 & m & 0 \\ 0 & 0 & 1 \end{pmatrix} , \qquad t = (1, 0, 0) \ . \tag{A.18}$$

The first component clearly describes the charged excitations; the other two sectors are called topological, because their neutral excitations do not propagate, i.e. $v_n = 0$. This choice modifies the time scaling of the electron correlator: for $1/3 < \nu < 1/2$, the multicomponent Luttinger theory predicts a constant exponent $\alpha = 3$, while the Lopez-Fradkin theory a varying one, $\alpha = 1/\nu$, which is in better agreement with the experimental results [98]. Note, however, that the m component Luttinger theory also predicts $\alpha = 1/\nu$ in the limit $v_n = 0$, while other experiments would favor $0 < v_n \ll v$ [45].

Another feature of Lopez-Fradkin theory is that the excitations are described by a subspace of the three dimensional charge lattice (1.13): the integers (n_1, n_2, n_3) labeling excitations are constrained by the condition of physical states, $n_2 = -n_3$. Therefore, the partition function has the general charge-lattice form (1.13), but it is not modular invariant due to this constraint.

The Coulomb peaks in this theory are equidistant because the modulations are proportional to $v_n/v = 0$: moreover, there is a single electron excitation and no level multiplicities because the two dimensional sub-lattice of (A.18) has no symmetries. For the same reason, the Coulomb peaks would be equally spaced even for $v_n > 0$.

In conclusion, we have shown that three proposed theories for the Jain states predict rather different patterns of conductance peaks at $T > 0$ that would be interesting to test experimentally. Other edge theories have been proposed whose peak patters remain to be investigated [99].

Appendix B

Modular transformations

In this Appendix, we collect some definitions, properties and modular transformations of the non-Abelian characters used in the text. A brief review on modular invariance and modular forms can be found in [72] and the reference therein; more extensive material is presented in [47].

B.1 Read-Rezayi

The properties and transformations of parafermion characters (3.44) and (3.45) are obtained from the coset construction [47][52][81]. The basic identity of the coset $\widehat{SU(2)}_k/\widehat{U(1)}$ (resp. $\widehat{SU(3)}_k/\widehat{U(1)}^2$ for the NASS state) is the following expansion of the affine $\widehat{SU(2)}_k$ (resp. $\widehat{SU(3)}_k$) characters χ^Λ:

$$\chi^\Lambda(\tau,\zeta) = \sum_{\lambda\in P/kQ} \chi^\Lambda_\lambda(\tau)\ \vartheta_\lambda(\tau,\zeta)\,, \tag{B.1}$$

where χ^Λ_λ are the parafermionic characters and ϑ_λ are classical theta function at level k associated to the root lattice Q of the Lie algebra [47]. The indices Λ and λ belong to the weight lattice P (cf. Section 3.4).

For the $SU(2)$ lattice, $\vartheta_{m/\sqrt{2}}(\tau,\zeta) = K_m(\tau,k\zeta;2k)$, the Abelian theta function (3.12), and $\chi^\Lambda_\lambda = \chi^\ell_m$ the $\mathbb{Z}_k$ parafermion characters. From (B.1) we also obtain the embedding index for the cosets, $2k$ and $2k\times 6k$ for $\widehat{SU(2)}_k/\widehat{U(1)}$ and $\widehat{SU(3)}_k/\widehat{U(1)}^2$, respectively. The modular transformations of the characters χ^ℓ_m are determined in such way that (B.1) reproduces the correct transformation of the $\widehat{SU(2)}_k$ characters:

$$\chi^\ell\left(\frac{-1}{\tau}\right) = \sum_{\ell'=0}^{k} s_{\ell,\ell'}\ \chi^{\ell'}(\tau)\ , \quad s_{\ell,\ell'} = \sqrt{\frac{2}{k+2}}\ \sin\frac{\pi(\ell+1)(\ell'+1)}{k+2}. \tag{B.2}$$

(For simplicity, we fix $\zeta=0$ in neutral characters). The combination of (B.1) and (B.2) yields the transformation of the characters χ^ℓ_m in (3.45).

The field identifications (3.44),(3.77), leading to symmetries among the parafermionic characters, follow from the properties of the modular transformations [81]. For example,

in the $\widehat{SU(2)}_k$ case the matrix $s_{\ell,\ell'}$ obeys the following symmetry under $\ell \to \mathcal{A}(\ell) = k-\ell$:

$$\mathcal{A}\left(s_{\ell',\ell}\right) \equiv s_{\mathcal{A}(\ell'),\ell} = s_{k-\ell',\ell} = (-1)^{\ell}\ s_{\ell',\ell}\,. \tag{B.3}$$

We now describe the modular transformation (3.48) of the Read-Rezayi extended characters θ^{ℓ}_{a} (3.46). After transformation of each term in their sum, the sum over the running index b yields:

$$\theta^{\ell}_{a}(-1/\tau) = \frac{k}{\sqrt{2\ k\ p}} \sum_{q'=0}^{p-1} \sum_{m'=0}^{2k-1} \sum_{\ell=0}^{k} \delta^{(k)}_{m',q'}\ e^{2\pi i \frac{2aq'-\hat{p}am'}{p}} s_{\ell,\ell'} K_{q'} \chi^{\ell'}_{m'}\,. \tag{B.4}$$

The mod-k delta function is solved by $m' = q' + \sigma k$ with $\sigma = 0,\ 1$; then, q' is re-expressed as $q' = a' + b'\hat{p}$, with a' mod $\hat{p}$ and b' mod k. The sum on q' and m' can be decomposed into $\sum_{\sigma=0}^{1} \sum_{a'=0}^{\hat{p}-1} \sum_{b'=0}^{k-1}$, and the phase is rewritten, $(-1)^{\sigma a}\ e^{-2\pi i \frac{Maa'}{2\hat{p}}}$. Using the identification (3.44) and (B.3), the sum on σ becomes $2\delta^{(2)}_{a,\ell}$ and finally the result (3.48) is obtained.

Calling the whole S-transformation of the θ^{ℓ}_{a} characters in (3.48) as $S^{\ell\ \ell'}_{a,a'}$, we now check its unitarity. We find that,

$$\sum_{\ell',a'} S^{\ell\ell'}_{a,a'} (S^{\dagger})^{\ell'\ell''}_{a',a''} = \frac{1}{\hat{p}} \sum_{\ell'=0}^{k} \delta^{(2)}_{a,\ell} \delta^{(2)}_{a'',\ell''} s_{\ell\ \ell'} s_{\ell'\ \ell''} \sum_{a'=0}^{\hat{p}-1} e^{2\pi i \frac{a'(a-a'')M}{2\hat{p}}}\ . \tag{B.5}$$

Since the non-Abelian part is unitary, we obtain $\delta^{(2)}_{\ell,\ell''}$ and thus $\delta^{(\hat{p})}_{(a-a'')M/2,0}$; the latter condition is equivalent to $\delta^{(2\hat{p})}_{aa''}$ because $\hat{p}$ and M are coprime, $(\hat{p}, M) = 1$.

B.2 NAF and $\overline{\mathrm{RR}}$

We now derive the modular transformation of the NAF characters θ^{ℓ}_{a} in (3.55). The transformation of the two terms in their expression leads to:

$$\theta^{\ell}_{a}(-1/\tau) = \frac{1}{\sqrt{2\hat{p}}} \sum_{q'=0}^{2\hat{p}-1} \sum_{\tilde{\ell}=0}^{k} e^{2\pi i \frac{aq'}{2\hat{p}}} \left(s_{\ell\ \tilde{\ell}} + s_{k-\ell\ \tilde{\ell}} e^{\pi i q'} \right) \chi^{\tilde{\ell}} K_{q'}\,. \tag{B.6}$$

The term in the parenthesis is $2s_{\ell\ \tilde{\ell}}\delta^{(2)}_{q',\tilde{\ell}}$, using (B.3); this condition can be solved by the following parameterization: $q' = a' + b'\hat{p}$ and $\tilde{\ell} = \ell'$ for $b' = 0$, and $\tilde{\ell} = k - \ell'$ for $b' = 1$, with $a' = 0$ mod $\hat{p}$ and $\ell' = a'$ mod 2. The sums on q' and $\tilde{\ell}$ become sums on $a',\ \ell'$ and b'. The sum on b' is,

$$e^{2\pi i \frac{aa'}{2\hat{p}}} \left(s_{\ell\ \ell'} K_{a'} \chi^{\ell'} + s_{\ell\ k-\ell'} e^{i\pi a} \chi^{k-\ell'} K_{a'+\hat{p}} \right) =$$

$$= e^{2\pi i \frac{aa'}{2\hat{p}}} \delta^{(2)}_{a\ \ell} s_{\ell\ \ell'} \left(K_{a'} \chi^{\ell'} + \chi^{k-\ell'} K_{a'+\hat{p}} \right)\,,$$

finally leading to (3.57).

The unitary of the modular transformation in (3.57) can be verified following the same steps of the previous section. For $\overline{\mathrm{RR}}$ fluids the computation is the same due to the reality of the $\widehat{SU(2)}_k$ S-matrix; a little difference is that $k + M$ is odd for NAF and M is odd for $\overline{\mathrm{RR}}$.

B.3 Bonderson-Slingerland states

The BS case is easier by changing the basis of characters from (3.72 to the one in (3.74), because the new Ising characters possess simpler transformations. This new basis is ($a = 0, 1, \ldots, nM$):

$$\begin{aligned}
\widetilde{\theta}_{a,0} = &\quad \tfrac{1}{\sqrt{2}}\left(\theta_{a,0} + \theta_{a,2}\right) = \textstyle\sum_{b=1}^{2n} K_{2an+b\hat{p}}\left(\tau, 2n\zeta; 2n\hat{p}\right)\ \Theta_b\ \widetilde{\chi}_0,\ m = 0 \\
\widetilde{\theta}_{a,1} = &\quad \theta_{a,1} = \textstyle\sum_{b=1}^{2n} K_{(2a+1)n+b\hat{p}}\left(\tau, 2n\zeta; 2n\hat{p}\right)\ \Theta_b\ \widetilde{\chi}_1, \qquad\qquad m = 1, \\
\widetilde{\theta}_{a,2} = &\quad \tfrac{1}{\sqrt{2}}\left(\theta_{a,0} - \theta_{a,2}\right) = \textstyle\sum_{b=1}^{2n} e^{i\pi b} K_{2an+b\hat{p}}\left(\tau, 2n\zeta; 2n\hat{p}\right) \Theta_b \widetilde{\chi}_2,\ m = 2,
\end{aligned} \tag{B.7}$$

The computation requires the modular transformation of $\widehat{SU(n)}_1$ characters [69]:

$$\Theta_b\left(-\frac{1}{\tau}\right) = \frac{1}{\sqrt{n}} \sum_{b'=1}^{n} \mathrm{e}^{-i2\pi\frac{bb'}{n}}\ \Theta_{b'}\left(\tau\right)\ . \tag{B.8}$$

Combining all the transformations in the factors of $\widetilde{\theta}_{a,i}$, we write:

$$\begin{aligned}
\widetilde{\theta}_{a,i} \quad = \quad & \frac{1}{\sqrt{n^2 2\hat{p}}} \sum_{b=1}^{2n} \sum_{q'=1}^{p} \sum_{\beta'}^{n} e^{2\pi i \frac{(2an+n\delta_{i,1}+b\hat{p})q' - 2\hat{p}b\beta'}{2n\hat{p}} + \pi i \delta_{i,2} b} \times \\
& \times K_{q'} \Theta_{\beta'} \sum_{i'=0}^{2} S^{\mathrm{Ising}}_{i,i'}\ \widetilde{\chi}_{i'}\ ,
\end{aligned} \tag{B.9}$$

where the modular transformation,

$$S^{\mathrm{Ising}} = \begin{pmatrix} 1 & 0 & 0 \\ 0 & 0 & 1 \\ 0 & 1 & 0 \end{pmatrix},$$

is defined according to (3.74). The sum on b gives the factor $\delta^{(2n)}_{q',2\beta'+n\delta_{i,2}}$, whose solution requires to parameterize q' as $q' = r' + \widetilde{b}\hat{p}$, with r' mod $\hat{p}$ and $\widetilde{b}$ mod $2n$. The delta function imposes,

$$r' - n\delta_{i,2} + 2\widetilde{b} - 2\beta' = 2ln\,, \qquad \text{i.e.} \qquad r' - n\delta_{i,2} = 2a'\,, \qquad \widetilde{b} - \beta' = \sigma n\,,$$

since $\widetilde{b}$ and β' are defined mod $2n$ and n, respectively, $\sigma = 0,\ 1$. It is convenient to write $r' = 2a' + n\delta_{i,2}$, with a' mod $\hat{p}/2$, which is coprime with n; therefore, we can write $r' = 2a'n + n\delta_{i,2}$. Note that β' is the index mod n of $\Theta_{\beta'}$, thus we can replace it with $\widetilde{b}$. After these substitutions in (B.9), we obtain the modular transformation of the Bonderson-Slingerland characters (B.7), with S reported in (3.75). The unitarity of

this matrix is:

$$\sum_{a',m'} S_{(a,m),(a',m')} S^{\dagger}_{(a',m'),(a'',m'')} = \sum_{a'} e^{2\pi i \frac{a'(a-a'')}{mM+1}} \times \begin{pmatrix} 1 & 0 & 0 \\ 0 & 0 & e^{i2\pi a' n/2(nM+1)} \\ 0 & e^{i2\pi a n/2(nM+1)} & 0 \end{pmatrix} \times \begin{pmatrix} 1 & 0 & 0 \\ 0 & 0 & e^{-i2\pi a n/2(nM+1)} \\ 0 & e^{-i2\pi a' n/2(nM+1)} & 0 \end{pmatrix} = \delta^{(mM+1)}_{a\ a''} \delta_{m\ m''} \,.$$

B.4 NASS states

The modular transformations of the $\widehat{SU(3)}_k/\widehat{U(1)}^2$ parafermion characters is found from (B.1): the S-matrix of the $\widehat{SU(3)}_k$ characters in the numerator of the coset is,

$$\chi^{\Lambda}\left(\frac{-1}{\tau}\right) = \sum_{\Lambda' \in P_k^+} s_{\Lambda\Lambda'}\ \chi^{\Lambda'}(\tau),$$
$$s_{\Lambda\Lambda'} = \frac{i}{\sqrt{3}(k+3)} \sum_{w \in W} (-1)^{|w|} \exp\left[2\pi i \frac{(w(\Lambda+\rho)\ ,\ \Lambda'+\rho)}{k+3}\right], \qquad \text{(B.10)}$$

where w is an element of the Weyl group W of $SU(3)$, $|w|$ is its length, and ρ is half of the sum of the positive roots [47]. The coset decomposition yields the following transformations of the parafermionic characters:

$$\chi^{\Lambda}_{\lambda}(-\frac{1}{\tau}) = \frac{1}{\sqrt{3}k} \sum_{\lambda' \in P/kQ} e^{-2\pi i \frac{(\lambda,\lambda')}{k}} \sum_{\Lambda' \in P_+^k} s_{\Lambda\Lambda'}\ \chi^{\Lambda'}_{\lambda'}(\tau)\,, \qquad \text{(B.11)}$$

where the ranges of the indices are explained in section 3.4. Useful properties of $s_{\Lambda\Lambda'}$ are its transformations under the automorphism $\mathcal{A}$ [81]:

$$\Lambda = (n_1, n_2) \mapsto \mathcal{A}(\Lambda) = (k - n_1 - n_2, n_1)\ ,$$
$$\mathcal{A}\left(s_{\Lambda',\Lambda}\right) \equiv s_{\mathcal{A}\Lambda',\Lambda} = s_{\Lambda',\Lambda}\ e^{2\pi i \frac{2n_1+n_2}{3}}; \qquad \text{(B.12)}$$

this is the $\widehat{SU(3)}_k$ version of (B.3): note that this map obeys $\mathcal{A}^3 = 1$. The field identifications (3.77) are deduced by studying the the modular matrix of the parafermionic characters [81]. Equation (3.77) can be rewritten as $\chi^{\Lambda}_{\lambda} = \chi^{\mathcal{A}(\Lambda)}_{\mathcal{A}(0)+\lambda} = \chi^{\mathcal{A}^2(\Lambda)}_{2\mathcal{A}(0)+\lambda}$.

In order to derive the modular transformation of NASS characters (3.94), we rewrite (3.90) as follows:

$$\Theta^{n_1 n_2}_{q,s}(\tau,\zeta) = \sum_{a,b=0}^{k-1} \sum_{\iota=0,1} K^{(Q)}_{q+\hat{p}(a+b)+\iota k\hat{p}}\ K^{(S)}_{s+(a-b)+\iota k}\ \chi^{n_1,\ n_2}_{\frac{q+s}{2}+2a+b,\frac{-q+s}{2}-a-2b}\,. \qquad \text{(B.13)}$$

After transformation of each term in this sum, we find

$$\Theta_{q,s}^{n_1 n_2}\left(-\frac{1}{\tau}\right) = \frac{1}{\sqrt{2kp}} \sum_{\iota=0,1} \sum_{a,b=0}^{k-1} \sum_{s'=0}^{2k-1} \sum_{c'=0}^{p-1} \sum_{\mu \in \frac{P}{kQ}} \sum_{\Lambda' \in P_+^k} S_{\Lambda\Lambda'}$$
$$\times \exp\left[2\pi i \left(\frac{(m+\hat{p}(a+b)+\iota k\hat{p})c'}{q} + \frac{(s+(a-b)+\iota k)s'}{2k} - \frac{(\lambda,\mu)}{k}\right)\right]$$
$$\times K_{c'}^{(Q)}\ K_{s'}^{(S)}\ \chi_\mu^{\Lambda'}(\tau) \tag{B.14}$$

where λ is an abbreviation for the subscript of χ_λ^Λ in (B.13). The sum on ι gives $2\delta^{(2)}_{c',s'}$. The next step requires to explicit the product (λ,μ); then, the sums on a and b give the conditions:

$$\frac{c'+s'}{2} - \mu_1 = 0 \mod k\,, \qquad \frac{c'-s'}{2} + \mu_2 = 0 \mod k\,. \tag{B.15}$$

These equations have three solutions in the fundamental domain $\mu \in P/kQ$ that should be taken into account. As before, we reparameterize the indices c' and s':

$$c' = \tilde{q} + \hat{p}(\tilde{a}+\tilde{b}) + \tilde{\iota}k\hat{p}\,, \qquad s' = \tilde{s} + (\tilde{a}-\tilde{b}) + \tilde{\iota}k\,. \tag{B.16}$$

Note that since $c' = s' \bmod 2$ also $\tilde{q} = \tilde{s} \bmod 2$. In this parameterization, the three solutions of (B.15) are,

$$\mu_1 = \frac{\tilde{q}+\tilde{s}}{2} + 2kN(\tilde{a}+\tilde{b}) + 2\tilde{a} + \tilde{b} + \tilde{n}k\ , \qquad \mu_2 = \frac{-\tilde{q}+\tilde{s}}{2} - 2\tilde{b} - \tilde{a} - \tilde{n}'k\ , \tag{B.17}$$

where the possible values of $(\tilde{n},\tilde{n}')$ are $(0,0)$, $(1,0)$ and $(1,1)$. The weight μ in (B.17) can be rewritten,

$$\mu = \tilde{\mu} + tA(0)\ , \qquad t = \tilde{n} + \tilde{n}' + 2N(\tilde{a}+\tilde{b})\,. \tag{B.18}$$

Using the automorphism (B.12), we find,

$$S_{\Lambda\Lambda'}\ \chi^{\Lambda'}_{\tilde{\mu}+tA(0)} = S_{\Lambda\Lambda'}\ \chi_{\tilde{\mu}}^{A^{-t}(\Lambda')} = S_{\Lambda A^t(\Lambda'')}\ \chi_{\tilde{\mu}}^{(\Lambda'')} = e^{2\pi i t(2n_1+n_2)/3} S_{\Lambda\Lambda''}\ \chi_{\tilde{\mu}}^{\Lambda''}\ ,$$

with $\Lambda'' = A^{-t}(\Lambda')$. Upon substituting in (B.14), the phase becomes,

$$2\pi i \left(-\frac{q\tilde{q}N}{3p} - \frac{q}{6}(\tilde{n}+\tilde{n}') - \frac{s}{2}(\tilde{n}-\tilde{n}) + \frac{qN(\tilde{a}+\tilde{b})}{3} + \tilde{\iota}\frac{q+s}{2} + \frac{t(2n_1+n_2)}{3}\right).$$

The sum on $\tilde{\iota}$ yields $\delta^{(2)}_{q,s}$. The sum on the three values of (n,n') leads to:

$$\delta^{(3)}_{-\frac{q+3s}{2}+2n_1+n_2,0} = \delta^{(3)}_{n_1-n_2,q}, \tag{B.19}$$

which is the triality condition. Finally, the result in (3.94) is recovered.

The unitary of the the S-matrix is:

$$\sum_{q'\Lambda'} S^{\Lambda\Lambda'}_{qq',ss'} (S^\dagger)^{\Lambda'\Lambda''}_{q'q'',s's''} =$$
$$= \delta^{(3)}_{n_1-n_2,q}\delta^{(3)}_{n_1''-n_2'',q''}\delta^{(2)}_{q,s}\delta^{(2)}_{q'',s''} \sum_{\Lambda'} s_{\Lambda\Lambda'}\ s^\dagger_{\Lambda'\Lambda''} \sum_{q'} e^{-2\pi i M \frac{q'(q-q'')}{3p}}\,. \tag{B.20}$$

This expression is zero for $n_1 - n_2 \neq n_1'' - n_2''$ mod 3. Then, for $n_1 - n_2 = n_1'' - n_2''$, i.e. $\Lambda - \Lambda'' \in Q$, the two delta mod 3 impose $q - q'' = 3n$ for an integer n; the sum on the two indices q' and Λ' plus the unitary of $s_{\Lambda\ \Lambda'}$ show that the l.h.s. of (B.20) is equal to $\delta^{(\hat{p})}_{(q-q'')N/3,0}\delta_{\Lambda,\Lambda''}$. For $N \neq 0$ mod 3, $\delta^{(\hat{p})}_{(q-q'')N/3,0} = \delta^{(\hat{p})}_{q-q'',0}$, since $(\hat{p}, N) = 1$, thus proving unitarity. Note that the case $N = 1$ includes the physically relevant fractions, $\nu = 2 + \frac{4}{7}$ and $\nu = 2 + \frac{2}{3}$, for $k = 2, 3$.

Bibliography

[1] J. K. Jain, *Composite Fermions*, Cambridge Univ. Press (2007), Cambridge.

[2] X. G. Wen, *Quantum Field Theory of Many-body Systems*, Oxford Univ. Press (2007), Oxford.

[3] R. A. Prange and S. M. Girvin, *The Quantum Hall Ef- fect*, Springer, Berlin (1990). S. Das Sarma and A. Pinczuk, ıPerspectives in Quantum Hall effects, Wiley, New York (1997). S. M. Girvin, *The Quantum Hall Effect: Novel Excitations and Broken Symmetries*, `arXiv:cond-mat/9907002v1 [cond-mat.mes-hall]`.

[4] A. Stern, *Anyons and the quantum Hall effect - a pedagogical review*, Ann. Phys. **323** (2008) 204.

[5] Patrick A. Lee, and T. V. Ramakrishnan, *Disordered electronic systems*, Rev. Mod. Phys. **57** (1985) 287.

[6] K. Von Klitzing, G. Dorda and M. Pepper, *New Method for High-Accuracy Determination of the Fine-Structure Constant Based on Quantized Hall Resistance*, Phys. Rev. Lett. **45**, 494-497 (1980).

[7] D. C. Tsui, H. L. Stormer, and A. C. Gossard *Two-Dimensional Magnetotransport in the Extreme Quantum Limit*, Phys. Rev. Lett. **48**, 1559 (1982).

[8] J. K. Wang and V. J. Goldman, *Edge states in the fractional quantum Hall effect*, Phys. Rev. Lett. **67**, 749 (1991); and reference therein.

[9] Horst L. Stormer, *Nobel Lecture: The fractional quantum Hall effect*, Rev. Mod. Phys. **71**, 875 (1999).

[10] J. S. Xia, W. Pan, C. L. Vicente, E. D. Adams, N. S. Sullivan, H. L. Stormer, D. C. Tsui, L. N. Pfeiffer, K. W. Baldwin, and K. W. West *Electron Correlation in the Second Landau Level: A Competition Between Many Nearly Degenerate Quantum Phases*, Phys. Rev. Lett. **93**, 176809 (2004)

[11] C. Nayak, *Lecture Notes for Physics 242a,b.* . A. M. Tsvelik, *Quantum Field Theory in Condensed Matter Physics*, Cambridge University Press.

[12] A. Cappelli, C. A. Trugenberger, G. R. Zemba, *Stable hierarchical quantum Hall fluids as $W_{1+\infty}$ minimal models*, Nucl. Phys. **B 448** (1995) 470; for a review, see: *$W_{1+\infty}$ minimal models and the hierarchy of the quantum Hall effect*, Nucl. Phys. *(Proc. Suppl.)* **B 45A** (1996) 112.

[13] F. D. M. Haldane, *Fractional Quantization Of The Hall Effect: A Hierarchy Of Incompressible Quantum Fluid States*, Phys. Rev. Lett. **51** (1983) 605. B. I. Halperin, *Statistics of quasiparticles and the hierarchy of fractional quantized Hall states*, Phys. Rev. Lett. **52** (1984) 1583 [Erratum-ibid. **52** (1984) 2390].

[14] G. Moore and N. Read, *Nonabelions in the fractional quantum hall effect*, Nucl. Phys. **B 360** (1991) 362.

[15] E. Ardonne, K. Schoutens, *New Class of Non-Abelian Spin-Singlet Quantum Hall States*, Phys. Rev. Lett. **82** (1999) 5096; E. Ardonne, N. Read, E. Rezayi, K. Schoutens, *Non-Abelian spin-singlet quantum Hall states: wave functions and quasihole state counting*, Nucl. Phys. **B 607** (2001) 549.

[16] E. Ardonne, F.J.M. van Lankvelt, A.W.W. Ludwig, K. Schoutens, *Separation of spin and charge in paired spin-singlet quantum Hall states* Phys. Rev. B **65**, 041305 (2002).

[17] R. B. Laughlin, *Anomalous quantum Hall effect: An incompressible quantum fluid with fractionally charged excitations*, Phys. Rev. Lett. **50** (1983) 1395.

[18] L. Saminadayar, D. C. Glattli, Y. Jin, and B. Etienne, *Observation of the e/3 Fractionally Charged Laughlin Quasiparticle*, Phys. Rev. Lett. **79**, 2526 (1997).

[19] F. E. Camino, Wei Zhou, and V. J. Goldman, *Realization of a Laughlin quasiparticle interferometer: Observation of fractional statistics,* Phys. Rev. B **72** 075342 (2005).

[20] X. G. Wen and A. Zee, *Classification of Abelian quantum Hall states and matrix formulation of topological fluids,* Phys. Rev. B **46**, 2290 (1992). J. Frohlich and E. Thiran, *Integral quadratic forms, Kac-Moody algebras,* and fractional quantum Hall
effect: An ADE-O classification. X. G. Wen, *Topological orders and edge excitations in FQH states,* Advances in Physics, 44, 405 (1995), [arXiv:cond-mat/9506066v2]. A. Lopez and E. H. Fradkin, *Fermionic Chern-Simons field theory for the fractional Hall effect*, [arXiv:cond-mat/9704055.]

[21] B. I. Halperin, *Theory of the Quantized Hall Conductance*, Helvetica Physica Acta, 56, 75 (1983).

[22] R. Willett, J. P. Eisenstein, H. L. Störmer, D. C. Tsui, A. C. Gossard, and J. H. English; *Observation of an even-denominator quantum number in the fractional quantum Hall effect*, Phys. Rev. Lett. 59, 1776 (1987).

[23] J. P. Eisenstein, R. Willett, H. L. Stormer, D. C. Tsui, A. C. Gossard and J. H. English *Collapse of the Even-Denominator Fractional Quantum Hall Effect in Tilted Fields*, Phys. Rev. Lett. 61, 997 (1988) .

[24] W. Pan, J.-S. Xia, V. Shvarts, D. E. Adams, H. L. Stormer, D. C. Tsui, L. N. Pfeiffer, K. W. Baldwin, and K. W. West ,*Exact Quantization of the Even-Denominator Fractional Quantum Hall State at $\nu = 5/2$ Landau Level Filling Factor* Phys. Rev. Lett. **83**, 3530 (1999) .

[25] J. P. Eisenstein, K. B. Cooper, L. N. Pfeiffer, and K. W. West, *Insulating and Fractional Quantum Hall States in the First Excited Landau Level*, Phys. Rev. Lett. **88**, 076801 (2002), http://arxiv.org/abs/cond-mat/0110477 [arXiv:cond-mat/0110477v1].

[26] S. Simon, $\nu = 5/2$ Talk at Conference "Quantum Matter in Low Dimensions: Opportunities and Challenges".

[27] N. N. Bogoliubov, V. V. Tolmachev and D. V. Shirkov, M. C. B. Abdalla and K. D. Rothe, *A new method in the theory of superconductivity*, Consultants Bureau, Inc. New York, 1959.

[28] N. Read and D. Green *Paired states of fermions in two dimensions with breaking of parity and time-reversal symmetries and the fractional quantum Hall effect*, Phys. Rev. B **61**, 10267 (2000).

[29] J. Zinn-Justin, *Quantum field theory and critical phenomena*, Int. Ser. Monogr. Phys. **92** (1996) 1.

[30] C. Nayak, S. H. Simon, A. Stern, M. Freedman and S. Das Sarma, *Non-Abelian anyons and topological quantum computation*, Rev. Mod. Phys. **80** (2008) 1083.

[31] R. Jackiw, *TOPICS IN PLANAR PHYSICS*, Nucl. Phys. Proc. Suppl. **18A**, 107 (1990). G. W. Semenoff, *Chern-Simons gauge theory and spin statistics connection in two-dimensional quantum mechanics. In *Banff 1989, Proceedings, Physics, geometry, and topology* 363-385. (see HIGH ENERGY PHYSICS INDEX 29 (1991) No. 16469).* G. V. Dunne, *Aspects of Chern-Simons theory,* [arXiv:hep-th/9902115].

[32] F. Wilczek, *Fractional statistics and anyon superconductivity, Singapore, Singapore: World Scientific (1990).*

[33] J. Preskill, *Topological quantum computation, lecture notes.* A. Y. Kitaev, *Anyons in an exactly solved model and beyond,* Annals Phys. **321** (2006) 2 [arXiv:cond-mat/0506438v3[cond-mat.mes-hall]].

[34] E. Witten, *Quantum field theory and the Jones polynomial*, Commun. Math. Phys. **121** (1989) 351.

[35] S. Elitzur, G. W. Moore, A. Schwimmer and N. Seiberg, *Remarks On The Canonical Quantization Of The Chern-Simons-Witten Theory,* Nucl. Phys. B **326** (1989) 108.

[36] X. G. Wen, *Topological Orders in Rigid States*, Int. J. Mod. Phys. B4, 239 (1990).

[37] C. C. Adams *The Knot Book: An Elementary Introduction to the Mathematical Theory of Knots* , Macmillan.

[38] M. Nielsen and I. Chuang, *Quantum Computation and Quantum Information.* Cambridge: Cambridge University Press. ISBN 0-521-63503-9. John Preskill Lecture notes on Quantum Computation, Chapter from 1 to 8.

[39] R. P. Feynman, *Simulating physics with computers*, Int. J. Theor. Phys. **21** (1982) 467.

[40] M. H. Freedman, A. Kitaev and Z. Wang, *Simulation of topological field theories by quantum computers*, Commun. Math. Phys. **227** (2002) 587; E. Rowell, R. Stong and Z. Wang, *On Classification of Modular Tensor Categories*, preprint arXiv:0712.1377, Commun. Math. Phys. in press; L. Fidkowski, M. Freedman, C. Nayak, K. Walker and Z. Wang, *From string nets to nonabelions,* Commun. Math. Phys. **287** (2009) 805.

[41] S. Trebst, M. Troyer, Z. Wang and A. W. W. Ludwig, *A Short Introduction to Fibonacci Anyon Models* Prog. Theor. Phys. Supplement No. 176 (2008) pp. 384-407.

[42] C. de C. Chamon, D. E. Freed, S. A. Kivelson, S. L. Sondhi, X. G. Wen, *Two point-contact interferometer for quantum Hall systems*, Phys. Rev. B **55**, 2331 (1997)

[43] L. Saminadayar, D. C. Glattli, Y. Jin, B. Etienne *Observation of the e/3 Fractionally Charged Laughlin Quasiparticles*, Phys. Rev. Lett. **79**, 2526 (1997).

[44] E. Fradkin, M. Huerta, G. Zemba, *Effective Chern-Simons Theories of Pfaffian and Parafermionic Quantum Hall States, and Orbifold Conformal Field Theories* Nucl.Phys. B **601** (2001) 591. P. Bonderson, A. Kitaev, K. Shtengel, *Detecting Non-Abelian Statistics in the $\nu = 5/2$ Fractional Quantum Hall State* , Phys. Rev. Lett. **96** (2006) 016803; W. Bishara, P. Bonderson, C. Nayak, K. Shtengel, J. K. Slingerland, *Interferometric signature of non-Abelian anyons,* Phys. Rev. **B 80** (2009) 155303. B. I. Halperin, A. Stern, I. Neder and B. Rosenow, *Theory of the Fabry-Perot Quantum Hall Interferometer*, `arXiv:1010.4598v1 [cond-mat.mes-hall]`.

[45] D. Ferraro, A. Braggio, M. Merlo, N. Magnoli, and M. Sassetti, *Relevance of Multiple Quasiparticle Tunneling between Edge States at $\nu = p/(2np + 1)$*, Phys. Rev. Lett. **101** (2008) 166805.

[46] R. L. Willett, L. N. Pfeiffer and K. W. West, *Measurement of filling factor 5/2 quasiparticle interference: observation of charge e/4 and e/2 period oscillations*, [arXiv:0807.0221].

[47] P. Di Francesco, P. Mathieu, D. Senechal, *Conformal Field Theory*, Springer (1999), Berlin.

[48] A. A. Belavin, A. M. Polyakov and A. B. Zamolodchikov, *Infinite conformal symmetry in two-dimensional quantum field theory,* Nucl. Phys. B **241** (1984) 333. P. Ginsparg, *Applied Conformal Field Theory*, Lectures given at Les Houches summer session, Jun 28 – Aug 5, 1988 [arXiv:hep-th/9108028v1]. G. Mussardo *Statistical Field Theory: An Introduction To Exactly Solved Models In Statistical Physics*, Oxford University Press M. R. Gaberdiel *An Introduction to Conformal Field Theory*, arXiv:hep-th/9910156v2.

[49] E. Kiritsis, *String Theory in a Nutshell*, Princeton University Press.

[50] C. Gomez, M. Ruiz-Altaba and G. Sierra, *Quantum Groups in Two-Dimensional Physics*, Cambridge University Press. G. Mussardo talk at the conference "Quantum Engineering of States and Devices: Theory and Experiments", web pages of the conference.

[51] Victor G. Kac, *Infinite dimensional Lie algebras*, Cambridge University Press.

[52] A.B. Zamolodchikov, V.A. Fateev, *Parafermionic Currents in the Two-Dimensional Conformal Quantum Field Theory and Selfdual Critical Points in Z(n) Invariant Statistical Systems*, Sov. Phys. JETP **62** (1985) 215; D. Gepner, Z. Qiu, *Modular invariant partition functions for parafermionic field theories*, Nucl. Phys. **B 285** (1987) 423. P. Jacob, P. Mathieu, *Parafermionic character formulae,* Nucl. Phys. B **587** (2000) 514.

[53] K. Huang, *Statistical Mechanics.*

[54] P. Bouwknegt, K. Schoutens *W-symmetry in Conformal Field Theory*, Phys.Rept. 223 (1993) 183-276.

[55] A. Cappelli, C. Itzykson and J. B. Zuber, *Modular Invariant Partition Functions in Two-Dimensions*, Nucl. Phys. **B 280** (1987) 445. For a review, see: A. Cappelli, J. B. Zuber, *A-D-E Classification of Conformal Field Theories,* Scholarpedia **5** (2010) 10314.

[56] R. Dijkgraaf, E. Verlinde, *Modular invariance and the fusion algebra*, Nucl. Phys. **B** (Proc. Suppl.) **5 B** (1988) 87; G. Moore, N. Seiberg, *Polynomial equations for rational conformal field theories*, Phys. Lett. **B 212** (1988) 451; *Naturality in conformal field theory*, Nucl. Phys. **B 313** (1989) 16; for a review, see: *Lectures on RCFT*, proceedings of the 1989 Banff Summer school, H. C. Lee ed., Plenum Press (1990), New York.

[57] J. Frohlich and E. Thiran, *Integral quadratic forms, Kac-Moody algebras, and fractional quantum Hall effect: An ADE-O classification.*

[58] E. Ardonne, K. Schoutens, *Wavefunctions for topological quantum registers*, Annals Phys. **322** (2007) 201.

[59] E. Keski-Vakkuri and X. G. Wen, *The Ground state structure and modular transformations of fractional quantum Hall states on a torus*, Int. J. Mod. Phys. B **7** (1993) 4227, [arXiv:hep-th/9303155].

[60] E. Ardonne, P. Fendley and E. Fradkin, *Topological order and conformal quantum critical points,* Annals Phys. **310**, 493 (2004) [arXiv:cond-mat/0311466].

[61] E. H. Fradkin, M. Huerta and G. R. Zemba, *Effective Chern-Simons theories of Pfaffian and parafermionic quantum Hall states, and orbifold conformal field theories,* Nucl. Phys. B **601** (2001) 591 [arXiv:cond-mat/0011143].

[62] A. Cappelli, G. V. Dunne, C. A. Trugenberger and G. R. Zemba, *Conformal symmetry and universal properties of quantum Hall states*, Nucl. Phys. B **398** (1993) 531 [arXiv:hep-th/9211071].

[63] A. Cappelli, L. S. Georgiev, I. T. Todorov, *A Unified Conformal Field Theory Description of Paired Quantum Hall States* Commun.Math.Phys. 205 (1999) 657-689.

[64] E. Ardonne, *A conformal field theory description of fractional quantum Hall states*, Ph. D thesis. Olaf Smits, *Clustered states in the fractional quantum Hall effect*, Ph. D. thesis.

[65] Chetan Nayak, Frank Wilczek, $2n$ *Quasihole States Realize* 2^{n-1}*-Dimensional Spinor Braiding Statistics in Paired Quantum Hall States*, arXiv:cond-mat/9605145v1]. J.K. Slingerland, F.A. Bais, *Quantum groups and nonabelian braiding in quantum Hall systems* Nucl.Phys. B612 (2001) 229-290.

[66] N. Read, E. Rezayi, *Beyond paired quantum Hall states: Parafermions and incompressible states in the first excited Landau level*, Phys. Rev. **B 59** (1999) 8084.

[67] A. Cappelli, L. S. Georgiev, I. T. Todorov, *Parafermion Hall states from coset projections of Abelian conformal theories*, Nucl. Phys. **B 599** (2001) 499.

[68] A. N. Schellekens and S. Yankielowicz, *Simple currents, modular invariant and fixed point*, Int. J. Mod. Phys. A **5** (1990) 2903.

[69] A. Cappelli, G. R. Zemba, *Modular invariant partition functions in the quantum Hall effect*, Nucl. Phys. **B 490** (1997) 595.

[70] K. Ino, *Modular invariants in the fractional quantum Hall effect*, Nucl. Phys. B **532** (1998) 783, [arXiv:cond-mat/9804198].

[71] A. Cappelli, L. S. Georgiev, G. R. Zemba, *Coulomb blockade in hierarchical quantum Hall droplets*, J. Phys. **A 42** (2009) 222001.

[72] A. Cappelli, G. Viola, G. R. Zemba *Chiral Partition Functions of Quantum Hall Droplets* Ann. Phys, **325** (2010) 465.

[73] A. Cappelli, G. Viola *Partition Functions of Non-Abelian Quantum Hall States* `[arXiv:1007.1732v2 [cond-mat.mes-hall]]`

[74] S.-S. Lee, S. Ryu, C. Nayak, M. P. A. Fisher, *Particle-Hole Symmetry and the $\nu = 5/2$ Quantum Hall State*, Phys. Rev. Lett. **99** (2007) 236807; M. Levin, B. I. Halperin, B. Rosenow, *Particle-hole symmetry and the Pfaffian state,* Phys. Rev. Lett. **99** (2007) 236806; W. Bishara, G. A. Fiete, C. Nayak. *Quantum Hall states at $\nu = 2/(k+2)$: Analysis of the particle-hole conjugates of the general level- k Read-Rezayi states*, Phys. Rev. **B 77** (2008) 241306.

[75] P. Bonderson, J. K. Slingerland, *Fractional Quantum Hall Hierarchy and the Second Landau Level,* Annals Phys. **323** (2008) 2709.

[76] B. Blok, X. G. Wen, *Many body systems with non-Abelian statistics*, Nucl. Phys. B **374** (1992) 615.

[77] N. Read, *Excitation structure of the hierarchy scheme in the fractional quantum Hall effect*, Phys. Rev. Lett. **65** (1990) 1502; J. Fröhlich, A. Zee, *Large scale physics of the quantum hall fluid*, Nucl. Phys. **B 364** (1991) 517; X.-G. Wen, A. Zee, *Classification of Abelian quantum Hall states and matrix formulation of topological fluids*, Phys. Rev. **B 46** (1992) 2290.

[78] A. Cappelli, G. R. Zemba, *Hamiltonian Formulation of the W-infinity Minimal Models*, Nucl. Phys. **B 540** (1999) 610.

[79] J. Fuchs, A. N. Schellekens, C. Schweigert, *A matrix S for all simple current extensions*, Nucl. Phys. B **473** (1996) 323.

[80] V.G. Kac, I.T. Todorov, *Affine orbifolds and rational conformal field theory extensions of W-1+infinity*, Commun. Math. Phys **190** (1997) 57.

[81] D. Gepner, *New Conformal Field Theories Associated with Lie Algebras and their Partition Functions*, Nucl. Phys. **B 290** (1987) 10; *Field Identification In Coset Conformal Field Theories*, Phys. Lett. **B 222** (1989) 207.

[82] P. Bonderson, C. Nayak, K. Shtengel *Coulomb Blockade Doppelgangers in Quantum Hall States,* Phys. Rev. **B 81** (2010) 165308.

[83] C. de C. Chamon, D. E. Freed, S. A. Kivelson, S. L. Sondhi, and X. G. Wen, *Two point-contact interferometer for quantum Hall systems*, Phys. Rev. **B 55**, (1997) 2331.

[84] N. R. Cooper, A. Stern, *Observable Bulk Signatures of Non-Abelian Quantum Hall States,* Phys. Rev. Lett. **102** (2009) 176807; K. Yang, B. I. Halperin, *Thermopower as a possible probe of non-Abelian quasiparticle statistics in fractional quantum Hall liquids*, Phys. Rev. **B 79** (2009) 115317.

[85] A. Stern, B. I. Halperin, *Proposed Experiments to Probe the Non-Abelian $\nu = 5/2$ Quantum Hall State*, Phys. Rev. Lett. **96** (2006) 016802; R. Ilan, E. Grosfeld, A. Stern, *Coulomb Blockade as a Probe for Non-Abelian Statistics in Read-Rezayi States*, Phys. Rev. Lett. **100** (2008) 086803;

[86] R. Ilan, E. Grosfeld, K. Schoutens, A. Stern, *Experimental signatures of non-Abelian statistics in clustered quantum Hall states*, Phys. Rev. **B 79** (2009) 245305.

[87] A. Stern, B. Rosenow, R. Ilan, B. I. Halperin, *Interference, Coulomb blockade, and the identification of non-abelian quantum Hall states*, preprint arXiv:0912.4394; R. Ilan, B. Rosenow, A. Stern, *Signatures of non-Abelian statistics in non-linear coulomb blockaded transport,* preprint arXiv:1005.4772.

[88] L. S. Georgiev, *Thermal broadening of the Coulomb blockade peaks in quantum Hall interferometers,* preprint arXiv:1003.4871.

[89] Y. Zhang, D. T. McClure, E. M. Levenson-Falk, C. M. Marcus, L. N. Pfeiffer, K. W. West, *Distinct Signatures For Coulomb Blockade and Aharonov-Bohm Interference in Electronic Fabry-Perot Interferometers* , Phys. Rev. **B 79** (2009) 241304; R.L. Willett, L.N. Pfeiffer, K.W. West, *Alternation and interchange of e/4 and e/2 period interference oscillations as evidence for filling factor 5/2 non-Abelian quasiparticles*, preprint arXiv:0911.0345.

[90] A. Cappelli, M. Huerta, G. R. Zemba, *Thermal Transport in Chiral Conformal Theories and Hierarchical Quantum Hall States*, Nucl.Phys. B636 (2002) 568. L. S. Georgiev,*A universal conformal field theory approach to the chiral persistent currents in the mesoscopic fractional quantum Hall states*, Nucl.Phys. B707 (2005) 347-380

[91] A. Kitaev, J. Preskill, *Topological Entanglement Entropy*, Phys. Rev. Lett. **96** (2006) 110404; M. Levin, X.-G. Wen, *Detecting Topological Order in a Ground State Wave Function*, Phys. Rev. Lett. **96** (2006) 110405; O. S. Zozulya, M. Haque, K. Schoutens, E. H. Rezayi, *Bipartite entanglement entropy in fractional quantum Hall states*, Phys. Rev.**B 76** (2007) 125310.

[92] P. Fendley, M. P. A. Fisher, C. Nayak, *Topological Entanglement Entropy from the Holographic Partition Function*, J. Statist. Phys. **126** (2007) 1111; *Boundary conformal field theory and tunneling of edge quasiparticles in non-Abelian topological states*, Annals Phys. **324** (2009) 1547.

[93] W. E. Chickering, J. P. Eisenstein, L. N. Pfeiffer, K. W. West, *Thermopower of two-dimensional electrons at filling factors $\nu = 3/2$ and 5/2*, Phys. Rev. **B 81** (2010) 245319.

[94] N. R. Cooper, B. I. Halperin, I. M. Ruzin, *Thermoelectric response of an interacting two-dimensional electron gas in a quantizing magnetic field*, Phys. Rev. **B 55** (1997) 2344.

[95] S. Hershfield, J. H. Davies, P Hyldgaard, C. J. Stanton, J. W. Wilkins, *Zero-frequency current noise for the double-tunnel-junction Coulomb blockade,* Phys. Rev. **B 47** (1993) 1967; for a review, see: M.J.M. de Jong, C.W.J. Beenakker, *Shot noise in mesoscopic systems,*, in *Mesoscopic Electron Transport*, L.L. Sohn, L.P. Kouwenhoven, G. Schoen eds. (Kluwer, Dordrecht, 1997).

[96] Z. Papic, B. A. Bernevig, N. Regnault, *Topological Entanglement in Abelian and non-Abelian Excitation Eigenstates*, `arXiv:1008.5087v1 [cond-mat.mes-hall]`. A. M. Läuchli, E. J. Bergholtz and M. Haque, *Entanglement scaling of fractional quantum Hall states through geometric deformations*, New J. Phys. **12** 075004 (2010).

[97] C. Itzykson, *Level one Kac-Moody characters and modular invariance*, Nucl. Phys. **B** (Proc. Suppl.) **5 B** (1988) 150.

[98] M. Grayson, D. C. Tsui, L. N. Pfeiffer, K. W. West, and A. M. Chang, *Continuum of Chiral Luttinger Liquids at the Fractional Quantum Hall Edge*, Phys. Rev. Lett. **80** (1998) 1062.

[99] See e.g.: D. Orgad and O. Agam, *Correlated Tunneling and the Instability of the Fractional Quantum Hall Edge*, Phys. Rev. Lett. **100** (2008) 156802.

[100] A. Lopez and E. Fradkin, *Universal structure of the edge states of the fractional quantum Hall states*, Phys. Rev. **B 59**, (1999) 15323.

[101] V. Kac and A. Radul, *Quasifinite highest weight modules over the Lie algebra of differential operators on the circle*, Commun. Math. Phys. **157** (1993) 429; H. Awata, M. Fukuma, Y. Matsuo and S. Odake, *Representation theory of the W(1+infinity) algebra*, Prog. Theor. Phys. (Supp.) **118** (1995) 343; E. Frenkel, V. Kac, A. Radul and W. Wang, $W_{1+\infty}$ *and* $\mathcal{W}(gl_N)$ *with central charge N*, Commun. Math. Phys. **170** (1995) 337.

[102] M. Huerta, $\widehat{U(1)} \times \widehat{SU(m)}$ *theory and* $c = m$ $W_{1+\infty}$ *minimal models in the hierarchical quantum Hall effect,* Int. J. Mod. Phys. **A 15** (2000) 915.

W. Pan, H. L. Stormer, D. C. Tsui, L. N. Pfeiffer, K. W. Baldwin and K. W. West, *Transition from an Electron Solid to the Sequence of Fractional Quantum Hall States at Very w Landau Level Filling Factor*, Phys. Rev. Lett. **88** (2002) 176802. J. S. Xia *et al.*, *Electron Correlation in the Second Landau Level: A Competition Between Many Nearly Degenerate Quantum Phases*, Phys. Rev. Lett. **93** (2004) 176809, `[arXiv:cond-mat/0406724v1 [cond-mat.mes-hall] ]`.